Adiabatic Invariance in Voluntary Rhythmic Human Motion

Victor Dehouck

THESE DE DOCTORAT DE L'ETABLISSEMENT UNIVERSITE BOURGOGNE FRANCHE-COMTE

PREPAREE AU LABORATOIRE COGNITION, ACTION ET PLASTICITE SENSORIMOTRICE – INSERM UMR1093

Ecole doctorale n°554

Environnements - Santé

Doctorat de Sciences et Techniques des Activités Physiques et Sportives

Par

M. DEHOUCK Victor

Invariance Adiabatique dans les Mouvements Rythmiques Volontaires Humains

Thèse présentée et soutenue à Dijon, le 22 novembre 2023

Composition du Jury :

Gentil Christian	Professeur des Universités, Université de Bourgogne	Président, Examinateur
Crèvecoeur Frédéric	Professeur, Université Catholique de Louvain	Rapporteur
Detournay Stéphane	Directeur de Recherche, Université Libre de Bruxelles	Rapporteur
Nisky Ilana	Professeur, Université Ben Gourion du Néguev	Examinatrice
Buisseret Fabien	Maître Assistant, Haute Ecole de Louvain en Hainaut	Examinateur
Dierick Frédéric	Maître de Recherche, Rehazenter	Examinateur
White Olivier	Professeur Associé, Université de Bourgogne	Directeur de thèse
Boulanger Nicolas	Professeur, Université de Mons	Codirecteur de thèse

ÉCOLE DOCTORALE
Environnements - Santé
Bourgogne | Franche-Comté

Titre : Invariance Adiabatique dans les Mouvements Rythmiques Volontaires Humains

Mots clés : Espace des Phases, Variables action-angles, Mouvements Humains

Résumé : Les mouvements humains sont toujours complexes. Même une tâche simple comme prendre un verre d'eau implique de nombreux degrés de liberté i.e., différents groupes de muscles, plusieurs articulations et un nombre infini de trajectoires possibles pour le bras. Néanmoins, les mouvements sont facilement disponibles aux sujets sains et semblent être naturellement optimisés par le système nerveux central. Cela est souvent modélisé par la minimisation d'un paramètre donné du système, tel que l'énergie ou l'à-coup, qui sont des candidats naturels. Malheureusement, ces approches sont souvent limitées dans leur portée et ne peuvent pas décrire les mouvements périodiques dans des environnements changeant dans le temps. Dans de tels systèmes, les invariants adiabatiques sont des observables pertinentes issues de la mécanique hamiltonienne. L'objectif de cette thèse de doctorat est d'étudier le rôle et l'utilisation des invariants adiabatiques dans le contrôle moteur humain. Pour ce faire, nous avons réalisé une série d'expériences. Tout d'abord, nous les avons étudiées en tant que contrainte pour la stabilité globale de la marche, même lorsqu'elle est exposée à une tâche altérant la variabilité, telle que le maintien d'un rythme dicté par un métronome. Ensuite, nous avons utilisé des résultats récents en physique pour évaluer la variabilité inhérente à la marche à longue distance en tant que phénomène de diffusion de la distribution des invariants adiabatiques. Enfin, nous les avons explorés dans des environnements temporels changeants, notamment en modifiant la "gravité" à la fois dans une centrifugeuse et dans un contexte de vol parabolique, où ils semblent être des quantités pertinentes pour montrer les changements dans les stratégies motrices. Les différents résultats de cette thèse indiquent que les invariants adiabatiques révèlent des contraintes génériques cachées affectant les mouvements humains périodiques.

Title : Adiabatic Invariance in Voluntary Rhythmic Human Motion

Keywords : Phase Space, Action-angle variables, Human Motion

Abstract : Human motion is inherently complex. Even an ordinary task like lifting a glass of water involves many degrees of freedom i.e., different muscle groups, multiple joints and an infinite number of trajectories for the arm. Nevertheless, motion is readily available to healthy subjects, and seems to be naturally optimized by the central nervous system. This is often modelized as the minimization of a given parameter of the system e.g., energy or jerk, which appear as natural candidates. Unfortunately, these approaches are often limited in their scopes, and cannot describe periodic motion in time-changing environments. In such systems, adiabatic invariants are relevant observables originating from Hamiltonian mechanics. The aim of this doctoral dissertation is to investigate the role and use of adiabatic invariants in human motor control. This was done in a series of experiments. First, we studied them as a constraint for the global stability of gait, even when exposed to a variability-altering task, such as metronome keeping. Then, we used recent results in physics to assess the inherent variability of long-range walking as a diffusion phenomenon of the distribution of adiabatic invariants. Finally, we explored them in time-changing environments, specifically by altering “gravity” both in a centrifuge and a parabolic flight context, where they seem to be relevant quantities to show changes in motor strategies. The different findings in this dissertation point to adiabatic invariants revealing generic hidden constraints affecting periodic human motion.

UBFC
UNIVERSITE
BOURGOGNE FRANCHE-COMTE

Université Bourgogne Franche-Comté
32, avenue de l’Observatoire
25000 Besancon

Funding

This thesis work was carried out with main funding from ISITE.
The work was also partially funded by the COMPLEXYS and HEALTH research institutes of UMONS.

complexys santé

INSTITUT DE RECHERCHE SUR LES SYSTEMES COMPLEXES DE L'UMONS

INSTITUT DE RECHERCHE EN SCIENCES ET TECHNOLOGIES DE LA SANTE DE L'UMONS

Publications

This thesis has led to these publications:

Published

- Boulanger N., Buisseret F., **Dehouck V.**, Dierick F., White O., (2020) **Adiabatic invariants drive rhythmic human motion in variable gravity**, *Physical Review E* DOI: 10.1103/PhysRevE.102.062403
- Boulanger N., Buisseret F., **Dehouck V.**, Dierick F., White O., (2021) **Motor strategies and adiabatic invariants: The case of rhythmic motion in parabolic flights**, *Physical Review E* DOI: 10.1103/PhysRevE.104.024403
- Buisseret F.[1], **Dehouck V.**[1] , Boulanger N., Henry G., Piccinin F., White O., Dierick F., (2022) **Adiabatic invariant of center-of-mass motion during walking as a dynamical stability constraint on stride interval variability and predictability**, *Biology* DOI: 10.3390/biology11091334
- Boulanger N., Buisseret F., **Dehouck V.**, Dierick F., White O., (2023) **Diffusion in phase space as a tool to assess variability of vertical centre-of-mass motion during long-range walking**, *Physics* DOI: 10.3390/physics5010013

In preparation

- White O.[1], **Dehouck V.**[1] , Boulanger N., Dierick F., Babič J., Goswami N., Buisseret F., **Resonance tuning of rhythmic movements is disrupted at short time scales: a centrifuge study**

This thesis has also led to this poster:

- **Dehouck V.**, White O., Boulanger N., Buisseret F., **Frequency tuning in human motion in variable gravity**, 9$^{\text{ème}}$ Journée Scientifique du Pôle Hainuyer; Mons, Belgium (2023)

[1]First co-authors

Contents

List of Figures

List of Tables

Chapter 1

French summary

Introduction

Les mouvements, et en particulier la locomotion, sont l'une des clés de voûte de la vie sur Terre. Tous les animaux sont mobiles ne serait-ce que pour une partie de leur vie, et les humains ne font pas exception. Que ce soit pour se nourrir, découvrir de nouveaux environnements ou se reproduire, la mobilité a formé l'arbre évolutif sur lequel nous nous tenons.

La nature des mouvements volontaires est riche. Ce qui apparaît comme automatique est en fait le résultat d'interactions sophistiquées. Par exemple, un martinet noir chassant des insectes semble glisser dans le ciel sans effort, alors qu'en réalité il doit intégrer des retours sensoriels complexes de son environnement, comme la vitesse et la direction du vent en temps réel pour garder un contrôle précis de ses ailes. Son système nerveux central possède une représentation des lois de la physique qui lui permet de prédire sa trajectoire ainsi que celle de l'insecte, le tout en volant avec des pointes à plus de 100 km/h.

Quoi qu'il en soit, qu'ils semblent simples ou complexes les mouvements sont inhéremment contraints par le corps, que ce soit physiologiquement ou neurologiquement. En effet, même le simple acte de marcher implique plusieurs combinaisons de flexions, extensions et rotations des trois articulations principales de la jambe, contrôlées par la contraction d'une dizaine de muscles (Rose and Gamble 2006, ch. 1). Ainsi que différentes structures neurales, avec des commandes émanant du système nerveux central et du réseau locomoteur spinal. Cela rend l'étude des mouvements particulièrement difficile puisque le nombre de variables à analyser est très large, c'est le problème de Bernstein (Bernstein 1967). Néanmoins, même à travers cette pléthore de combinaisons et la taille de l'espace de configuration, le système nerveux central semble automatiquement choisir la meilleure stratégie motrice en temps

réel (Rose and Gamble 2006, ch. 5).

En plus de ces considérations biomécaniques, les mouvements sont aussi contraints par l'environnement direct. Par exemple, marcher sur de l'herbe, de l'asphalte ou du sable est légèrement différent, c'est aussi le cas pour des environnements plus exotiques comme une centrifugeuse ou la station spatiale internationale. Le système nerveux central intègre ces retours environnementaux pour corriger des erreurs perçues. Bien qu'évident, il est aussi bon de rappeler que le corps humain est fondamentalement un objet physique et doit donc suivre ses lois.

Contrôle moteur

Dans la vie courante, tous les êtres humains sont amenés à réaliser des mouvements volontaires, qui nous semble automatiquement disponibles. Néanmoins, ces mouvements doivent être planifiés. Pour un individu sain, attraper une balle est une tâche simple, mais cette apparente simplicité est en réalité le résultat d'une série d'interactions complexes entre différentes structures, tels que les muscles, les nerfs périphériques et le système nerveux central. Tout d'abord, la position de la balle par rapport au corps est perçue par différents sens (vision, proprioception, etc.) La masse, la forme et la trajectoire de la balle doivent aussi être estimées pour prédire la posture adaptée à la réception. Ses informations nerveuses sont ensuite envoyées aux différents muscles pour pouvoir adopter cette posture. Chacune de ces étapes encourt des délais. Néanmoins, les êtres humains sont capables de réaliser ce genre de tâches qui requiert des timings précis. Pour ce faire, le système nerveux central essaye en permanence de prédire et d'anticiper les événements qui prennent place autour de nous, et de s'adapter à eux (Rosenbaum 2009).

Ce mécanisme a lieu grâce aux modèles internes (Kawato 1999). Un exemple simple d'exécution motrice avec un modèle direct, est le suivant : quand une commande motrice est générée par le système nerveux central, une copie de cette commande est envoyée à un modèle interne qui prédit les conséquences de cette commande en même temps qu'elle est effectuée. Toute différence entre l'action exécutée et la prédiction faite est envoyée au système nerveux central pour corriger et adapter la commande motrice. Dans notre exemple cela signifie que si une rafale de vent perturbe la trajectoire de la balle, la commande motrice envoyée à l'effecteur n'est plus pertinente, puisqu'elle n'est plus cohérente avec la prédiction faite par le modèle interne qui interprète les retours de l'environnement en permanence. Cette différence est signalée au système nerveux central qui modifie alors la commande motrice pour prendre en compte la perturbation.

Ces modèles internes et leurs prédictions rendent nos mouvements parti-

culièrement adaptables, puisqu'ils nous permettent de deviner les propriétés de notre environnement et prédire des stratégies motrices optimales, même face à des contextes (relativement) nouveaux puisque nous pouvons corriger nos mouvements presque en temps réel.

Bien que ces représentations internes expliquent en partie notre adaptabilité à des situations nouvelles, un autre problème courant du contrôle moteur est le suivant: comment le système nerveux central choisit-il la commande motrice à envoyer en premier lieu ?

En effet, le corps humain possède de très nombreux degrés de liberté redondants disponibles pour réaliser n'importe quelle tâche (Bernstein 1967). Même un mouvement apparemment anodin comme attraper une balle implique en réalité plusieurs groupes de muscles avec différents niveaux d'activation possibles, plusieurs articulations pouvant se combiner avec divers angles et un nombre infini de trajectoires. Néanmoins, quand on réalise des mouvements le système nerveux central semble rapidement et automatiquement choisir une commande motrice précise. Il semble impossible que le système nerveux essaye de prédire et de traiter l'information d'un nombre infini de possibilités et il est raisonnable de supposer que celui-ci se repose sur des principes physiques ou généraux pour réduire le nombre de configurations à explorer. Ces principes sont couramment étudiés dans le contexte de la théorie du contrôle optimal. Ces principes reposent souvent sur la minimisation de certaines grandeurs, comme le temps, la force, la quantité de mouvement, le coût énergétique ou le jerk, à savoir la dérivée de l'accélération (Nelson 1983).

Ce jerk est couramment utilisé pour décrire les mouvements du bras, par exemple. Originellement proposé par (Hogan 1982), ce principe propose que les mouvements naturels tendent à être lisses, c'est-à-dire sans à-coup ou soudaines accélérations, ce qui revient à minimiser le jerk. Cela peut être formalisé comme la minimisation de l'action:

$$S = \int_{t_0}^{t_1} \dddot{x}^2 dt. \tag{1.1}$$

Où t_0 et t_1 représentent respectivement le temps de début et de fin du mouvement. x représente la position de l'effecteur, par exemple la main. Cela signifie que les mouvements sont étudiés en terme d'espace extracorporel, ce qui rend ce modèle facile d'utilisation puisqu'il ne fait pas d'hypothèse par rapport à la biomécanique du bras.

Cependant, les solutions issues de ce genre de principes ne sont pas périodiques. Ce n'est donc pas une approche adaptée pour étudier les mouvements rythmiques telle que la marche. L'étude de ces mouvements nous

conduit donc à explorer de nouveaux modèles.

Gravité

Par sa nature omniprésente, la gravité est intuitivement comprise et difficile à isoler. Par exemple, bien que ce soit une contrainte universelle dans les mouvements terrestres, pesant constamment à $g = 9{,}81 m/s^2$, il n'y a pas d'organe unique dédié à sa mesure, et son intégration par le système nerveux central est nécessairement un processus multisensoriel. Néanmoins, elle est prise en compte par le système nerveux pour planifier des mouvements optimaux.

Par exemple, lorsque l'on pointe horizontalement du doigt d'un objet à un autre, le profil de vitesse réalisé par le bras est symétrique: le bras accélère pendant la première partie du mouvement et décélère dans la deuxième moitié. Ce n'est pas le cas pour les mouvements verticaux, c'est-à-dire dans la direction où la gravité agit. En effet, un mouvement dirigé vers le haut atteint son maximum de vitesse plus tôt qu'un mouvement dirigé vers le bas. Cette intégration de la gravité dans le mouvement aide à réduire le coût énergétique des mouvements verticaux, où le bras se laisse accélérer et décélérer par la force de gravité (Pozzo et al. 1998).

Pour étudier la robustesse des théories et des représentations de la gravité, il est particulièrement intéressant de pousser les expériences hors de la zone de confort du système nerveux central et dans des environnements où la "gravité" est différente. Il existe deux tels régimes : l'hypergravité ($g > 1$) typiquement étudié dans les centrifugeuses, où la rotation et la force centripète résultante permettent de générer des environnements avec de grandes accélérations; et le régime hypogravitaire ($g < 1$) typique des chutes libres, comme celles survenant dans les vols paraboliques ou dans la station spatiale internationale.

Malheureusement, les phases de transitions d'un environnement gravitaire à un autre sont difficilement modélisables. C'est en général le cas pour tout changement de paramètre au cours du temps.

Physique

Face à ces deux problèmes, à savoir la difficulté de modéliser des mouvements périodiques et des mouvements avec des changements de paramètres extérieurs au cours du temps, la physique semble offrir une solution de choix avec les invariants adiabatiques.

Ces derniers sont naturellement apparus dans le contexte de la mécanique hamiltonienne. En effet, l'une des premières choses à faire pour comprendre un système physique est trouver les grandeurs qui restent constantes au cours

du temps. Une méthode courante pour trouver ces grandeurs consiste en un changement de variables –procédure rendue simple par l'utilisation de transformations dites canoniques, qui conservent la forme des équations décrivant l'évolution d'un système– spécifiquement pour les variables d'action-angle, où la variable d'action I est constante par définition.

La variable d'action est définie comme telle (Landau and Lifchitz 1988):

$$I_\alpha \equiv \frac{1}{2\pi} \oint_{\mathcal{C}_\alpha} p_\alpha \mathrm{d}q^\alpha \tag{1.2}$$

où α est une projection de l'espace des phases, p un moment conjugué, q une position et $\mathcal{C}$ une courbe fermée dans l'espace des phases. Cette équation a une interprétation simple puisqu'elle donne l'aire de la courbe $\mathcal{C}_\alpha$ à un facteur $1/2\pi$ près.

Pour un oscillateur harmonique, modèle fréquent de mouvements périodiques, d'équation

$$H = \frac{p^2}{2} + \frac{\omega^2 q^2}{2} \tag{1.3}$$

cela donne

$$I = \frac{E}{\omega} \tag{1.4}$$

où E est l'énergie cinétique et ω la pulsation du mouvement. Comme I est une constante du mouvement, cette interprétation implique une contrainte forte sur les mouvements périodiques harmoniques: le rapport de l'énergie et de la pulsation doit rester constant d'un cycle à l'autre du mouvement.

Trouver des constantes du mouvement est rendu difficile quand le système est susceptible d'évoluer dans le temps. Heureusement, la mécanique hamiltonienne a aussi une solution dans ce cas: le théorème adiabatique qui indique que, si la dépendance temporelle du système est suffisamment lente, il existe des variables qui restent approximativement constantes. Ces variables sont les variables d'actions (Landau and Lifchitz 1988).

Pour un oscillateur harmonique dont la fréquence dépend du temps $\omega = \omega(t)$, la relation (1.4) implique alors que lorsque la fréquence du mouvement augmente, l'énergie doit changer proportionnellement, de manière à garder I constant.

Dans cette thèse, nous assimilons les mouvements humains périodiques à des oscillateurs harmoniques, et nous les étudions à travers le cadre des invariants adiabatiques.

Objectifs et hypothèses

Planifier des mouvements est une tâche importante pour correctement atteindre des objectifs moteurs et s'adapter à des nouvelles situations. Cependant, il est difficile de savoir comment le système nerveux central sonde ou ignore les stratégies inintéressantes face à l'infinité de possibilités résultantes de la redondance des degrés de liberté de notre corps. En effet, dans la vie courante les individus sains sont capables de produire des commandes motrices pertinentes de manière apparemment automatique.

Pour expliquer ce phénomène, plusieurs principes sont supposément employer par le système nerveux central, tel que la minimisation du jerk, avec son propre domaine d'application et ses limites. En effet, une limite commune de ses principes est la caractérisation des mouvements périodiques ou des changements de paramètres du système au cours du temps. Dans ce contexte, nous proposons de calculer des grandeurs pertinentes : les invariants adiabatiques. Ces invariants se basent sur les lois de la physique décrites par la mécanique hamiltonienne. Ceci représente une approche purement mécanique et extra-corporelle qui est donnée *a priori* et qui ne repose sur aucune hypothèse par rapport à la biomécanique du système. L'objectif de cette thèse est d'étudier ce nouveau modèle mécanique des mouvements périodiques dans une variété de contextes expérimentaux.

Dans une première expérience, avant de sonder des environnements plus complexes, nous testons la dynamique générale de notre modèle (1.4) dans le cas de la marche, sans changement de paramètres. Par la nature générale du modèle nous faisons l'hypothèse qu'il est maintenu quelles que soient les conditions expérimentales. Pour explorer cette hypothèse nous utilisons deux conditions connues comme produisant des structures temporelles largement différentes: la marche libre et la marche sous métronome.

Dans une seconde étude de la même expérience, nous testons la capacité qu'a notre approche à modéliser une facette importante de la motricité humaine: la variabilité. En effet, nous traitons les mouvements comme étant la réalisation d'un oscillateur harmonique qui devrait être parfaitement régulier, ce qui n'est clairement pas le cas dans les mouvements humains. Des arguments récents de physique suggèrent que l'addition d'un terme perturbatif à l'hamiltonien du système est suffisant pour imiter la distribution de l'invariant adiabatique dans l'espace des phases, ce qui est assimilable à la variabilité. Nous testons cette théorie dans le cas humain.

Enfin, dans une deuxième et troisième expérience avec des protocoles relativement similaires, nous testons la capacité de notre modèle à caractériser les mouvements dans des environnements changeants dans le temps. Spécifiquement, nous avons utilisés des données expérimentales issues de sessions de centrifu-

gation et de vols paraboliques qui représentent des environnements extrêmes où la "gravité" change. Bien que le système nerveux central ne soit pas familier avec ces environnements, nous faisons l'hypothèse que notre approche mécanique est maintenue.

De manière générale, cette thèse vise à mieux comprendre les contraintes du contrôle moteur en proposant et en explorant une nouvelle manière de modéliser les mouvements volontaires périodiques humains dans des environnements susceptibles de changer au cours du temps.

Première expérimentation

Dans une première expérience (Buisseret et al. 2022), nous avons examiné le rôle des invariants adiabatiques dans le contexte de la marche humaine. En effet, la marche est un processus simultanément globalement stable et localement variable, i.e., la forme générale de la foulée reste constante pendant le mouvement, mais de petites variations apparaissent d'un pas à l'autre. La variabilité de la marche a fait l'objet de nombreuses études, cependant il existe toujours des inconnues quand à l'origine de cette stabilité globale. Dans ce contexte, les invariants adiabatiques semblent pertinents puisqu'ils définissent des quantités qui restent constantes pendant les mouvements périodiques.

Pour cette expérience, nous avons recruté vingt-cinq participants sains pour marcher pendant dix minutes à une allure confortable, avec et sans métronome indiquant la fréquence préférée de marche, une condition connue comme altérant la variabilité dans l'intervalle de foulée, comme définie par des paramètres tels que l'exposant de Hurst, la dimension fractale ou l'entropie d'échantillon, mais dont l'effet sur la stabilité n'est pas connu.

Nous avons réitéré un résultat connu: calquer sa foulée sur un métronome change la variabilité du mouvement d'autocorrélée à presque aléatoire. En revanche, l'invariant adiabatique est préservé dans les deux conditions expérimentales, rendant compte de la stabilité globale de la marche. Par conséquent, les invariants adiabatiques semblent révéler des contraintes sur la stabilité globale qui sont cachées derrière l'apparente variabilité locale de la marche.

Deuxième expérimentation

Au cours d'une deuxième expérience (Boulanger et al. 2023), nous avons examiné une nouvelle manière de modéliser la variabilité à long terme de la marche, avec une méthode basée sur l'effet du bruit sur le modèle théorique esquissé dans l'expérimentation précédente. En effet, des développements récents en mécanique hamiltonienne ont montré que des perturbations stochas-

tiques influent sur les valeurs que prennent les invariants adiabatiques qui obéissent désormais à une équation de Fokker-Planck décrivant leur distribution statistique avec une dépendance temporelle.

Comme nous le savons, il est impossible de réaliser deux fois le même exact mouvement. Il est donc attendu que la marche humaine, étudiée par le déplacement vertical du centre de masse, puisse être modélisée comme un système dynamique perturbé stochastiquement. Cela résulterait en une diffusion dans l'espace des phases, i.e., les cycles du mouvement seraient légèrement déformés d'un cycle au suivant.

Nous avons étudié cette possibilité en travaillant sur la marche de vingt-cinq participants sains marchant pendant dix minutes à vitesse spontanée. Nous avons en effet observés de la variabilité d'un cycle à l'autre résultant en une diffusion dans l'espace des phases qui est compatible avec une solution de l'équation de Fokker-Planck. Cette distribution constitue un nouvel outil pour étudier la variabilité à long terme de la foulée, et est une autre contrainte inhérente à la marche humaine. Nous avançons l'hypothèse que la forme de cette distribution statistique change avec des facteurs tels que l'âge, l'environnement ou encore des pathologies.

Troisième expérimentation

Au cours de cette troisième expérience (Boulanger et al. 2020), nous avons investigué le réel potentiel des invariants adiabatiques, à savoir leurs caractères approximativement constants quand les paramètres du système qu'ils représentent varient lentement dans le temps, ce qui est une limite typique des modèles courants du mouvement. Bien qu'il y ait plusieurs paramètres candidats à varier pendant un mouvement, l'une des quantités les plus fondamentales pour les mouvements sur Terre est la gravité. Celle-ci apparaît comme un candidat naturel puisqu'elle est incorporée par le système nerveux central pour optimiser les mouvements de manière routinière. De plus, très peu de personnes auront expérimenté avec des environnements loin de 1 g pendant des périodes de temps prolongées, ainsi étudier ce genre d'environnement permettrait de sonder la manière qu'à le système nerveux central à réagir à ces situations.

Pour ce faire, nous avons exposé six participants à deux sessions de centrifugation de manière à ce que l'accélération ressentie le long du corps varie de un à trois g. Pendant ces sessions, les participants ont réalisé des mouvements rythmiques du bras à une allure libre.

Bien que les participants n'ont jamais connu de tels environnements gravito-inertiels, nous observons maintenant une relation linéaire entre l'invariant adiabatique et l'accélération ressentie, comme attendu par la théorie adiaba-

tique. Cela met davantage en évidence que les invariants adiabatiques semblent révéler des contraintes génériques du mouvement naturellement prises en compte dans les environnements changeant avec le temps.

Quatrième expérimentation

Pour cette quatrième expérience (Boulanger et al. 2021), nous avons continué de varier des paramètres fondamentaux de l'environnement, à savoir la gravité, et sommes allés plus loin en sondant des mouvements plus complexes et le cas singulier où g = 0. Nous avons aussi sondé la capacité d'adaptation des mouvements périodiques humains à des nouveaux environnements sous contraintes, de nouveau avec une tâche de maintien de rythme signalé par un métronome.

Pour cette expérience, le protocole expérimental a été réalisé à bord d'un vol parabolique, où le pilote réalise une série de manœuvres qui expose les participants à 0, 1 et 1,8 g. Onze participants ont été recrutés pour réaliser des mouvements du bras en forme de lemniscate pendant six paraboles. Les participants ont été divisés en deux groupes, allure libre et métronome.

Le lien linéaire entre la gravité ressentie et l'invariant adiabatique est une fois de plus observé pour les deux contraintes dans la direction verticale du mouvement, et ça même dans le cas extrême g = 0. Comme attendu, l'invariant adiabatique reste constant dans la direction horizontale, là où la gravité n'agit pas. Une dynamique relevant de dérivées d'ordre supérieur apparaît dans la troisième direction, suggérant de nouveaux axes de recherche.

Conclusion

L'objectif de cette thèse a été d'introduire la robustesse du cadre de la mécanique hamiltonienne à l'étude du mouvement humain. Cela a été fait en utilisant les invariants adiabatiques pour étudier un problème courant du contrôle moteur: les mouvements périodiques dans des environnements avec des dépendances temporelles. Notre approche mécanique simple est capable de prédire le comportement observé dans ces systèmes sans devoir faire d'hypothèse sur la biomécanique de l'effecteur et ce même dans des environnements pourtant inconnus du système nerveux central, le tout en se reposant sur des principes physiques établis *a priori*.

Étant par nature exploratoire, cette thèse est ouverte et prévoit de nombreuses perspectives de recherche. Premièrement, notre modèle est basé sur l'oscillateur harmonique. Bien que ce soit un candidat naturel pour les mouvements périodiques, les mouvements humains le sont rarement. Pour représenter au mieux les mouvements réels il faudrait alors ajouter des termes

anharmoniques ou utiliser d'autres types d'oscillateurs, comme l'oscillateur de Duffing dont les mouvements horizontaux de notre expérience en vol parabolique se rapprochent. Il est intéressant de noter que l'oscillateur de Duffing peut présenter des régimes chaotiques.

De plus, des dérivées d'ordre supérieur sont parfois nécessaires pour correctement décrire et modéliser les mouvements. Malheureusement, la précision expérimentale de nos expériences ne nous a pas permis d'explorer ces questions, qui pourraient révéler de nouvelles perspectives et trouver des parallèles avec d'autres méthodes utilisant les dérivées supérieures tels que les modèles minimisant le jerk.

Par ailleurs, l'interaction de différentes caractéristiques du mouvement pourrait être étudier en changeant certaines conditions expérimentales. Par exemple, les transitions d'un environnement gravito-inertiel à un autre dans notre expérience en centrifuge sont très rapides, ce qui génère du stress. Des transitions plus lentes permettraient de sonder l'adaptation du système nerveux central sans pour autant le mettre à mal. Cela permettrait aussi de tester la théorie adiabatique qui précise que si les changements d'accélération sont suffisamment lents, l'invariant adiabatique du système resterait complètement constant. Néanmoins, le système nerveux central cherche constamment à adapter les mouvements en fonction des retours qu'il obtient de son environnement pour être plus efficace, et pourrait donc naturellement changer de stratégie pendant ces transitions. Les échelles de temps de ces interactions sont inconnues.

Ces perspectives ne représentent qu'un petit nombre des directions de recherches possibles issues de cette thèse et nous invitons la communauté du contrôle moteur à se saisir de ces concepts et de les explorer.

Chapter 2

Introduction

Motion, and in particular locomotion, is one of the hallmark of life on Earth. Every animal is motile for at least part of its life, and the vast majority is motile throughout it; and humans are no exception. Whether it is to feed, to reproduce, or to discover and conquer new environments, motility has shaped the very evolutionary tree we stand on.

The nature of volitional motion is rich and complex. What appears automatic, innocuous and trivial to us is in fact the very opposite. For example, a common swift hunting for insects appears to glide effortlessly across the sky, but in reality it has to integrate complex feedback from its environment like wind speed and direction in close to real time to keep precise control of its wing angle. Its central nervous system has a deep understanding of physics to predict the trajectory of the insect and its own all the while flying with peak speeds at over 100 km/h. The swift also breeds and sleeps while flying (Hedenström et al. 2016).

Even the unconscious act of level walking in healthy adults includes changes in direction and speed, variability across a basic periodic pattern, multiple muscles and joints, complex neural commands and structures (Rose and Gamble 2006). This is further complicated by factors like age, pathology, direct environment, etc.

All in all, what appears as a simple or complex motion is inherently constrained by the body, in both a physiological and neurological sense. Indeed, for the walking example, it necessarily involves many combinations of flexions, extensions and rotations of the three main leg joints, controlled by contractions of tens of muscles. This also involves different neural structures, with command emanating from the central nervous system, and central pattern generators (their structure and role in human beings is still debated (Minassian et al. 2017).) This makes the study of motion a particularly complex endeavor as the number of variables to analyze or isolate (for those

which can be isolated) is very large. This is known as Bernstein's degree of freedom problem (Bernstein 1967, ch. 3.5). Nevertheless, even through this plethora of combinations and the size of configuration space, the nervous system automatically chooses and adjusts to the best strategy (by some definition of best, as we discuss in section 3.4.2) in real time (Rose and Gamble 2006, ch. 5).

In addition to these biomechanical considerations, motion is constrained by its direct environment. Indeed walking on grass, concrete or asphalt is slightly different. This is before taking into account things like treading on water or more exotic environments like centrifuges, the International Space Station or the Moon. The central nervous system though, having evolved with many of those constraints, can efficiently integrate and even take advantage of them. For example, gravity –one of the most fundamental constraint on motion– is routinely taken into account when performing vertical motion where it helps accelerate downward movements and decelerate upward ones, giving rise to asymmetric speed profiles (Pozzo et al. 1998). The central nervous system is also not passive during motion, but can integrate sensory feedback –be it by sight, sound, haptics, proprioception, etc.– to correct for perceived errors, whether explicitly or implicitly. This is particularly relevant to periodic motion where feedback from one cycle of motion can be applied to the next. While obvious, it is also important to recall that the human body, or any animal for that matter, is fundamentally a physical system and therefore obeys the laws of physics. As with the swift example, the brain is thought to have an intuitive understanding of these laws (Zbären et al. 2023).

Finally, task-specific requirements also constrain motion, e.g. walking while being on the phone is cognitively demanding and therefore affects motion (Sarvestan et al. 2022), a task might require high speed or high precision, resulting in a well known speed-accuracy trade-off (Fitts 1954).

Nevertheless, through the sheer complexity and interconnectedness of it all, motion is readily available to us, and the central nervous system automatically picks optimal, energy-minimizing, strategies in real time. This fact leads some neuroscientists to argue that movement production is the reason for the existence of brains in the first place (Wolpert 2011).

Over the years, many models of human motion have been put forward to try and solve the different problems cited above. Each with its successes and drawbacks. Modern approaches rely on minimizing a certain parameter or functional of a system representing the task at hand. For example, in the context of reaching tasks, minimum-jerk approaches have been very successful at modeling non-periodic human motion (Flash and Hogan 1985). This technique is based on the minimization of the magnitude of the jerk, i.e., the

derivative of acceleration: $\dot{a} = \dddot{x}$. It can be interpreted as maximizing the smoothness of motion. In Lagrangian mechanics, this would be formulated as the minimizing of the action

$$S = \int_{t_i}^{t_f} \dddot{x}^2 \quad dt. \tag{2.1}$$

Unfortunately, this type of principle does not give rise to periodic solutions, and is therefore unable to model locomotion. Another limiting factor is the need for precise and therefore expensive instrumentation as differentiating numerically can lead to errors, as we discuss later in chapter 8.

Another natural candidate for minimization, from a biological and physical point of view, is energy. Indeed, it stands to reason that reducing metabolic costs is an evolutionary advantage; it is also common for physical systems to tend to their lowest energy state. This has been applied to periodic motion, such as walking. It also appears to be a guiding principle of locomotion, as a change in minimum due to exterior forces results in a change of gait parameters (Abram et al. 2019). Nevertheless, this also has limitations as energy conservation principles are no longer guaranteed when time-dependent external forces act on a system during motion.

In this work, we propose a new general mechanistic approach based on Hamiltonian mechanics to model motion in the case of a (quasi-)periodic movement, all the while allowing for time-dependent perturbations, so that mechanical energy is not conserved. One motivation for this approach relies on a point made earlier: as a mechanical system the body necessarily obeys the laws of physics. The robust framework of Hamiltonian mechanics can unearth some of the physical constraints inherent in motion in a model-independent way and guide towards a new description and a more powerful analysis of motion.

Hamiltonian mechanics as a framework is based on the coordinates q and momenta p, which we identify as the position x and speed v in this work, and the geometric properties of phase-space, that is the plane (q, p). While most approaches are based on the study of $x(t)$, Hamiltonian mechanics proposes to describe periodic motion without an explicit time dependency. This might lead to new perspectives and insights as to the nature of human motion.

One tool particularly useful in the context of Hamiltonian mechanics are adiabatic invariants I (Landau and Lifchitz 1988). They can be defined in multiple ways, but their most important property is that they stay approximately constant when changes to the physical system they represent is slow. Geometrically, adiabatic invariants I for periodic systems represent the normalized area enclosed by the curve that the system draws in phase-space

(q, p). We discuss their origins and give a more complete overview of the theoretical aspects of the thesis in chapter 3.

This work also relies on experimental data obtained in various studies. Greater experimental context is given in chapter 3.

After setting the theoretical and experimental background, we discuss the hypotheses and goals of this thesis in chapter 4.

In chapter 5, based on our publication (Buisseret et al. 2022), we probe the use of adiabatic invariants in the most common of periodic motion: walking. Indeed, a definition of the adiabatic invariant reveal a strong constraint on periodic motion: without external perturbations, the ratio of average kinetic energy to the frequency of a cycle remains constant cycle to cycle, i.e.

$$I = \frac{\bar{E}_k}{\pi f} = cst. \tag{2.2}$$

This is indeed what we observe experimentally, even with external factors known to drastically alter movement variability such as metronome keeping.

In reality, motion is noisy and it is impossible to perform the exact same movement twice. This implies stochastic perturbations that impact modelization: there is diffusion in phase-space (Bazzani et al. 1994a). This phenomenon is investigated through statistical mechanics tools such as Fokker-Planck equations, in chapter 6, recounting our paper (Boulanger et al. 2023).

Then, we use adiabatic invariants to their full potential by varying parameters during motion. Adiabatic theory is still adapted to this kind of environment: the area of phase space now depends linearly in the perturbed variable. One such variable, also the most fundamental parameter on Earth, is gravity. We use data from two "gravity-changing" experiments to probe its usefulness in chapter 7, published in (Boulanger et al. 2020), with simple harmonic motion. In chapter 8, published as (Boulanger et al. 2021), we study the limit $g = 0$ case and more complex motion.

To summarize, the plan of the thesis is as follows: in chapter 3, we lay out the theoretical aspects of the physics and motor control concepts needed and we detail the different experimentations that were carried out or used. We explore the use of adiabatic invariants in human gait in chapters 5 and 6; and in more challenging environments in chapters 7 and 8. Finally, we give perspectives and conclude in 9.

At the beginning of each experimental chapter, we give a brief summary of the analyses performed and results obtained.

Chapter 3

Theoretical background

3.1 Action-angle variables

In physics, there exist many ways to describe a given movement: Newtonian, Lagrangian or Hamiltonian mechanics. Each formulation has its own peculiarities and interests (Jose and Saletan 1998).

Newtonian mechanics is of particular historic interest as it is the first physical theory to use the concept of derivatives, as such it was the foundation of classical mechanics and of the theories that followed. It relies on Newton's laws of motion making it easy to use.

In turn, Lagrangian mechanics rely on the principle of least action, i.e., the trajectories of motion are stationary points (minima, maxima, or saddle points) of the system's action functional, an action being a quantity of a system, like energy or momentum, with SI units $\mathrm{kg{\cdot}m^2{\cdot}s^{-1}}$. The action functional is

$$S[q(t)] = \int_{t_1}^{t_2} L(q(t), \dot{q}(t), t)dt, \tag{3.1}$$

where q is the generalized coordinate, $\dot{q} = dq/dt$ its associated velocity and L the Lagrangian of the system, that is a function that contains all the relevant information on a system and the forces acting on it, usually the difference between kinetic and potential energy. In essence, for a system with Lagrangian L, among all possible trajectories $q(t)$ between points $q_1 = q(t_1)$ and $q_2 = q(t_2)$, the trajectory that the system actually follows is one that minimizes, maximizes or saddles the action S, this is summarized in figure (3.1).

The stationary points of equation (3.1) are the trajectories q that satisfy

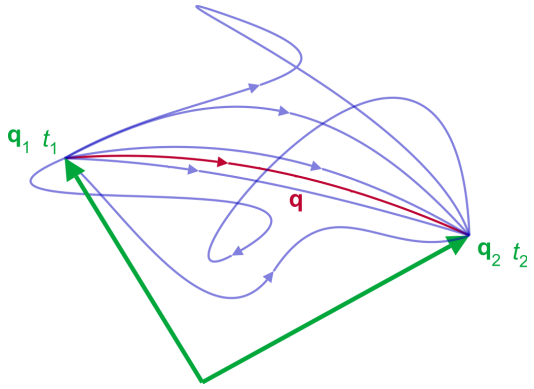

Figure 3.1: Representation of the least action principle. Blue lines represent possible trajectories, the actual trajectory is a stationary point of (3.1) represented in red. *Public domain by Maschen retrieved from* `https://commons.wikimedia.org/wiki/File:Least_action_principle.svg` *on 29/06/2023.*

the Euler-Lagrange equation:

$$\frac{\partial L}{\partial q} - \frac{\mathrm{d}}{\mathrm{d}t}\frac{\partial L}{\partial \dot{q}} = 0. \tag{3.2}$$

Although the Lagrangian formulation of mechanics has shown great success with results of crucial importance such as Noether's theorem, or the fact that it is the basis for the standard model of particle physics, it is not always the easiest or best suited set of techniques to solve physical problems. Indeed, Lagrange's formalism relies on the computation of the generalized coordinates q and velocities $\dot{q}$, and while the first derivatives of q are simple, derivatives of $\dot{q}$ are present in the Euler-Lagrange equation which can make computations difficult.

Hamiltonian mechanics avoids this problem by proposing a first-order reformulation of a system's dynamics based on momenta

$$p_\alpha = \frac{\partial L}{\partial \dot{q^\alpha}} \tag{3.3}$$

rather than generalized velocities $\dot{q}$. Here, α specifies a projection of phase space, i.e. if motion takes place in the space (x, y, z), α refers to one of those direction. This allows for a more geometric interpretations of dynamics since motion is now studied in what is referred to as phase space, the space (q, p), in our case we can assimilate it to (x, v_x). In this space, every degree of freedom and every state of a dynamical system are uniquely represented. It

is also a departure from "classical" ways to study motion as there is now no direct time dependence. An illustration of phase space for a pendulum is given in figure (3.2).

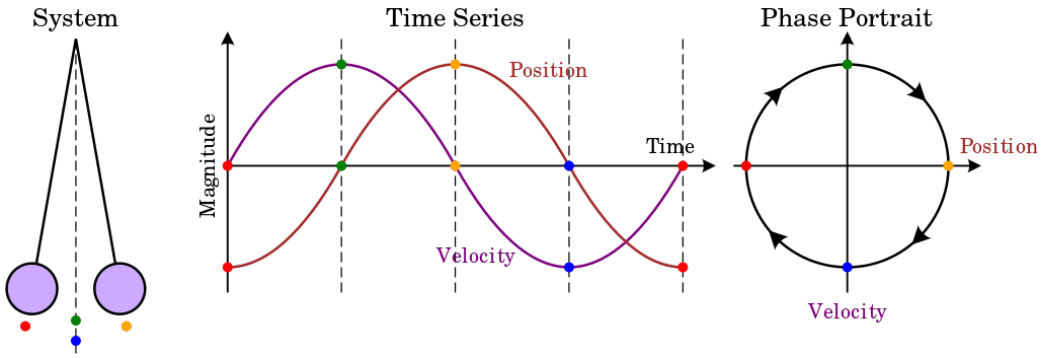

Figure 3.2: Typical time series and phase space for a pendulum. Different states of the system are highlighted with colored dots. *CC BY-SA 4.0 by Krishnavedala retrieved from* `https://commons.wikimedia.org/wiki/File:Pendulum_phase_portrait_illustration.svg` *on 29/06/2023.*

Another benefit is found in easier computations as the first derivatives of both p and q can be derived via Hamilton's canonical equations:

$$\dot{q^\alpha} = \frac{\partial H}{\partial p_\alpha}, \tag{3.4}$$

$$\dot{p_\alpha} = -\frac{\partial H}{\partial q^\alpha}. \tag{3.5}$$

where H is the Hamiltonian of the system, i.e. a function that, given initial conditions $(q_0^\alpha, p_{\alpha,0})$, describes the evolution of the system. The interested reader will find more details about Hamiltonian mechanics in (ch.8 Goldstein et al. 2002; Landau and Lifchitz 1988). Formulating a problem in terms of Hamilton's canonical equations makes it usually easier to solve as they are first order differential equations, a type of equation for which many techniques were developed both analytically and numerically (Hairer et al. 1993).

Even this formulation of mechanics cannot lead to analytical solutions for the equations of motion of most dynamical systems. However, there are ways to obtain qualitative information about even the most complex of systems.

Indeed, one advantage of Hamilton's formulation of mechanics is that it offers a lot of freedom in performing changes of (q^α, p_α) coordinates that do not alter the form of Hamilton's canonical equations. The transforma-

tions that preserve the form of the canonical equations are called canonical transformations.

A common idea is then to perform a canonical transformation from an open domain of phase space (q^α, p_α) to (ϕ^α, I_α) where the local variable I_α is a constant of motion (with dimensions of an action, i.e., energy $\times$ time) and ϕ is called an angle variable. Therefore, the new phase space variables are called action-angle variables (Landau and Lifchitz 1988). While this type of transformation is not strictly always possible to carry out, it can be done in the limited case of periodic motion we study. The usefulness of such variables is that, for some class of systems:

$$H(q,p) \xrightarrow{\text{C.T.}} H'(I) = K \tag{3.6}$$

Here, C.T. refers to any kind of canonical transformation. This transformation defines a new Hamiltonian K that is dependent on the constants of motion by virtue of Hamilton's canonical equations.

$$\dot{\phi} = \frac{\partial H'}{\partial I}, \quad \dot{I} = -\frac{\partial H'}{\partial \phi} = 0. \tag{3.7}$$

In this new set of coordinates, I is a constant of motion and K is a constant that can be set to zero with no loss of generality, we give details below.

For an integrable system with one degree of freedom, if the motion is bounded in phase space then it is restricted to closed curves, which are topologically similar to circles meaning that they can be continuously distorted into one. Similarly, for a system with two degrees of freedom closed curves appear in both (ϕ^1, I_1) and (ϕ^2, I_2). Therefore, motion takes place on the product of two circles, a torus. Different sets of variables (ϕ, I) will results in different non-intersecting closed curves and thus different non-intersecting tori.

While this makes for a neat visualization of motion, it can be quite a hard task to guess the coordinates for which a system's dynamics can be expressed on such tori. Action-angle variables (I, ϕ) are new coordinates that directly specify both the specific curves and the point on the curves on which motion is performed.

We can write the generating function of this canonical transformation in terms of q^α and I_α since I_α specifies the curve in the α projection of phase space and q^α gives, up to the sign of p_α, the point on this curve. We set

$\tilde{W}(q^\alpha, I_\alpha)$ a second type generating function, that is

$$p_\alpha = \frac{\partial \tilde{W}}{\partial q^\alpha}, \tag{3.8}$$

$$\phi^\alpha = \frac{\partial \tilde{W}}{\partial I_\alpha}. \tag{3.9}$$

Because we want the variable ϕ^α to describe a point on a closed curve, we assimilate it to an angle and we normalize it as such

$$\oint_{\mathcal{C}_\alpha} \mathrm{d}\phi^\alpha = 2\pi. \tag{3.10}$$

With the previous definitions:

$$2\pi = \oint_{\mathcal{C}_\alpha} \mathrm{d}\phi^\alpha, \tag{3.11}$$

$$= \oint_{\mathcal{C}_\alpha} \frac{\partial^2 \tilde{W}}{\partial q^\alpha \partial I_\alpha} \mathrm{d}q^\alpha, \tag{3.12}$$

$$= \frac{\partial}{\partial I_\alpha} \oint_{\mathcal{C}_\alpha} \frac{\partial \tilde{W}}{\partial q^\alpha} \mathrm{d}q^\alpha, \tag{3.13}$$

$$= \frac{\partial}{\partial I_\alpha} \oint_{\mathcal{C}_\alpha} p_\alpha \mathrm{d}q^\alpha. \tag{3.14}$$

This relation defines the action variable (Landau and Lifchitz 1988):

$$I_\alpha \equiv \frac{1}{2\pi} \oint_{\mathcal{C}_\alpha} p_\alpha \mathrm{d}q^\alpha. \tag{3.15}$$

which equals the area enclosed in the curves $\mathcal{C}_\alpha$, up to a factor $1/2\pi$.

Because the action variable I specifies an invariant torus, it itself is invariant. Therefore,

$$\dot{I}_\alpha = -\frac{\partial H}{\partial \phi^\alpha} = 0 \tag{3.16}$$

and in the new coordinates (ϕ, I) the Hamiltonian is only a function of the action variable I.

The other canonical equation reads

$$\dot{\phi^\alpha} = \frac{\partial H}{\partial I_\alpha}. \tag{3.17}$$

Because the I are constants of motion, this is

$$\phi^\alpha(t) = \frac{\partial H}{\partial I_\alpha} t + \delta. \tag{3.18}$$

With the normalization of ϕ^α and its interpretation, $\partial H/\partial I_\alpha = \omega^\alpha$ are constants representing the 2π times the frequencies at which the curve $\mathcal{C}_\alpha$ is passed through. ϕ^α progresses linearly in time and δ is the initial angle, at $t = 0$.

3.2 Adiabatic theory

An important task in order to gain insight on the dynamics of a given physical system is to find the constants of motion within that system. As we have just shown, there are systematic ways to find these constants through canonical transformations. Unfortunately, it is usually not trivial for Hamiltonians without any time dependency as we will show in the next section, and is even harder for time dependent systems. This problem is partly solved by adiabatic theory which states that when the time dependence within the Hamiltonian of the system is sufficiently slow, as parameters change so does the action variable I. In that case it is called an adiabatic invariant. In some cases, I even stays constant (Jose and Saletan 1998).

Let $H(q, p, \lambda)$ be a completely integrable Hamiltonian. Here, $\lambda = \lambda(t)$ is the parameter through which the time-dependency is borne. In our thesis, we make "gravity" time-dependent so we can assimilate $g(t) = \lambda(t)$. In general, $\lambda(t)$ could represent time-dependent muscle tension or any other physiological parameter given that human motion is inherently variable with time. Of course, if no change in the parameter $\lambda(t)$ occur then H does not change with time. This is the case for overground walking where $\lambda(t) = g$ stays constant, hence I stays constant.

The action-angle variables associated with the system will depend on the parameter λ:

$$I(q, p, \lambda)$$
$$\phi(q, p, \lambda).$$

To probe how this new time dependence impacts the Hamiltonian of the system, we can compute

$$\dot{H} = \frac{\partial H}{\partial q}\dot{q} + \frac{\partial H}{\partial p}\dot{p} + \frac{\partial H}{\partial \lambda}\dot{\lambda}. \tag{3.19}$$

Hamilton's canonical equations (3.4 and 3.5) cancel out the first terms meaning that it is indeed λ that carry the change in the Hamiltonian, and if we are interested in the change in H within a given time ΔT, we are left with

$$\Delta H = \int_0^{\Delta T} \frac{\partial H}{\partial \lambda}\dot{\lambda}\mathrm{d}t. \tag{3.20}$$

As previously stated, the adiabatic theory only works for slow rate of change in the parameter λ, we therefore assume that $\dot{\lambda}$ is constant in the integration interval and can be written as

$$\dot{\lambda} \simeq \frac{\Delta\lambda}{\Delta T}, \tag{3.21}$$

injecting in 3.20, we have

$$\Delta H = \frac{\Delta\lambda}{\Delta T}\int_0^{\Delta T} \frac{\partial H}{\partial\lambda}\mathrm{d}t. \tag{3.22}$$

For I to be an adiabatic invariant under a slow change of parameter, or

$$I(\Delta T) \simeq I(0), \tag{3.23}$$

we need to show that the areas of phase space at $t = 0$ and $t = \Delta T$ are equal. Since $E = H(q, p, \lambda(t))$ it is required that ΔH is sufficiently small, that is obtained under the adiabatic condition:

$$\tau\frac{\Delta\lambda}{\Delta T} \ll \lambda. \tag{3.24}$$

where τ is the period of motion. This condition means that the change of parameter have to be small compared to the typical cycle of motion.

For quantitative arguments as to the exact change in I incurred by changes in λ in different physical systems we refer the reader to (ch.12.3 Goldstein et al. 2002)

Adiabatic invariants have a wide range of applications. They are used in thermodynamics, plasma physics, classical dynamics and have been studied during the early Solvay Conferences where they were the basis for early quantum theories (Pérez 2008).

In the next section, we show two derivations for the adiabatic invariants of two common systems in physics.

3.3 Examples

3.3.1 Harmonic oscillator

A common example of an adiabatic system is a weight experiencing a force proportional to its displacment, i.e., a mass on a spring. In mechanics this is called a harmonic oscillator. The Hamiltonian for such a system is (Landau and Lifchitz 1988):

$$H = \frac{p^2}{2} + \frac{\omega^2 q^2}{2}. \tag{3.25}$$

With the canonical equations, we find

$$q = \sqrt{\frac{2E}{\omega^2}} \sin(\omega t) \tag{3.26}$$

$$p = \sqrt{2E} \cos(\omega t) \tag{3.27}$$

As defined in 3.15, the action variable I can be computed for this system:

$$I = \oint p dq \tag{3.28}$$

by substituting p and q, we find:

$$I = \frac{2E}{\omega} \int_0^{2\pi} \cos^2 \theta d\theta = \frac{2\pi E}{\omega} \tag{3.29}$$

In terms of frequency, this is:

$$I = \frac{E}{f}. \tag{3.30}$$

In this thesis, we assume that basic periodic motion can be assimilated to harmonic oscillations and we do so in every experiment. It is specifically this property of harmonic motion that we study in this work. Without external perturbations this is a constant of motion, linking the energy and frequency of harmonic motion.

In reality, an harmonic oscillator is a small-angle approximation of the planar pendulum, an analytically more complicated case. Fortunately, even for angles up to 23°, the difference in period is less than 1% (Lima and Arun 2006), a seemingly reasonable error in the context of motor control experiments. Nevertheless, we show the computation for the action variable in the case of the pendulum in the next section for completeness.

As discussed in the previous section, the real strength of the action variables are their capacity to stay (approximately) constant with regards to slow external changes to the system. Let us explore that property by making ω explicitly dependent on time. In that case, the equation of motion for I becomes (ch. 12.5 Goldstein et al. 2002):

$$\dot{I} = -\frac{\dot{\omega}}{\omega} I \cos(4\pi\omega_0). \tag{3.31}$$

ω_0 representing the pulsation for the unperturbed system. As previously stated, adiabatic invariance is only observed for slow and small changes, this is the case if we assume

$$\frac{\dot{\omega}}{\omega} = \epsilon \tag{3.32}$$

ϵ being short-hand for a small positive parameter, i.e., $\epsilon \ll 1$. This is observed for frequencies of the form (ch. 12.5 Goldstein et al. 2002):

$$\omega \approx \omega_0(1 + \epsilon t). \tag{3.33}$$

In this thesis, we assume frequencies of this type when parameters, like gravity, change. We explore this phenomenon in more detail in chapters (7) and (8).

Note that adiabatic invriance means that as I stays approximately constant, a change in frequency must now results in a corresponding change in the energy, to keep their ratio constant.

3.3.2 Pendulum

Generally, the adiabatic invariant of a system is not that easy to find. In this section we compute the action variable for a more complicated system, the planar frictionless pendulum. This system is drawn in figure 3.3. In this section, m refers to the mass of the bob, g to the gravitational acceleration, l to the length of the pendulum's arm and θ to the angle of the pendulum. This is an original derivation.

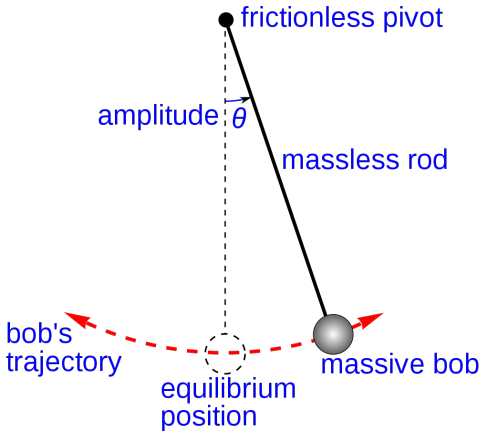

Figure 3.3: Schematic of a simple pendulum oscillation. *Public domain by Chetvorno retrieved from* `https://commons.wikimedia.org/wiki/File:Simple_gravity_pendulum.svg` *on 29/06/2023.*

Such a system has for Lagrangian

$$L = \frac{m}{2} l^2 \dot{\theta}^2 + mgl\cos\theta, \tag{3.34}$$

and energy

$$E = \frac{m}{2} l^2 \dot{\theta}^2 - mgl\cos\theta. \tag{3.35}$$

Because the energy is conserved we have

$$E = E_0 = -mglcos\theta_0. \tag{3.36}$$

where θ_0 denotes the maximum angle, if the pendulum is initially released with no velocity it is also the initial angle.

To compute the action variable, we need to obtain expressions for p and q. Clearly in this system $q = \theta$ and,

$$p = \frac{\partial L}{\partial \dot{\theta}} = ml^2\dot{\theta}. \tag{3.37}$$

We do not know $\dot{\theta}$, so we invert the previous equation to get

$$\dot{\theta}^2 = \frac{p^2}{m^2 l^4} \tag{3.38}$$

to inject in E

$$E = \frac{p^2}{2ml^2} - mgl\cos\theta. \tag{3.39}$$

This allows us to get an expression of p with no dependency in $\dot{\theta}$:

$$p^2 = 2ml^2(E + mgl\cos\theta) = 2m^2 l^3 g(\cos\theta - \cos\theta_0). \tag{3.40}$$

With trigonometry rules, this can be rewritten as

$$p^2 = 4m^2 l^3 g(\sin^2\frac{\theta_0}{2} - \sin^2\frac{\theta}{2}). \tag{3.41}$$

We set

$$k^2 = \sin^2\frac{\theta_0}{2} \quad \text{and,} \quad n^2 = \frac{g}{l} \tag{3.42}$$

for convenience.

In our case,

$$I = \frac{1}{2\pi}\oint p\mathrm{d}q = \frac{4}{2\pi}\int_0^{\theta_0} p\mathrm{d}\theta \tag{3.43}$$

since to complete an entire cycle of motion the pendulum m has to go from $\theta = \theta_0$ to $\theta = 0$, from 0 to $-\theta_0$, from $-\theta_0$ to 0 and back to θ_0.

We can finally compute the action variable

$$I = \frac{4}{2\pi}\int_0^{\theta_0} p\mathrm{d}\theta = \frac{8}{2\pi} l^2 mn \int_0^{\theta_0} \sqrt{k^2 - \sin^2\frac{\theta}{2}}\mathrm{d}\theta. \tag{3.44}$$

To find this integral we set

$$\sin\frac{\theta}{2} = k\sin\varphi, \quad \varphi \in \mathbb{R}. \tag{3.45}$$

Simplifying,

$$k^2 - \sin^2\frac{\theta}{2} = k^2\left(1 - \sin^2\varphi\right) = k^2\cos^2\varphi. \tag{3.46}$$

We change the variable of integration to φ. The Jacobian of the transformation is

$$\frac{1}{2}\cos\frac{\theta}{2}\mathrm{d}\theta = k\cos\varphi\mathrm{d}\varphi. \tag{3.47}$$

The limit of integration becomes

$$\varphi_0 = \frac{\pi}{2} \tag{3.48}$$

leaving us with a new integral:

$$I = \frac{16}{2\pi}l^2mn\int_0^{\pi/2}\frac{k^2\cos^2\varphi}{\cos\frac{\varphi}{2}}\mathrm{d}\varphi. \tag{3.49}$$

With the usual trigonometric formula we find

$$k^2\cos^2\varphi = k^2 - k^2\sin^2\varphi. \tag{3.50}$$

The action angle for a pendulum is then

$$I = \frac{8}{2\pi}l^2mn\left[2\int_0^{\pi/2}\frac{k^2-1}{\sqrt{1-k^2\sin^2\varphi}}\mathrm{d}\varphi + 2\int_0^{\pi/2}\sqrt{1-k^2\sin^2\varphi}\mathrm{d}\varphi\right] \tag{3.51}$$

We recognize the well-known complete elliptic integral of the first and second kinds (Lozier et al. 2010):

$$K(k) = \int_0^{\pi/2}\frac{\mathrm{d}\varphi}{\sqrt{1-k^2\sin^2\varphi}}$$
$$E(k) = \int_0^{\pi/2}\sqrt{1-k^2\sin^2\varphi}\mathrm{d}\varphi$$

With these simplified notations

$$I = \frac{16}{2\pi}ml^2n\left([k^2-1]K(k) + E(k)\right). \tag{3.52}$$

This can be somewhat simplified again. First by noting the fact that the period of oscillation is

$$T = \frac{4}{n}K(k), \tag{3.53}$$

and remembering

$$E = -mgl\cos\theta_0, \tag{3.54}$$

one finds

$$I = \frac{4}{\pi}mgl\left(2E(k) - (cos\theta_0 + 1)\frac{nT}{4}\right), \tag{3.55}$$

$$= -\frac{m}{\pi}gl(1 + cos\theta_0)T + \frac{8}{\pi}mnl^2E(k), \tag{3.56}$$

$$= -\frac{m}{\pi}gl + \frac{ET}{\pi} + \frac{8}{\pi}mnl^2E(k). \tag{3.57}$$

As we have reviewed,

$$\frac{\partial(2\pi I)}{\partial E} = T. \tag{3.58}$$

From naive derivation of (3.57) it seems that

$$\frac{\partial(2\pi I)}{\partial E} = 2T. \tag{3.59}$$

This simply means that a dependency in E is hidden in the $E(k)$ term.

The dependency can be found using a property of complete elliptic integral, namely

$$E(k) = (1 - k^2)\left[k\frac{\mathrm{d}K}{\mathrm{d}k} + K(k)\right]. \tag{3.60}$$

Taking an earlier definition, we have

$$2\pi I = 16mnl^2(1 - k^2)k\frac{\mathrm{d}K}{\mathrm{d}k}. \tag{3.61}$$

With another elliptic integral property (Lozier et al. 2010),

$$\frac{\mathrm{d}}{\mathrm{d}k}\left[k(1 - k^2)\frac{\mathrm{d}K}{\mathrm{d}k}\right] = kK, \tag{3.62}$$

we have

$$\begin{aligned}\frac{\mathrm{d}(2\pi I)}{\mathrm{d}k} &= 16mnl^2kK(k)\\ &= 4mglkT,\end{aligned}$$

or

$$T = \frac{1}{4mgl}\frac{1}{k}\frac{\mathrm{d}(2\pi I)}{\mathrm{d}k}. \tag{3.63}$$

Furthermore,

$$\begin{aligned}\frac{\mathrm{d}(2\pi I)}{\mathrm{d}E} &= \frac{\mathrm{d}(2\pi I)}{\mathrm{d}(mgl[2k^2-1])} \\ &= \frac{\mathrm{d}k}{\mathrm{d}(mgl[2k^2-1])}\frac{\mathrm{d}(2\pi I)}{\mathrm{d}k} \\ &= \frac{1}{4mgl}\frac{1}{k}\frac{\mathrm{d}(2\pi I)}{\mathrm{d}k}.\end{aligned}$$

We finally find that

$$\frac{\mathrm{d}(2\pi I)}{\mathrm{d}E} = T, \tag{3.64}$$

which is a similar expression to the one found for the harmonic oscillator.

Here, we computed the action variable for a system with no time dependency, in this case $I(t) = I$ is trivially an adiabatic invariant. However, for a slow enough change of parameter, for example slowly lengthening the pendulum arm, motion would have to change to ensure that the derivative of the first order complete elliptic integral counteracts the change of arm length.

As seen in this section, even for a relatively complicated system the action variable and its property allow for a universal method to probe the relationships between parameters of a problem, revealing the strength of this approach.

3.4 Motor Control

In everyday life, all humans are led to perform voluntary motion, and motion is readily available to us, even unconsciously. Nevertheless, voluntary motion must be planned: by its very nature it refers to intentional, planned movements in pursuit of a goal.

For healthy individuals, catching a ball is a simple task, but that apparent simplicity is ultimately the result of a complex series of interactions between different bodily structures such as muscles, peripheral nerves and the central nervous system. This voluntary action also necessitates multiple steps. For example, the position of the ball in the air, and also relative to the body is perceived by different sensory stimuli (e.g. vision, proprioception, etc). The mass and shape of the ball must also be estimated in order to correctly predict the stance required to successfully execute the task, i.e. catching it.

The required nervous inputs to prepare that stance must then be sent to the relevant muscle groups. This is not performed instantaneously as there are delays at every one of those steps, whether it is the time it takes to receive sensory information from the different sensory structures, to process that information, or simply to send it to the next structure in the chain. Nevertheless, even through those inherent delays, humans can perform precise motion, like catching a ball, which requires tight timings. To overcome this, the central nervous system constantly tries to predict and anticipate events all around us (Rosenbaum 2009).

To plan and predict motion, the central nervous system must be able to simulate the responses from the body and from the environment that would results from said motion. The dynamics from the body and the environment are also in constant evolution, in mechanical terms: the Hamiltonian describing one individual's movement may be time-dependent, either because of individual variability or external changes. This results in errors –be it because of variability or poor planning– around the motion actually performed, that must be compared to the predicted motion in order to correct the system's behavior and update the models involved, if needed. Before generating any voluntary motion, the central nervous system has to go through these different steps. It first plans a motor command and simulates its effects, and then executes the command, and possibly corrects it. This is done through what are called internal models.

3.4.1 Internal models

An internal model is a process that simulates the input and/or output of the motor apparatus, through their representation of the body, their environment, etc (Kawato 1999).

There exists two main types of internal models: inverse models and forward models (Kawato 1999).

The simplest model, the inverse model, generates the motor command with regards to the current state of the system and the desired state. In the ball-catching example, this means that the central nervous system takes into account two things: first, the current state of the individual and of the ball (their positions and trajectories, for example) and second, the desired state i.e., the ball is caught, to generate the appropriate motor command.

The forward model is different as it predicts the consequences of the motor command at the same time that the command is executed. Any discrepancy between the executed action and its prediction is sent to the central nervous system, to correct and adapt the motor command. In our example, this means that if a gust of wind blows the ball off course, the motor command

is no longer relevant to the task, and the forward model constantly accruing feedback sees this discrepancy and modifies the motor command to account for the perturbation. This is illustrated in figure 3.4.

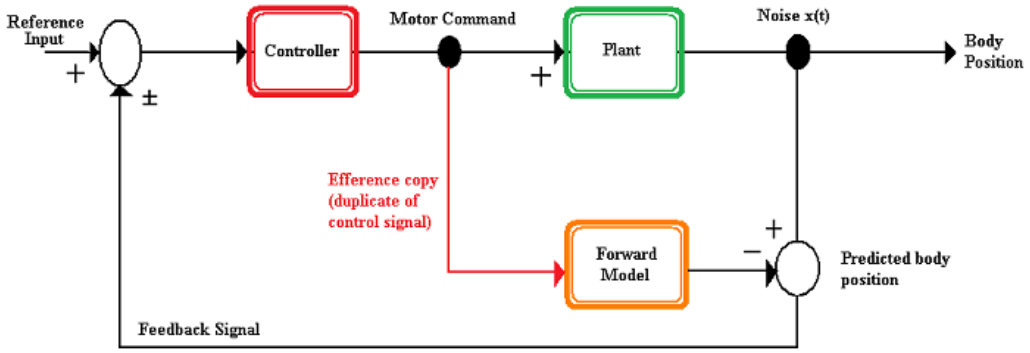

Figure 3.4: Schematic modelization of an internal model. *CC SA 3.0 by Easportz retrieved from* `https://commons.wikimedia.org/wiki/File:Basic_Internal_Model.png` *on 29/06/2023.*

These internal models, and their prediction and feedback mechanisms make our movements particularly adaptable as we can guess properties of our environment and predict optimal strategies, even when faced with (relatively) new contexts as we can correct motion in (near) real time.

The training of our internal models happens through exploring multiple types of environments, but also through repetition. The experience that comes from repeating a movement gives rise to adaptability and optimizations, in terms of speed, both of execution and reaction (Ariani et al. 2020), precision (Gentili et al. 2006), cost of treating relevant information (Fisk and Schneider 1984) and overall energetic costs, for example. These optimizations are particularly relevant in our framework as they show that the central nervous system possesses an intuitive understanding of the laws of physics, as we discuss in the next sections. The feedback also occurs through many different channels (sight, proprioception, discussed below). The redundant information is necessary for the central nervous system to have a robust representation of the environment.

3.4.2 Optimal control

While these internal representations of the environment, motion and their consequences represent a complex process, another issue appears to the central nervous system whenever motion is present: the human body possesses a

very large number of degrees of freedom. Indeed, even a simple arm motion, like grabbing a glass, involves multiple muscle groups and joints, and can be done via different activation levels and an infinite number of trajectories. This is Bernstein degrees of freedom problem (Bernstein 1967). In Hamiltonian mechanics, phase-space contains all the degrees of freedom (q^α, p_α) of a system, as such it appears to be the natural theoretical domain in which to study motor control. In that context, Bernstein's problem could be reformulated as follows: the optimal motor strategy chosen by an individual is contained in a subspace of the total phase-space.

Nevertheless, when performing motion the central nervous system seems to quickly and automatically pick one specific motor command. It seems impossible that the central nervous system would try to predict and treat the information from an infinite number of possibilities and it can reasonably be argued that it would rely on physical and other overarching principles to reduce the number of configurations to explore and produce motion. In the next three sections we explicit some of those principles.

Speed-accuracy trade-off

The speed-accuracy trade-off is a fundamental property of human movement coordination. It essentially is the observation that the faster we move the less accurate we are, and vice versa. Movements being therefore characterized by a balance between speed and accuracy.

The trade-off has been modeled by Fitts's law in (Fitts 1954):

$$MT = a + b \log_2 \left(\frac{2D}{W} \right) \tag{3.65}$$

where MT stands for movement time, a and b are constants, D the distance between starting point and target, and W the width of the target which can be interpreted as error tolerance. In that case, a wider target and thus a lesser needed accuracy leads to a faster movement time.

While it was originally stated for human-computer interface, it has been shown to apply to a large variety of conditions with few exceptions (Hoffman 1991; Kerr 1973). By this seemingly universal nature, the speed-accuracy trade-off might be one of the principles taken into account by the central nervous system when planning motion.

Once again, phase space seems to be the natural setting for this principle as it relates coordinates q to their associated momentum p.

Other principles are proposed in the framework of optimal control theory. Here optimal is used in the sense of mathematical optimization, i.e., maximizing or minimizing a function and does not necessarily mean "ideal" or

"efficient". Many such minimizing principles have been proposed, like with the minimization of: time, force, impulse, energy or jerk (Nelson 1983). We briefly present two extensively studied cases: jerk and energy.

Energetic cost minimization

Another natural candidate from a biological and physical point of view is energetic cost minimization. It is particularly well studied in gait, where it is posited to be one of the biggest factor involved in determining the parameters of our gait, alongside stability and maneuverability, for example (Rose and Gamble 2006).

This is a general assumption present almost everywhere in gait literature, and it appears true at least for healthy normal level walking, where changing one's preferred gait results in an increase in metabolic cost, which is not preferable. When faced with new constraints on gait through pathology (i.e. fracture, amputation, etc.) or synthetically, we naturally adapt and update our internal models to the new pattern with minimal energetic cost (Abram et al. 2019; Selinger et al. 2019).

Nevertheless, it cannot constitute the only general principle for the production of motion as it is rarely the regime in which humans walk, for example. Indeed, there are other implicit task goals that are not easily quantifiable, like adhering to social norms and cues or preventing fall, that compete with the goal of energy minimization. These other goals are relevant in the context of rehabilitation, where energy-optimal gaits might not be reachable or even desirable goals.

This is also true for minimum-jerk approaches (and optimal control theory in general). Motion is complex, and it is reasonable to assume that it does not come from a single objective function, but rather a complex interaction of continuously changing goals.

Jerk minimization

A popular principle for motion production was originally proposed by Hogan in (Hogan 1982), and further studied in (Flash and Hogan 1985; Hogan 1984). This principle posits that natural motion tends to be smooth, i.e. without sudden hitches or acceleration transients, which would mean minimizing the derivative of acceleration ($\dddot{x} = \ddot{v} = \dot{a}$): jerk. A representation of position, speed, acceleration and jerk is given in figure 3.5.

This can be formalized in variational calculus as the minimization of the action:

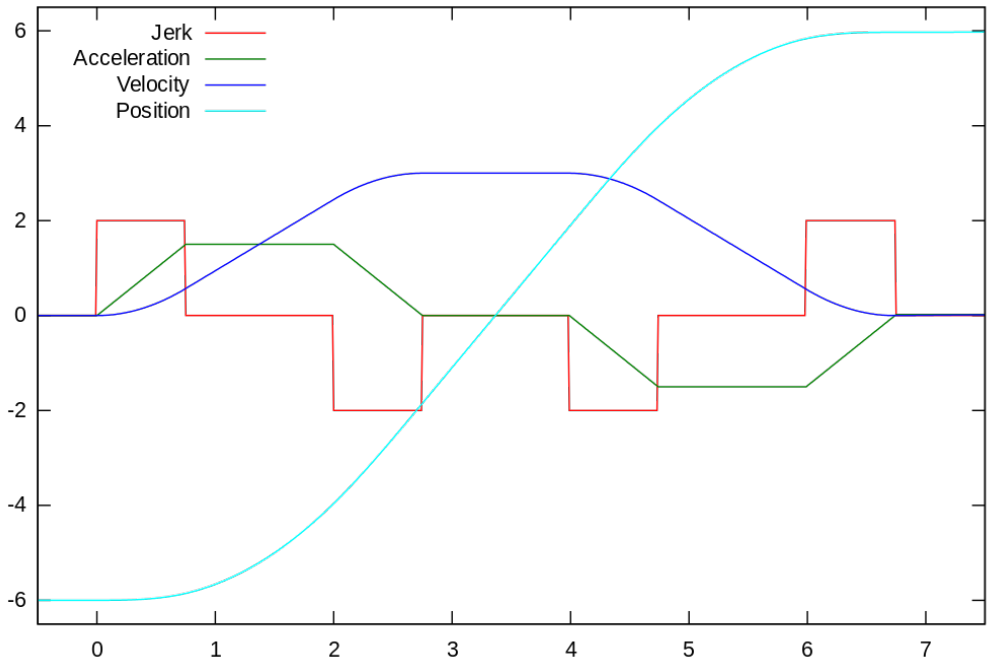

Figure 3.5: Generic profile for position, speed, acceleration and jerk for a unidirectional movement. *CC BY-NC-SA 4.0 by Autopilot retrieved from* `https://commons.wikimedia.org/wiki/File:Schematic_diagram_of_Jerk,_Acceleration,_and_Speed.svg` *on 29/06/2023.*

$$S = \int_{t_0}^{t_1} \dddot{x}^2 dt \tag{3.66}$$

in the case of unidirectional motion.

Here the variable x is the position of the end of the effector, e.g., the position of the hand. This means that this model studies motion in term of extracorporal space and not in terms of joints angles, etc. This makes this model easy to use as it makes no assumption with regards to the dynamics of the arm or the neural inputs required to produce motion. We note that action principles involving higher derivatives go beyond standard, Newtonian, mechanics. They are known to generally lead to unstable movements, unless restricted to very specific models, see (Pais and Uhlenbeck 1950). Such higher-derivative models can be expressed in phase-space too thanks to Ostrograski's method (Tai-jun et al. 2013). It has been shown that adiabatic invariants can be defined for models allowing bounded trajectories

(Boulanger et al. 2019), but the action principle (3.66) does not belong to the latter models.

There is a good fit between experimental data from arm movement and trajectories computed from the minimum-jerk principle which points towards motion being planned in extracorporal space, with higher level planning of the trajectory and then a lower level translating the desired trajectory into neural commands to produce the required torques and forces to perform the motion.

Unfortunately for our case, minimizing the action S does not give rise to periodic solution and it might therefore not be how the central nervous system plans rhythmic movements such as gait. Some variational principles generalizing harmonic oscillators –and therefore periodic motion– with higher-derivatives exist, but they have not yet been studied in the case of human motion.

These models are similar to the one we propose, as they do not make assumptions with regards to the biomechanical and neural structures involved with motion. A more complete view of human motion would surely involve investigating these aspects of motion, this is beyond the scope of this thesis.

3.4.3 Rhythmic motion

Central Pattern Generators

Periodic motion is an important subset of human motion. Indeed, one of the very aspects that makes us human is bipedal motion, or walking, which is periodic by nature. The basic neural structures that govern bipedal motion are called central pattern generators (CPG). They are a network of neurons located in the spinal chord that can produce rhythmic signals even in the absence of rhythmic input, there structure is schematized in figure 3.6. Furthermore, once started, they can produce periodic motion without receiving commands from the motor cortex (Steuer and Guertin 2019).

Of course, internal or external changes in the system happen during motion, making it necessary for CPG to integrate feedback, this is done through other nervous structures, like the vestibular system discussed in the next section. During periodic motion incorporating feedback is particularly relevant as it can usually be done at the timescale of the period of motion, thus responses to changes in the environment can be integrated from one cycle of motion to the next. Studying those changes can therefore reveal the adaptative mechanisms of the body. Moreover, human motion is noisy. As it is impossible to perform the exact same motion twice, motion cannot be strictly periodic but is at most quasi-periodic, i.e. holding a basic pattern

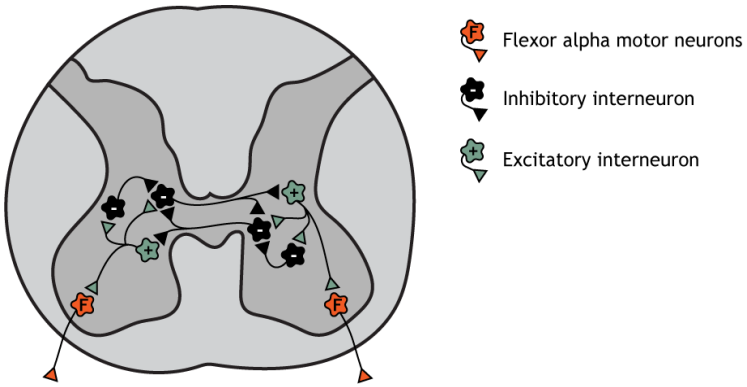

Figure 3.6: Structure of a central pattern generator. *CC BY-NC-SA 4.0 by Casey Henley retrieved from* `https://openbooks.lib.msu.edu/neuroscience/chapter/spinal-control-of-movement/` *on 22/06/2023.*

over which variations are experienced, Bernstein called it "repetition without repetition" (Bernstein 1967). This can make modelizing motion complicated as we need new measures and indices to characterize this behavior of motion, usually from fractal or chaos theory such as Sample Entropy, the Hurst exponent, the Lyapunov exponent, etc. In mechanics, the study of chaotic systems provide many examples of quasi-periodic motion, e.g., a Van der Pol oscillator (Jose and Saletan 1998).

While "noise" around the repeating pattern used to be smoothed out or completely removed, it now appears to be an important feature of dynamic systems. Indeed, variability can be characteristic of many situations. It can arise from errors in motor performance, and is expected to diminish with skill acquisition, but it can also reflect the abundance of motor strategies and the adaptability of a skilled expert. It can also denote health or pathologies in human beings for example (Stergiou and Decker 2011). In all these cases, the general structure of "noise" differ.

Treadmill and variability

While gait is not the only quasi-periodic motion experienced by humans, it is the most commonly studied. This is usually done with treadmills, which consist of a large conveyor belt driven by a motor allowing the user to walk or run in place. Like any experimental device this comes with advantages and limits.

The advantages of treadmill studies are that they can be conducted irrespective of the weather, and more particularly in controlled conditions

(e.g., with control of the temperature, wind, speed, ascent/descent angle etc.) They can also be conducted in a laboratory setting, with access to relevant equipment. This is useful as studying the oxygen consumption ($\dot{V}O_2$) of a participant outdoors requires them to carry equipment, which might hinder more realistic (e.g. unencumbered) measures for example. Another obvious advantage of the treadmill is the ability to walk or run without changes in direction or elevation for long periods of time, which can make analysis more complicated for experiments ran in stadium settings. Finally, treadmills have been common for a long time and the study of there effect on health has been going on since at least the nineteenth century (Hutchinson 1823).

Unfortunately, there are also drawbacks to using treadmills for experimental (or clinical) purposes. The most evident limit is that treadmills are driven at a constant speed, which is not usually the case for human gait, normally experiencing varying periods of slower and higher speeds. Studying rough terrains or simply different ground surfaces is also not doable. Moreover, the conveyor belt is usually made of rubber and is slightly suspended, which makes the ground reaction forces experienced during gait on a treadmill uncharacteristic of regular ground surfaces. These differences with regards to usual walking or running conditions can produce differences in angular and temporal kinematics, but also in variability of gait in treadmill compared to overground (Hooren et al. 2019; Terrier and Dériaz 2011).

Typical dynamic gait measurements established on treadmills are speed, stride length and interval. Physiological measurements can also be made such as the maximal oxygen consumption ($\dot{V}O_{2,\max}$) or heart rate and heart rate variability or electromyograms, the kinematics of motion can also be established such as joint angles. Because of the peculiarities of individuals, these measurements are often particular to the participant and cannot always be meaningfully compared to other individuals and comparisons are usually done against different groups (i.e., healthy vs pathologic). In this thesis, the study of gait was limited to its dynamics.

Periodic motion is not limited to the dynamics of the lower body and specifically gait. During this thesis we also studied motion performed by the arm, for which studies are rarer and protocols are usually developed on a study-by-study basis.

We studied free-pace and metronome walking on a treadmill in experiments (5) and (6).

3.5 Gravity

By its ubiquitous nature, the force of gravity is both intuitively understood and complex to isolate. For example, even though it is a universal constraint on motion on Earth, weighing constantly at $g = 9.81\text{m/s}^2$, there is no one organ dedicated to measuring its effects, and its integration by the central nervous system is necessarily a multisensory affair.

In humans, there exist three main systems that integrate gravitational information. First, the vestibular system which creates the sense of balance and spatial orientation that are needed to maintain postural control. It is situated in the inner ear and is comprised of two main structures: the semicircular canals capable of perceiving rotational motion and the otoliths which measure linear accelerations (Angelaki and Cullen 2008). Their shape within the inner ear is given in figure 3.7. This is enough to meaningfully integrate any movement as they can always be broken down into a series of rotations and translations. For example, even without any other stimulus, a person riding an elevator can intuitively tell whether it is accelerating up or down. Unfortunately, this system cannot always be relied upon (Lawson and Riecke 2014) and illusions of moving when one is static or rotating when one is not can be dangerous. For example, it is of particular concern when training plane pilots (Kritzinger 2016). Lucikly, it is not the only system that the central nervous system relies upon.

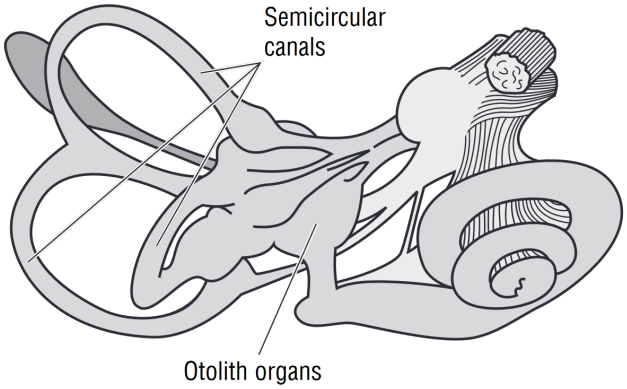

Figure 3.7: The organs forming the vestibular system. *Public domain retrieved from* `https://www.nasa.gov/pdf/58294main_The.Brain.in.Space.pdf` *on 30/06/2023.*

The somatosensory system is the network of structures capable of perceiving temperature, pain and most importantly in our case, touch and proprioception, the sense of body position. The sense of touch is relevant to

the representation of gravity as we constantly are in contact with a surface. For example, when standing upright, the reaction force from the constant pull of gravity is felt through the mechanoreceptors of the feet, relating once again indirect information to the central nervous system. The proprioception information relates the position of body parts to each others via muscle and tendon tension. In this case, the sag of the arms while standing upright is also relevant information processed by the central nervous system to take part in its representation of gravity.

The visual system performs many tasks. In the context of motor control it is mostly used to ground oneself in its direct environment, for precise motor control (notably through eye-hand coordination), and for motion perception. The role of the visual system in the perception of gravity is obvious: the environment around us continuously sends stimuli of the direction of gravity. This is the direction in which trees take their roots, branches stoop and rain falls, when picking up a glass of water, it is the force we have to overcome. This gives us a constant appreciation for local up and down.

It is the integration of those three systems that is responsible for our internal representation of gravity. Having experienced this field for our entire lives, human beings have a deep understanding of it, and consequently the central nervous system takes it into account to plan and use it innately to optimize motion.

For example, when pointing from one point to another horizontally, the speed profile is symmetric, as the arm is first accelerated during the first half of the motion, and then decelerated during the second phase and stops upon reaching the target. This is not the case when there is a vertical component to the motion, i.e. in the direction gravity acts. Indeed, upward motion of the forearm reaches its maximum velocity sooner than a downward one (Pozzo et al. 1998), as can be seen in figure 3.8. This means that for upward motion more time is spent decelerating than accelerating, and inversely for downward motion. This integration of gravity into motion planning helps reduce the energetic cost of up-down motion, as the arm is also accelerated and decelerated by the external force of gravity (Gaveau et al. 2014).

3.5.1 Variable gravity

As a way to study the robustness of our theories and humans' representation of gravity, it is of particular interest to push experiments outside of the comfort zone of the central nervous system and into environments where "gravity" is variable. Here, there exist two regimes, hypergravity, where the acceleration felt is greater than 1 g, and hypogravity, lower than 1 g. It is significantly easier to probe the hypergravity regime as we can simulate

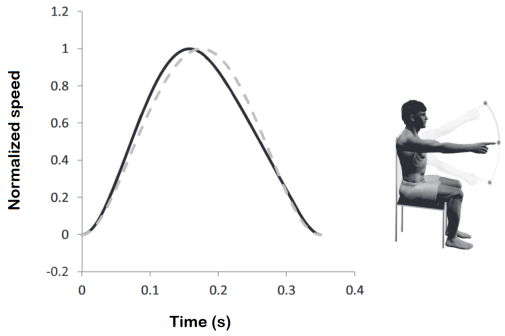

Figure 3.8: Typical velocity profile for up-down motion around the shoulder. Grey indicates downward motion, black upward. Inset represents the motion performed. Adapted from (Gaveau et al. 2014).

acceleration with the centripetal force, as is the case in centrifuges.

Centrifugation

There are multiple different designs of centrifuges, but they are all comprised of the same basic components. A gondola, where the participant is placed to perform an experiment, with equipment to constantly monitor their state, like cameras, microphones and electrocardiographs data being fed to a control room. The gondola is attached to an arm while it itself is fixed to an engine responsible for the rotation of the whole apparatus.

The acceleration felt in the gondola caused by the centrifugation depends on the speed of rotation and the length of the centrifuge's arm. The direction of the acceleration also depends on the orientation of the gondola which can usually be varied to simulate different environments. The perceived acceleration, $\vec{g}(t)$ is the sum of gravity and the rotational acceleration in the centrifuge, i.e., $\vec{g}(t) = \vec{g} + \vec{a_c}(t)$. In our case, we simulate acceleration in the vertical direction of the body, i.e., the direction in which gravity is usually felt.

As said previously, it is rare for human beings to be exposed to accelerations far from 1 g for extended period of times and we are not particularly made to withstand these conditions, it can therefore have adverse effects. Most obviously, it affects our weight (recall that $\vec{P} = m\vec{g}$) which can make moving particularly difficult. Transitions between different accelerational environments can also cause motion sickness. Transitions around 1 g are particularly nauseogenic and it is recommended not to move the head during centrifugation. In the case of vertical downward acceleration, it also pushes blood to the lower limbs and away from the brain, making loss of conscious-

Figure 3.9: The long-arm centrifuge at the QinetiQ Flight Physiological Centre in Linköping, Sweden. Credit: QinetiQ.

ness a real concern during centrifugation. Tolerance to centrifugation varies significantly from individuals, and can be trained (Whinnery and Forster 2013).

During this thesis we used data from centrifugation sessions performed in the centrifuge pictured in figure (3.9). This is developed in chapter (7).

Centrifuges are mainly used to train and test pilots and astronauts, but they are also used in research to study the effect of higher accelerational environments on humans, animals, plants, plasmas, etc. Unfortunately, centrifuges are not capable of producing accelerations lower than 1 g, and this regime must be explored in other experimental contexts, like free-fall.

Parabolic flights

The best environment to perform experiments with low gravity is space. Unfortunately, this is usually not doable because of the exorbitant cost of space freight, the limited space and personnel aboard the International Space Station, and the stringent constraints that any object must follow to even be allowed on the station. Luckily, weightlessness can be achieved on Earth, albeit for short times in drop towers or parabolic flights.

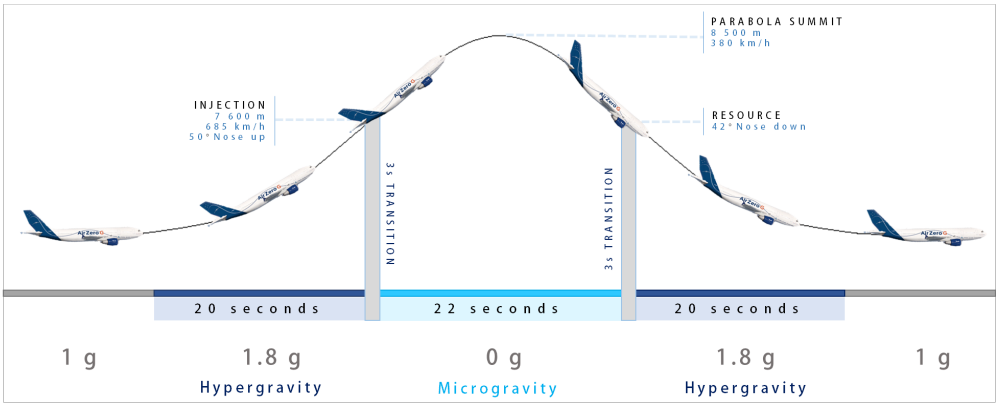

Figure 3.10: Diagram of a typical parabola. Credit: ESA

A parabolic flight is performed by a specially modified plane, an Airbus A310 ZeroG in the case of the French National Centre for Space Studies (CNES). It consists of a series of maneuvers that allows the passenger to experience hyper- and zero-gravity for a short time (typically ∼20 s). The maneuver, called a parabola, is composed of multiple phases represented in figure 3.10. First, the plane is flying horizontally experiencing 1 g, then the plane climbs to a 50° pitch angle with a speed of 685 km/h. This gives rise to a sensation of 1.8 g for about 20 s. The plane then lowers its speed to 380 km/h while lowering its nose, during this phase passengers experience free-fall (0 g) for ∼20 s. After reaching a 42° angle of negative pitch, the airplane stabilizes back to horizontal flight, during this transition the passengers experience hypergravity of around 1.8 g for ∼20 s once again. The airplane then stays in horizontal flight for a few minutes, before performing another parabola. A typical parabolic flight operated by the CNES performs 31 such parabola, for a total of around 30 min of altered gravity, 10 min of which are in weightlessness.

While experimenting in parabolic flights is easier than in the International Space Station, it still comes with constraints. First, the phases of altered gravity are very short and do not allow to study the behavior of systems (e.g., the central nervous system, a mechanical system, etc.) at long timescales. This can be problematic as the internal modelization of gravity comes from a lifetime of experience that cannot *a priori* be replicated in such a flight. Secondly, the abrupt changes of environment can cause a lot of stress to the body and it is therefore complicated to interpret baseline readings in flight, as they are necessarily "polluted". Finally, like in the case of centrifuges, the change of accelerational environment can cause motion sickness and nausea, appropriately planes operating parabolic flights are often nicknamed "vomit

comets". To combat that, passengers are usually given the drug Scopolamine, which can have side effects such as tachycardia or bradycardia.

Effects of such flights are further explored in chapter (8).

During our thesis we used both experimental contexts to study how participants adapt to changes in $\vec{g}(t)$ when performing rhythmic motion.

Because of the prohibitive cost of those experimental contexts, it is rarely possible to include large numbers of participants, the number of participants is therefore limited for our studies. For similar reasons and the involved nature of those contexts, probing populations such as young participants, participants with pathologies should first be done in simpler experiments, e.g., with overground walking.

Chapter 4

Hypothesis and goals

Globally, this work aims to better understand the underpinnings of motor control by proposing and exploring a new way to model voluntary rhythmic motion in human in time-varying environments.

As discussed in the previous chapter, planning motion is a very important task to be able to correctly achieve motor goals and adapt to new situations. However, it is not clear how the central nervous system probes or weeds out uninteresting strategies in the face of the infinite possibilities laid out by the redundancy in the degrees of freedom of our body. Indeed, in everyday life people routinely reach their motor goals seemingly without having to think about it. To explain this phenomenon, many strategies have been purported to be employed by the central nervous system, like the minimization of the jerk or the energy of the motion, each with its domain of application and limits. A common issue in these principles is the characterization of periodic motion or changes in the environment during motion. Here, we propose to compute relevant quantities in this context: adiabatic invariants, which are based on Hamiltonian mechanics. This is a purely extracorporal mechanistic approach that is given *a priori* and that makes no assumptions with regards to the biomechanics of the system, and simply requires slow (if any) changes in the environment in which motion takes place. The goal of this thesis is to study this novel mechanistic physical property of rhythmic motion in humans in a variety of experimental contexts.

In our first experiment (chapter 5), before turning to more complex environments, we first probe the general motor behavior of our model in the well studied context of gait, without changing any parameter during the experimentation. By its general nature we hypothesize that the model should hold whatever the experimental conditions are. To explore this claim, we look at two different experimental conditions that are known to have widely different temporal structures, free-pace and metronome-keeping gaits.

In a second study (chapter 6) of the same experiment, we test the capacity of our approach to model an important aspect of human motion: variability. Indeed, we assume that motion is akin to an harmonic oscillator which should be perfectly regular. Statistical mechanics arguments suggest that the addition of a small noise term should be enough to mimic diffusion in phase space. We test that theory in the case of human motion and noise.

In our second and third experiment (chapters 7 & 8), in two somewhat similar protocols, we finally probe the capacity that our model has to characterize motion in time-changing environments. Specifically, we studied experimental data from centrifugation sessions and parabolic flights which are extreme environments where "gravity" changes. Even though the central nervous system has a hard time planning efficient motion in these environments, we hypothesize that our mechanistic model still holds.

Chapter 5

Adiabatic invariants and human walking

5.1 Summary

In this first experiment, we have examined the role of adiabatic invariants in the context of human walking. Indeed, human walking is both simultaneously a globally stable and locally variable process, i.e. while the general shape of strides stays constant during motion, it is variable from one step to the next. The variability of gait has been well studied, unfortunately it is still not clear what drives global stability. In that context, adiabatic invariants seem relevant as they define quantities that stay constant during periodic motion, despite fluctuations of other parameters such as energy or frequency (Landau and Lifchitz 1988).

For that purpose we recruited twenty five healthy participants to walk for ten minutes at a comfortable pace, with and without a metronome indicating preferred step frequency, a condition known to alter variability in the stride interval, as defined by parameters such as the Hurst exponent, fractal dimension or sample entropy, but whose effect on stability is unknown (Kantz and Schreiber 2003). Global stability was assessed by quantifying the whole-body center-of-mass motion while local dynamic variability, predictability and complexity was assessed using the stride interval.

We reiterate a previous result: metronome keeping indeed alters the stride interval variability and predictability, from autocorrelated to almost random dynamics. However, the adiabatic invariant is preserved in both the normal and metronome condition, assessing the global stability of gait. Therefore, it appears that adiabatic invariants reveal global stability constraints that are "hidden" behind apparent local stride variability.

The content of this chapter as been published as Buisseret F.[1] , **Dehouck V.**[1] , Boulanger N., Henry G., Piccinin F., White O., Dierick F., (2022) **Adiabatic invariant of center-of-mass motion during walking as a dynamical stability constraint on stride interval variability and predictability**, *Biology* DOI: 10.3390/biology11091334.

5.2 Introduction

Human gait can be considered a quasiperiodic phenomenon. Despite the apparent stability of walking at a constant speed, gait exhibits an inherent local variability that can be observed at the level of basic parameters such as the stride-to-stride interval time or simply referred to as the stride interval (SI). The global stability during gait is typically assessed by quantifying the whole body centre-of-mass (COM) motion. Local variability can be modulated to maintain global stability (Emmerik et al. 2016).

It is well known that gait variability is a hallmark of healthy individuals and has properties that are far more complex than stochastic variability. Since the seminal works of Haussdorff et al. (Hausdorff et al. 1995; Hausdorff et al. 1997), it has been shown that the variability, more exactly the predictability, of SI over a long period of time – typically several hundred gait cycles – is autocorrelated, just as it is in chaotic systems. These autocorrelations can be assessed by computing the Hurst exponent or H Hurst 1951; Kantz and Schreiber 2003, which typically ranges from 0.7 to 0.9 in young healthy adults (Ravi et al. 2020). Note that H= 0.5 implies random variability. Although the physiological mechanism that generates SI autocorrelations is still controversial, neurodegenerative diseases significantly alter SI variability (Moon et al. 2016), and the use of indices other than H can help distinguish between different pathologies (Dierick et al. 2021; Phinyomark et al. 2020). Other disturbances during walking, such as the execution of a cognitive task (Dierick et al. 2020) or following a rhythmic auditory cue (Terrier and Dériaz 2012) also alters SI variability.

Realistic values for H can be obtained by resorting to simple mechanical models of the inverted pendulum type, in which one or two parameters are randomly updated at the beginning of each step (Ahn and Hogan 2013; Gates et al. 2007). Although mechanical approaches are used to model gait variability, it is worth noting that developments in Mechanics, such as action-angle

[1]First co-authors

variables in the Hamiltonian formalism, have proven remarkably successful in finding conserved quantities for complex and even chaotic systems (Jose and Saletan 1998; Landau and Lifchitz 1988), *i.e.* quantities with invariant value over time. Identifying such a conserved quantity for human gait would be to find dynamical constraints "hiding" behind SI variability that could provide new insights into how dynamical systems, in which behaviors evolve over time, maintain their current state or stability while allowing for variability/predictability. Whereas energy is not necessarily conserved over time with stochastic variation in system parameters, adiabatic invariants are good candidates for (almost) conserved quantities. An adiabatic invariant, I, is a quantity that remains approximately constant during the evolution of a dynamical system even under slow external changes, *i.e.* an adiabatic transformation (Landau and Lifchitz 1988). One way to define an adiabatic invariant, I, relevant to the analysis of rhythmic human motion for a given degree of freedom $Q(t)$ for which the kinetic energy has the standard form $E_k = \frac{m}{2}\dot{Q}^2$ (Boulanger et al. 2021), with m a mass scale, is through

$$\overline{E_k} = \pi\, I\, f \ , \tag{5.1}$$

where $\pi = 3.1415\ldots$, f is a given cycle frequency (the inverse of its duration) and $\overline{E_k}$ is the averaged kinetic energy on the cycle under consideration. In the model (Eq. 5.1), $\overline{E_k}$ and f are assumed to change significantly over time, but their ratio, which is proportional to I, should remain invariant. Here, $\overline{E_k}$ during each gait cycle will be computed from the whole body COM vertical displacement. The term "adiabatic invariant" will therefore refer to the quantity (5.1) computed from the vertical displacement of the COM. It is an important restriction since, in principle, adiabatic invariants may be found in the other directions and for other degrees of freedom while walking. Another important remark is the following. The term "invariant" will be used to denote a function of the dynamical variables whose value does not change over time during the evolution of a dynamical system, while the word "constant" will be used for a parameter whose value is not modified by the experimental condition. A textbook example is that of a simple pendulum without friction: Total energy is invariant but not constant since it depends on the amplitude.

Biological systems are the most noteworthy nonconservative systems that derive forces from internal energy reservoirs (Kugler et al. 1990). In previous work, the adiabatic invariant has been successfully applied to human movement (Kugler et al. 1990). In biological systems, it is also important to note that adiabatic invariants can be considered only as an approximation and are not rigorously but rather approximately invariant

Previous work has shown that the relations (5.1) holds for rhythmic arm movements (Kadar et al. 1993; Kugler et al. 1990) and for walking (Turvey et al. 1996). In the latter work, participants walked for 3 minutes, and SI variability was not examined. More, limit cycle attractors in phase-space $(Q, \dot{Q})$, *i.e.* the average gait cycle of a participant, were not drawn while they can also be used as visual representation of gait pattern. Human motion, and particularly walking is indeed highly stereotyped, though noisy, and gait patterns are highly consistent for an individual over time (Broscheid et al. 2018). The attractors may also distinguish between walking and running, as the transition from walking to running can be viewed as a change from one stable attractor to another (Raffalt et al. 2020). Therefore, these attractors could help distinguish between participants and conditions. The area enclosed by the phase-space trajectory of system over one cycle is the adiabatic invariant I.

From the perspective of understanding the role played by the neuromusculoskeletal system in constraining coordination and reducing the degrees of freedom (Bernstein 1967), adiabatic invariants of motion are relevant quantities since two or more variables are linked by a single invariant. Therefore, the primary objective of this study is to investigate whether the adiabatic invariant model (5.1) holds in a population of healthy young adults walking at spontaneous speed on a motorized-treadmill during a sufficient number (typically more than 500) of cycles to also assess SI variability, predictability, and complexity. The secondary objective is to understand how a constraint applied on the system, in our case a rhythmic auditory cue (metronome) indicating preferred step frequency, impact global stability (assessed by the adiabatic invariant I) and SI variables. Our hypotheses were that equation (5.1) holds during walking on a treadmill regardless of the metronome constraint, and that the latter constraint significantly alters variability and predictability indices as shown in (Terrier and Dériaz 2012).

5.3 Materials and Methods

Protocol

The protocol was performed in a session of approximately 60 minutes. It has been validated by the Academic Ethical Committee Brussels Alliance for Research and Higher Education (protocol B200-2021-123). Participants were healthy students recruited in the Department of Physiotherapy of the Haute Ecole Louvain en Hainaut (Montignies-sur-Sambre, Belgium). After being informed about the study, each participant signed an informed consent. The

same experimenters (F.P. and G.H.) were responsible for the measurements.

First, participants' age and biometric data (mass and height) were collected. Participants were asked to wear a tight outfit. Participants' pelvic movements were recorded by a Vicon opto-electronic system (Vicon Motion Systems Ltd, Oxford Metrics, Oxford, United Kingdom) composed of 8 cameras (Vero v.2.2) with a sampling frequency of 120 Hz. Four 14-mm-diameter reflective markers were placed on the pelvis of the participants following the Plug-In-Gait model (Oxford Metrics, Oxford, United Kingdom): Left Anterior Superior Iliac Spine [LASI], Right Anterior Superior Iliac Spine [RASI], Left Posterior Superior Iliac Spine [LPSI], and Left Posterior Superior Iliac Spine [RPSI].

Then, participants took place on the belt of an instrumented motorized-treadmill (N-Mill, Motekforce Link, The Netherlands). The vertical ground reaction force and center of pressure of each foot was recorded at a sampling rate of 500 Hz using the manufacturer's software (CueFors 2, Motekforce Link, The Netherlands). Spontaneous walking speed was determined and recorded during a 3-minute habituation period. After a 1-minute rest, the participant walked at a spontaneous speed on the treadmill for 10 minutes (control condition, CTRL). The average step frequency, f, was automatically computed by the CueFors 2 software. The positions of the 4 markers, $\vec{x}_a$, were recorded with the Vicon system via the Vicon Nexus software (v.2.7.1, Oxford Metrics, Oxford, UK). After a short break of 3 minutes, the participant walked on the treadmill at a spontaneous speed for 10 minutes with instructions to synchronize his or her steps with the clicks of a metronome whose tempo corresponded to the number of steps per minute calculated in the CTRL condition (metronome condition, METRO). This allowed the participants to adjust their gait tempo on a step basis whilst ensuring they adopted their own comfortable pace. The duration of the successive gait cycles and the positions of the 4 markers were recorded in the METRO condition.

To estimate the whole body COM vertical trajectory, $Q(t)$, the mean vertical position of all pelvic markers (RASI, LASI, LPSI, RPSI) was taken at each time step. Furthermore, to reduce measurement artefacts, $Q(t)$ was filtered using a low-pass fourth order Butterworth filter adjusted to each time series so that it kept 99.99% of the signal's power. In order to alleviate the low sampling rate of the measurement system a cubic spline interpolation was conducted on the data, multiplying the frequency by 10 to 1200 Hz. The speed and acceleration were then obtained through a finite difference scheme. The data was processed using R software (v. 4.1.0) (R Core Team 2021). Typical phase-space trajectories are shown in Fig. 5.1.

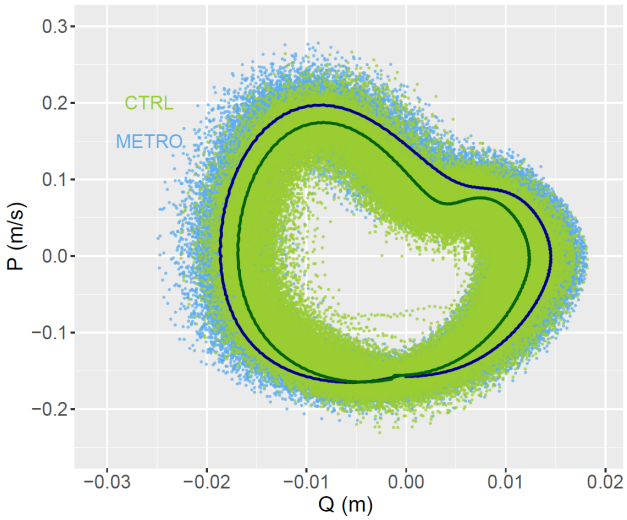

Figure 5.1: Two typical plots of whole body COM vertical trajectories in phase-space (Q, P) in the two studied conditions: CTRL (green) and METRO (blue). Attractors, computed as the mean cycle in phase-space, are also displayed in the two studied conditions: CTRL (dark green line) and METRO (dark blue line). The same subject has been chosen in both conditions.

Adiabatic invariant I (global stability)

We assume that the vertical motion of the whole body COM during walking is governed by the Hamiltonian $H = \frac{1}{2}(P^2 + Q^2)(\omega + \epsilon\,\xi(t))$ with $0 < \epsilon \ll 1$ and $\xi(t)$ a stochastic noise. This model is based on a forced harmonic oscillator with a frequency that fluctuates randomly around a mean ω. The noise accounts for physiological noise (i.e., the impossibility for the human locomotor system to be steadily in the same state) and should be low in healthy individuals. The momentum P is defined as $P = \dot{Q}$ as in standard Hamiltonian mechanics. This general class of Hamiltonians fits the form considered in the Appendix A, where the computational details are given. As developed in this Appendix, the action variable (5.1) is an adiabatic invariant of the system: its value does not change over time except for small random fluctuations around the mean. In summary, the linear relationship (5.1) is to be expected in the analysis of the vertical motion of COM in healthy walking individuals.

A step is defined by the collection of data points between two maxima in $Q(t)$. A gait cycle consists of two consecutive steps. For each gait cycle identified, denoted C_i, the frequencies f_i and the average kinetic energy $\overline{E_{ki}}$ were computed. Recall that i typically ranges from 1 to 500. For a given

participant in a given condition we computed $E_{km} = \boldsymbol{E}(\overline{E_{ki}})$, $f_m = \boldsymbol{E}(f_i)$ and $I = \frac{E_{km}}{\pi f_m}$, where $\boldsymbol{E}(x_i)$ denotes the arithmetic mean of an arbitrary set of values x_i. Equation (5.1) is valid for all values of $(f_i, \overline{E_{ki}})$ and we assume that I is constant according to adiabatic invariant theory (Landau and Lifchitz 1988). Taking into account Eq. (5.1) together with $E_{km} = \pi\, I\, f_m$ leads to

$$\frac{\overline{E_{ki}}}{E_{km}} = \frac{f_i}{f_m}. \tag{5.2}$$

Therefore, a prediction of our model is that $\frac{\overline{E_{ki}}}{E_{km}}$ versus $\frac{f_i}{f_m}$ should behave as a straight line with slope 1 and a zero intercept.

After each gait cycle was identified, an average cycle was computed. To do this, each cycle was normalized to a unit duration and a spline of 1200 equally spaced points was computed for each cycle. Then 1200 bins -one for each frame- were created and filled with the data from the splines of all cycles of a given participant in a given condition. The mean and standard deviation were computed for each bin.

SI variability, predictability, and complexity

Time series $\boldsymbol{T}$ with durations T_i of successive gait cycles were computed from heel strikes of the right foot identified by CueFors 2 software. At the end of the session, two time series were generated for each subject in the CTRL and METRO conditions. Typical plots are shown in Fig. 5.2.

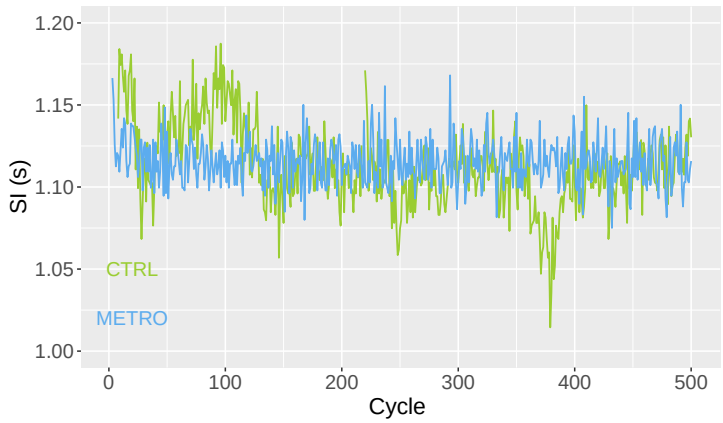

Figure 5.2: Typical plots of the SI time series obtained in the two studied conditions: CTRL (green) and METRO (blue). Parameters in CTRL condition are: SI= 1.12 s, CV=0.0282, H=0.988, S=1.59, D=1.35. Parameters in METRO condition are: SI= 1.12 s, CV=0.0132, H=0.383, S=2.20, D=1.51.

First, the average SI was computed as well as the coefficient of variation, CV=$SD(\boldsymbol{T})/SI$, estimating the magnitude of SI fluctuations. The Hurst exponent, H, was then computed by resorting to Detrended Fluctuation Analysis following the guidelines in (Ravi et al. 2020); more technical details about the algorithm we used can be found in (Dierick et al. 2017). By definition, H is mainly a measure of time series' predictability (Hurst 1951; Kantz and Schreiber 2003). Therefore, it is relevant to complement it with other variability indices (Crevecoeur et al. 2010; Dierick et al. 2021; Phinyomark et al. 2020), of which we have chosen the Minkowski fractal dimension, D, (Dierick et al. 2017), and the sample entropy, S, both as measures of complexity (Emmerik et al. 2016). Computational details for D can be found in (Dierick et al. 2017), while S was computed using the method described in (Yentes et al. 2013). All SI data analysis was performed with R (v. 4.1.0).

Fig. 5.2 gives a first hint of SI variability, predictability, and complexity. Fluctuations around the mean value have a smaller magnitude in METRO condition (smaller CV), but a simpler temporal structure. Indeed, the latter fluctuations show increasing or decreasing trends during several tenths of cycles in CTRL conditions, resulting in a larger predictability (larger H). The lower predictability in METRO condition also results in a larger sample entropy, meaning that the fluctuations are closer to a random process in METRO condition. Indeed, S is maximal for a random process.

As discussed in Appendix A, CV provides an estimate of ϵ, the magnitude of the time-dependent noise modelling the quasiperiodic nature of human motion. As our approach is only valid for ϵ well smaller than 1, the measured values of CV must be well smaller than 1 too for our approach to be consistent.

Statistical analysis

Data assessing SI variability, predictability, and complexity were tested for normality (Shapiro-Wilk) and equality of variance. A paired t-test was performed and used to examine the effects of condition (CTRL or METRO) on SI, CV, H, D and S. The significance level was set at $p = 0.05$. In the case of a failed normality test, a Wilcoxon signed rank test was performed. The adiabatic invariant I was compared in CTRL and METRO conditions using the same methodology. All these statistical procedures were performed with SigmaPlot software version 11.0 (Systat Software, San Jose, CA).

An ANCOVA with zero intercept and significance level $p = 0.05$ was performed to compare the linear trends of $\frac{\overline{E_k}}{E_{km}}$ versus $\frac{f}{f_m}$ in conditions CTRL

and METRO, *i.e.* according to model

$$\frac{\overline{E_k}}{E_{km}} = k\,\frac{f}{f_m}, \tag{5.3}$$

where k is the experimentally observed slope. A linear regression with zero intercept of $\frac{\overline{E_k}}{E_{km}}$ versus $\frac{f}{f_m}$ was also performed independently of the condition, and the 95% confidence interval of the slope was computed. ANCOVA was performed with R software (v. 4.1.0).

Dynamic Time Warping (DTW), an algorithm developed to measure "distances" between similarly patterned time series, was then run to compare the distance between CTRL and METRO conditions for each participant whole body COM vertical position (Q) and speed (P) as a function of time. The distances were computed for Q and compared to that computed for P using a paired t-test. The 'dtw' package in R was used and the time series were z-normalized before comparison between time series.

5.4 Results

Population

The general characteristics of our participants can be found in Table 5.1.

Table 5.1: General characteristics of our population. Results are reported in the form mean± SD. The number of gait cycles performed by the participants in 10 minutes is reported in the form median [q1-q3] regardless of the condition.

N	25
Age (years)	22.8±5.2
Mass (kg)	68.1±13.6
Height (m)	1.65±0.32
Sex (M/F)	9/16
Gait cycles	532 [513-552]

M: male; F: female

SI variability, predictability, and complexity

A comparison of the results obtained in the CTRL and METRO conditions in the analysis of the SI time series is shown in Table 5.2. SI and D are not significantly changed. CV and H significantly decreased in the METRO

condition, with H> 0.5 in CTRL condition and < 0.5 in METRO condition. S marginally increased in the METRO condition. The significant differences are shown in Fig. 5.3 graphically.

Table 5.2: Comparison between results in conditions CTRL and METRO for the SI analysis. Results are reported in the form mean±SD if a paired t-test was performed, or median and first-third quartiles [q1-q3] if a Wilcoxon signed rank test was performed. Significant p-values are in bold.

Condition	SI (s)	CV	H	D	S
CTRL	1.184 [1.126-1.269]	0.0261±0.0071	0.848 [0.781-0.951]	1.633±0.116	1.759±0.228
METRO	1.187 [1.119-1.273]	0.0193±0.0060	0.373 [0.265-0.560]	1.667±0.129	1.891±0.249
p	0.258	**0.001**	**< 0.001**	0.282	0.063

SI: stride interval; CV: coefficient of variation; H: Hurst exponent; D: Minkowski fractal dimension; S: sample entropy.

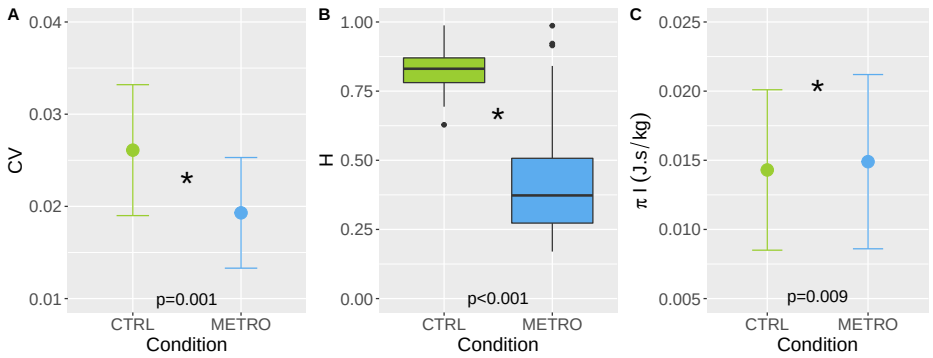

Figure 5.3: (A) Comparison of the mean values of CV in CTRL and METRO conditions. The error bar is equal to 1 SD. (B) Boxplots comparing the distribution of H in CTRL and METRO conditions. (C) Same graphical representation as in (A) for πI. The stars (*) denote significant differences between the means or medians between the two conditions.

Phase-space dynamics

The adiabatic invariant is significantly increased in METRO condition: πI =0.0149±0.0063 J.s/kg against πI =0.0143±0.0058 J.s/kg ($p = 0.009$). The difference is displayed in Fig. 5.3.

The linear trend (Eq. 5.3) is confirmed by the ANCOVA ($p < 0.001$), and the slope does not depend on the condition ($p = 0.700$). The observed slope has a 95% confidence interval of [0.998, 1.002]: $k = 1$ is compatible with

the latter interval. The quality of the linear regression can be graphically appraised in Fig. 5.4A. Figure 5.4B shows the dispersion of the data around the linear relation (5.2). It can be seen that the values of $\frac{\overline{E_k}}{E_{km}} - \frac{f}{f_m}$ are well peaked around the zero value, which is related to the high value reached for R^2 .

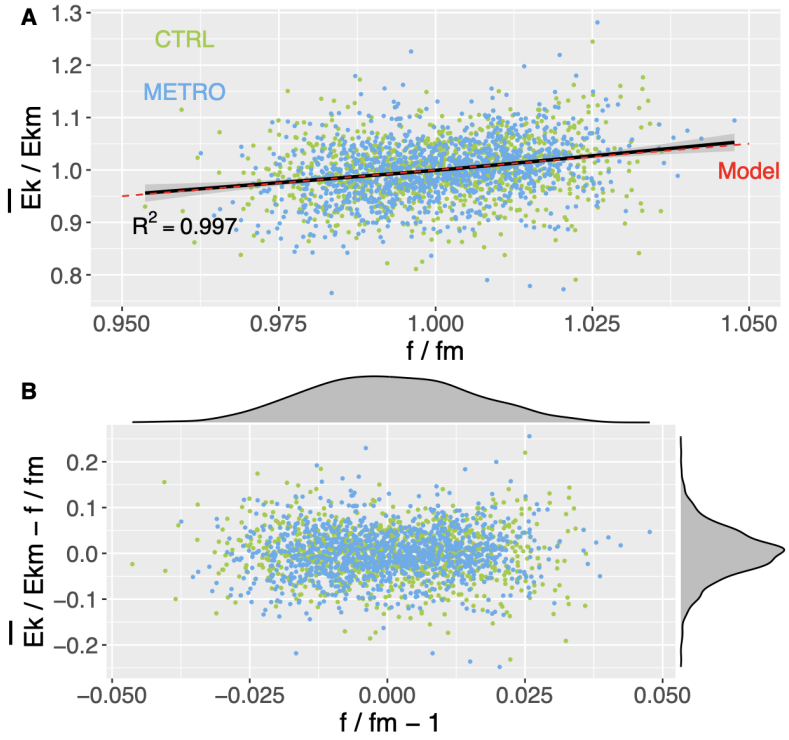

Figure 5.4: (A) Computed pairs $\left(\frac{f}{f_m}, \frac{\overline{E_k}}{E_{km}}\right)$ (points) compared to a global regression of the form (Eq. 5.3) (black line and gray band indicating the 95% confidence interval). The coefficient of determination R^2 of the regression is indicated. The model (Eq. 5.2) is also shown (dashed red line). (B) Computed pairs with the linear trend (5.2) removed $\left(\frac{f}{f_m} - 1, \frac{\overline{E_k}}{E_{km}} - \frac{f}{f_m}\right)$. The densities of the points along the two axes are shown above (density of $\frac{f}{f_m}$) and to the right side of the plot (density of $\frac{\overline{E_k}}{E_{km}} - \frac{f}{f_m}$).

The average DTW distance between CTRL and METRO conditions was 10.3 ± 3.8 for Q and 12.9 ± 7.4 for P. A paired t-test finds these values not statistically different with $p = 0.099$.

5.5 Discussion

The objectives of this study were twofold: (1) to investigate whether the adiabatic invariant model (Eq. 5.1) holds in a population of healthy young adults walking at spontaneous speed on a motorized-treadmill, and (2) to understand how a constraint applied on the system i.e. a metronome impacts global stability and SI variables. The major findings were that: (1) the invariant model was verified, and (2) SI variabilty (CV) and predictability (H) significantly decreased in the METRO condition, and global stability (I) significantly increased in the METRO condition.

The originality of this work is that it simultaneously measured the global stability, and local variability, predictability, and complexity of motorized-treadmill walking in two conditions. In the first, CTRL, participants walked at spontaneous speed. In the second, METRO, participants adjusted heel strikes to a tone emitted by a metronome whose frequency matched each participant's preferred frequency. The latter condition is known to induce significant changes in step-to-step variation (Terrier and Dériaz 2012), and this was also the case in our study. We first comment on the SI variability, predictability, and complexity results. The values we found are typical of the long-range variability observed in healthy young adults; see, e.g. (Dierick et al. 2017; Phinyomark et al. 2020) for CV, H, and D, and (Crevecoeur et al. 2010) for S. A salient feature of our results is the decrease of H from correlated (H=0.848) to anti-correlated (H=0.373) values. This phenomenon was previously observed in (Terrier and Dériaz 2012). The metronome that clicks at the spontaneous frequency of a participant "destroys" the normal SI autocorrelation pattern (Terrier and Dériaz 2012). This can be interpreted by the additional constraint that the metronome imposes. Here, the participant is not free to adapt his/her variability as would be the case with an optimal motor strategy, but must inhibit any change in SI variability to remain synchronous with the metronome. This blocking mechanism leads to anti-correlation and also to a much smaller CV in the METRO condition. Note that CV is well smaller than 1 in both conditions, so it is consistent with our mechanical approach where the magnitude of the time-dependent noise is assumed to be small. S is almost significantly higher in the METRO condition. This could be related to the fact that q3 value of H in METRO condition is equal to 0.56: a non-negligible fraction of our participants has H around 0.5, and random variability has maximum entropy.

Our major observation is that the model (5.3) holds in both CTRL and METRO conditions. Although the participants change their SI variability and predictability, the dynamical stability constraint induced by the adiabatic invariance is verified: $\overline{E_k}$ of the whole body COM and f of a given cycle

are linearly correlated. Note that the model (5.3) does not forbid changing the value of I in the different conditions. By the way, the adiabatic invariant I is significantly higher in the condition METRO. On the one hand $I = \frac{\overline{E_k}}{\pi f}$. On the other hand, f does not change significantly in the METRO condition because T does not change. Thus, the increase in I is associated with a higher $\overline{E_k}$ per gait cycle. Regarding phase-space dynamics, the DTW distance for P is not significantly different from that for Q. This result does not allow to infer that the change in I is mostly due to a change of behaviour in one of the variables P or Q. Instead it shows that the change in I is due to a simultaneous change of both P and Q behaviours.

Strategies for human locomotion based on adiabatic invariance have already been developed and computed from the total (translational and rotational) body's kinetic energy per stride (Turvey et al. 1996). In this study, they used a multi-segmental model in which the body segments were treated as an ensemble of systems in motion, each characterized within a stride by the summed changes in kinetic energies from and about their respective centers-of-mass. In this model, walking is viewed as a sequence of joint rotations and is referred to as a "segmental" approach (Tesio and Rota 2019). Here, we extend the results of this previous work, as we were able to show the validity of the theory of adiabatic invariance in walking using a single-point kinematic model represented by the vertical component of the whole body COM. The latter is known to provide summarized information about all body segments during walking. In contrast to the previous model, walking is considered as achieving a forward motion of the whole body system (Tesio and Rota 2019). Even more interesting is that the vertical displacement of the whole body COM is related to the metabolic cost (Ortega and Farley 2005). Therefore, we hypothesize that I is related to the metabolic cost of walking and that participants are able to follow the metronome constraint at the expense of a larger oxygen consumption ($\dot{V}O_2$). This picture is coherent with (Rock et al. 2018), in which it is shown that an altered SI variability correlates with higher $\dot{V}O_2$. However, the changes in variability in the latter study were due to different walking speeds, which are not comparable with our protocol. It has also been shown that the nervous system uses predictions of the optimal gait to optimize the energetic cost of each new step (Selinger et al. 2019). This has also been demonstrated in other activities such as pedalling (Takaishi et al. 1994). We think that keeping a constant value for I during walk with a given set of external conditions is one of the constraints involved in the prediction of the nervous system. The presence of such a constraint may actually improve the efficiency of prediction by excluding irrelevant motor strategies and reducing the degrees of freedom of

the neuro-musculoskeletal system (Bernstein 1967).

From a methodological viewpoint, we choose to compute $\overline{E_k}$ of the whole body COM only in the vertical direction (sagittal plane motion) and not in the anteroposterior and mediolateral directions (horizontal and transverse plane motion). This choice could be justified by the methodology implemented for SI variables assessment requiring numerous gait cycles. Walking on a motorized-treadmill is not similar to walking on the ground and station-keeping on the belt is impossible and surely less important than not falling (Wang and Srinivasan 2014). Displacement of the whole body COM in the horizontal and transverse planes is mainly related to foot placement dynamics on the belt that may be affected by the motion strategy adopted by the participants, for example if they want to avoid the belt's edge (Wang and Srinivasan 2014). Therefore, the displacement of the COM in horizontal and transverse planes was excluded from our analyses since the motion in this plane is not representative of a spontaneous motion from a walk on the ground. Moreover, a drift correction method should have been considered before calculating the adiabatic invariants, which is out of the scope of our paper. As a consequence only one adiabatic invariant has been computed while, from the separability hypothesis, three adiabatic invariants should be possibly computed from the COM motion during walk, one per direction. Further studies are now necessary to explore this statement.

The present study has some limitations that should be addressed. First, we considered the CTRL condition as a reference to compare the effects of the metronome. However, walking on a motorized-treadmill results in an anti-correlated pattern in the stride speed fluctuations (Terrier and Dériaz 2012). Therefore, the best reference condition is walking on the ground, but recording the kinematics of the pelvis during a large number of cycles is not possible without moving to half-turns in the calibrated volume, which would lead to a disturbance of the locomotor rhythm. Second, $\dot{V}O_2$ was not measured during walking. However, a direct relationship between total body kinetic energy and $\dot{V}O_2$ was previously observed at various constant walking speeds (Turvey et al. 1996). Measurement of $\dot{V}O_2$ would have allowed us to test our hypothesis formulated above regarding the relationship between I and the metabolic cost of walking. Third, we use a reduced kinematic pelvic model with four markers to estimate the whole body COM position instead of a whole body kinematic model. However, we believe that our pelvic model is more robust than the single sacral marker method that is a too rough approximation of COM given that the latter can move with respect to the sacrum (Tesio and Rota 2019). The pelvic model is also theoretically controlled for pelvic tilt motion (Saini et al. 1998) and assume that the pelvis position could be an approximation of the whole body COM position (Wang

and Srinivasan 2014). More, the pelvic model is favoured by clinicians during routine gait analysis to reduce the experimental and postprocessing times. Therefore, we hope that the reduced kinematic pelvic model used here will be an incentive to test the existence of global stability of the whole body COM in pathological populations.

In summary, we have shown for the first time that an adiabatic invariant, I (see Eq. (5.1)), is a robust dynamical stability constraint on SI variability and predictability. In other words, the vertical speeds and positions of one individual's COM during successive walking cycles are not arbitrary but such that I is invariant. The value of the adiabatic invariant does not change during walk as expected from a mechanical model, although external perturbations (here, rhythmic auditory cues from a metronome + physiological noise) may change the latter value, arguably because a larger I is related to a larger energy expenditure in response to external perturbation. To what extent this constraint still holds in patients with motor disorders – e.g. Parkinson's disease – and unveiling its relationship with physiological mechanisms are open problems that we hope address in future work.

Author contributions **Conceptualization**, N. Boulanger, F. Buisseret, F. Dierick, O. White and V. Dehouck; **methodology**, N. Boulanger, F. Buisseret, F. Dierick, O. White and V. Dehouck; **software**, V. Dehouck, G. Henry and F. Piccinin; **formal analysis**, N. Boulanger and F. Buisseret; **data acquisition**, G. Henry and F. Piccinin; **data curation**, V. Dehouck, G. Henry and F. Piccinin; **writing–original draft preparation**, N. Boulanger, F. Buisseret, F. Dierick, O. White and V. Dehouck; **writing–review and editing**, N. Boulanger, F. Buisseret, F. Dierick, O. White, V. Dehouck, G. Henry and H. Piccinin. All authors have read and agreed to the published version of the manuscript. More information about the authors can be found in the published version: (Buisseret et al. 2022).

Chapter 6

Phase-space diffusion and human walking

6.1 Summary

In the previous study we have found adiabatic invariance to be a phenomenon present at the population level when treating gait as a realization of an harmonic oscillator. Here, we propose to look at the variability of gait through a perturbation of that oscillator. At this order, we can interpret variability as a diffusion process in phase-space.

Particularly, in this second study, we have examined a new way to model the long-range variability of walking, one that is based on the effect of noise on the theoretical model outlined in the previous experimentation. Indeed, recent developments in Hamiltonian mechanics have shown that stochastic, time-dependent perturbations influence the values of the adiabatic invariants that then obey a specific probability distribution that changes with time, informed by a Fokker-Planck equation.

As we know, it is impossible to exactly perform the same motion twice, and it is therefore expected that human walking, as framed by the vertical displacement of the body's center-of-mass as in the previous experimentation, can be modeled as a stochastically perturbed dynamical system. This would result in a diffusion in phase space, i.e. the cycle of motion is slightly deformed from one cycle to the next.

We examine this possibility by studying the gait of twenty five healthy participants walking for ten minutes at spontaneous speed. We indeed observe variability from one cycle to the next that results in diffusion in phase space that is compatible with the solution of a Fokker-Planck equation. This distribution constitutes a new tool for studying long-range variability in walk-

ing and is another constraint inherent in human walking. We hypothesize that the shape of that distribution changes with things such as age, pathology, the environments or task-specific requirements.

The content of this chapter as been published as Boulanger N., Buisseret F., **Dehouck V.**, Dierick F., White O., (2023) **Diffusion in phase space as a tool to assess variability of vertical centre-of-mass motion during long-range walking**, *Physics* DOI: 10.3390/physics5010013.

6.2 Introduction

Action-angle coordinates $(I_\alpha, \theta^\alpha)$, with $\alpha = 1, \ldots, n$, are of central importance in the study of deterministic classical systems with finitely many degrees of freedom. A time-independent integrable Hamiltonian may indeed be formulated as a separable function of the action variables only: $H = \sum_{i=\alpha}^{n} H_{0\alpha}(I_\alpha)$. The equations of motion for such a system read (Landau and Lifchitz 1988, Ch. 45):

$$\dot{I}_\alpha = -\frac{\partial H}{\partial \theta^\alpha} = 0, \quad \dot{\theta}^\alpha = \frac{\partial H}{\partial I_\alpha} =: \omega_\alpha \, . \tag{6.1}$$

The action variables are constants of the motion and therefore ω_α is also constant, implying that the angle coordinates read $\theta^\alpha = \omega_\alpha t + \theta_0^\alpha$ where $\omega_\alpha = \frac{2\pi}{T_\alpha}$ and T_α is the period of the motion in the plane $(I_\alpha, \theta^\alpha)$. Since the Kolmogorov-Arnold-Moser theorem (see (Arnold 1963; Kolmogorov 1954; Möser 1962) and (Dumas 2013) for a historical overview) and the work of Nekhoroshev (Nekhoroshev 1972, 1977), the action-angle variables have proven to be the most useful for the study of stability of dynamical systems, including chaotic systems. We now restrict our formalism to systems with $n = 1$, whose sole degrees of freedom consist in the pair (I, θ).

Suppose that H depends on a function $\lambda(t)$. The action variable I then becomes time-dependent and is called an adiabatic invariant. On the one hand, if λ changes slowly during the typical period of a cycle, then the adiabatic invariant also changes slowly: $\dot{I} \sim \dot{\lambda}$ (Henrard 1993; Jose and Saletan 1998; Landau and Lifchitz 1988). On the other hand, if λ is a perturbative stochastic noise, the adiabatic invariant also becomes randomly time-dependent and the deviation from its average value remains perturbative. Detailed demonstrations and bounds for the deviation may be found in

(Cogburn and Ellison 1992; Khasminski 1966). Moreover, for a Hamiltonian $H(I, \lambda(t))$ with perturbative stochastic noise $\lambda(t)$, it has been shown that the density $\rho(I, t)$ of the values of the adiabatic invariant as a function of time obeys a Fokker-Planck equation (Bazzani et al. 1995, 1994b; Bazzani and Beccaceci 1998). The latter phenomenon is a diffusion process in phase space. Besides its intrinsic interest, such a formalism has already found an important application in plasma physics, where it allows to relax standard simplifying assumptions and describe the problem in a less model-dependent way (Kominis et al. 2010). The Fokker-Planck equation has also been recently applied to the study of robustness in gene expression (Degond et al. 2020).

Biomechanical models of voluntary rhythmic movements in humans (of which walking has been studied most extensively) may also benefit from the above results. Such movements are quasi-periodic because of physiological noise, which prevents an individual from being in the same invariant state during repeated movements. The resulting variability has motivated many studies of human gait, most of which rely on the computation of nonlinear indices to assess variability (Hurst exponent, fractal dimension, etc.). See (Hausdorff et al. 1995; Hausdorff et al. 1997) for the pioneering studies and (Ravi et al. 2020; Stergiou 2018) for recent reviews. To our knowledge, the variability of gait has never been studied by assessing the shape and time evolution of the distribution $\rho(I, t)$. In the present work, we show that that the distribution $\rho(I, t)$ in human walking indeed obeys a Fokker-Planck equation, i.e. that diffusion in phase space is experimentally observable in walking. Biomechanical models can then inherit the advantages of this formalism.

The paper is structured as follows. In section 6.3, diffusion in phase space and its use in modelling human walking is proposed. Then, in section 6.4, the experimental setup is presented and numerical results are given in section 6.5. Finally, in section 6.6, the results are discussed and concluding remarks are given.

6.3 Diffusion in phase space

Generalities

Let us consider a one-dimensional Hamiltonian $H_0(I)$, where I and θ are the action and angle coordinates, respectively. Suppose that a time-dependent stochastic perturbation is added to H_0 and that the latter Hamiltonian satisfies the stability assumptions underlying the Nekhoroshev theorem (Nekhoroshev 1972, 1977). The total Hamiltonian H may be written as follows:

$$H = H_0(I) + \epsilon\, \xi(t)\, \mathcal{V}(I,\theta)\ , \tag{6.2}$$

where $0 < \epsilon \ll 1$, and where $\xi(t)$ is a stochastic noise with vanishing mean value. Under the dynamics controlled by H, the action variable becomes time-dependent and the deviation from the initial value I_0 is of order $\sqrt{\epsilon}$ up to a time of order $1/\epsilon$ or even better (Cogburn and Ellison 1992; Khasminski 1966). More precisely, $|I(t) - I_0| = O(\sqrt{\epsilon})$ and a time-dependent density distribution $\rho(I,t)$ of the values of the adiabatic invariant can be associated with its time evolution $I(t)$. As shown and illustrated in (Bazzani et al. 1995, 1994b; Bazzani and Beccaceci 1998), the density distribution $\rho(I,t)$ obeys a particular Fokker-Planck equation given by

$$\partial_t \rho = \partial_I (D(I) \partial_I \rho)\ , \tag{6.3}$$

where the function $D(I)$ is called the diffusion function and $\partial_I \equiv \partial/\partial_I$. Considering the Fourier decomposition $\mathcal{V}(I,\theta) = \sum_k \mathcal{V}_k(I)\, \mathrm{e}^{ik\theta}$ of the perturbation function that appears in the Hamiltonian, the following expression is obtained (Bazzani and Beccaceci 1998) for the diffusion function:

$$D(I) = \frac{\epsilon^2}{2} \sum_k k^2 |\mathcal{V}_k(I)|^2 \tilde{\phi}(k\omega)\ , \tag{6.4}$$

where $\tilde{\phi}(\nu)$ is the noise spectral density, i.e. $\tilde{\phi}(\nu) = \int_{-\infty}^{+\infty} \phi(u) \cos(\nu u)\, du$ with the autocorrelation function

$$\phi(u) = \lim_{T\to+\infty} \frac{1}{T} \int_0^T \xi(t)\xi(t+u)\, du\ . \tag{6.5}$$

Two particular cases can be highlighted. First, when $H = (\omega + \epsilon\, \xi(t))I$, only the $k = 0$ mode $\mathcal{V}_0$ is nonzero and $D = 0$. There is no diffusion in a pure harmonic oscillator with randomly perturbed frequency (Bazzani et al. 1994b). Second, in the case of constant diffusion coefficient, the normalised solution of (6.3) on the interval $I \in [0, +\infty[$ with boundary conditions $\rho(I,0) = \delta(I - I_0)\, \Theta(t)$, Θ being the Heaviside step function, and $\rho(0,t) = 0 = \lim_{I\to+\infty} \rho(I,t)$, may be obtained:

$$\rho(I,t) = \Theta(t)\, \frac{\mathrm{e}^{-\frac{(I-I_0)^2}{4Dt}} - \mathrm{e}^{-\frac{(I+I_0)^2}{4Dt}}}{\sqrt{4\pi D t}\ \mathrm{erf}\left(\frac{I_0}{\sqrt{4Dt}}\right)} = \Theta(t)\, \frac{\mathrm{e}^{-\frac{(I-I_0)^2}{4Dt}}}{\sqrt{4\pi D t}}\, \frac{1 - \mathrm{e}^{-\frac{I\, I_0}{Dt}}}{\mathrm{erf}\left(\frac{I_0}{\sqrt{4Dt}}\right)}\ . \tag{6.6}$$

The normalisation is such that $\int_0^{+\infty} \rho(I,t)\, dI = \Theta(t)$. Hereafter, we will be interested in the second case of a constant but non-vanishing diffusion fonction.

For a general discussion about the construction of solutions of the Fokker–Planck equation, see (Risken and Caugheyz 1991), and (Fa 2005; Lin and Ho 2012) for explicit solutions with non-constant and nonzero diffusion and drift coefficients.

Application to human walking

It is known that the vertical displacement of the body's centre-of-mass (COM) during human bipedal walking at spontaneous speed is compatible with a simple, spring-mass-like, model, see for example the seminal work (Cavagna et al. 1976). It is therefore tempting to model the vertical motion of the COM by the harmonic oscillator Hamiltonian $H_0 = \frac{1}{2}(P^2 + \omega^2 Q^2) = \omega\, I$, where P and Q are the vertical momentum and position of the COM, respectively. By definition, and assuming the standard relation $P \propto \dot{Q}$, one has

$$I = \frac{1}{2\pi} \oint_\Gamma P\, dQ = \frac{T\overline{E_c}}{\pi} , \tag{6.7}$$

with Γ a cycle in phase space, T the duration of the cycle and $\overline{E_c}$ the averaged kinetic energy over Γ.

Some phenomena suggest that the inclusion of other terms, at least in the perturbation, is necessary to obtain a more realistic model. First, the minimum (maximum) of the potential energy and the maximum (minimum) of kinetic energy are not reached at exactly the same time: a time shift of about 3 % of the gait cycle duration is observed (Cavagna and Legramandi 2020). Such a feature requires a time-dependent correction to be added. Second, the Hamiltonian H_0 corresponds to a linearised pendulum only in the limiting case of small amplitudes. Anharmonic corrections should be added. The interested reader will find in (Whittington and Thelen 2008) a more explicit model of the pendulum in which the potential term is nonlinear, and in (Brizard 2013) a computation of action-angle variables for the fully non-linear pendulum with Hamiltonian $H_0 = \frac{P^2}{2} + 1 - \cos Q$. Third, the parameters of the model (ω in our case) must have some time-dependent variability due to physiological noise; the state of a complex system like the human body is not identical from one gait cycle to another.

In view of the above discussion, a Hamiltonian of the form (6.2) in which H_0 is not a pure harmonic oscillator seems to be a relevant model of the vertical COM dynamics in action-angle formalism. As far as the perturbation $H_1(I, \theta) = \epsilon\, \xi(t)\, \mathcal{V}(I, \theta)$ is concerned, we will consider the simplest nontrivial ansatz with a constant but non-vanishing diffusion coefficient D. Referring to (6.4), this implies that all the functions $\mathcal{V}_k(I)$ are constant so that $H_1(I, \theta)$

only depends on the angle variable θ. It does not depend on the total amount of action or energy in the system but only on time through the stochastic noise $\xi(t)$ and on the position in the cycle through $\mathcal{V}(\theta)$. Therefore, we assume that the influence of physiological noise on walking is related to the position in the gait cycle and not to the total action or the averaged kinetic energy of the walker – recall that $I \sim \overline{E_c}$.

Consequently, Eq. (6.3) with a nonzero diffusion coefficient yields the heat equation

$$\partial_t \rho = D\, \partial_I^2 \rho \,, \tag{6.8}$$

and the diffusion of the adiabatic invariant should be observable experimentally.

6.4 Experimental setup

Protocol

The protocol was validated by the Academic Ethical Committee Brussels Alliance for Research and Higher Education (B200-2021-123). Participants were healthy students recruited in the physiotherapy department of the Haute-Ecole Louvain en Hainaut (Montignies-sur-Sambre, Belgium). After being informed about the study, each participant signed an informed consent form.

Biometric data were first collected (age, weight, height), as well as information on the wearing of orthopaedic insoles and the participant's medical and trauma history. The participant is then asked to put on a tight-fitting garment. In order for his or her movements to be recorded by a Vicon optoelectronic system (Vicon Motion Systems Ltd, Oxford Metrics, Oxford, UK) consisting of 8 cameras (Vero v.2 .2) with a recording frequency of 120 Hz, 4 reflective markers with a diameter of 14 mm were placed on the participant according the Plug-In-Gait model (Oxford Metrics, Oxford, United Kingdom): Left Anterior Superior Iliac Spine [LASI], Right Anterior Superior Iliac Spine [RASI], Left Posterior Superior Iliac Spine [LPSI], and Left Posterior Superior Iliac Spine [RPSI].

After this preparatory phase, the participant walked for 3 minutes on an N-Mill instrumented treadmill (Motekforce Link, The Netherlands). The purpose of this familiarisation phase is to determine the participant's spontaneous walking speed. No other data were recorded during this period. After the walking speed was recorded, the participant walked on the treadmill for 10 minutes at the previously determined spontaneous speed. During these 10 minutes, the average number of steps per minute was measured by

Table 6.1: Features of the population. Results are written under the form median [Q1–Q3], with Q1 and Q3 being the first and third quartiles, respectively.

Participants (n)	25
Age (years)	23 [20−23]
Mass (kg)	65.0 [58.8−73.4]
Height (cm)	169 [164−176]
Walking speed (km/h)	3.9 [3.5−4.2]
Sex (men/women)	9/16
Gait cycles	532 [513-552]

the treadmill and the three-dimensional trajectory of the 4 markers, $\vec{x}_a(t)$, was recorded by the Vicon system using the Vicon Nexus software (v.2.7.1, Oxford Metrics, Oxford, UK).

The general characteristics of our participants are listed in Table 6.1. Let us not that an initial analysis of these data was presented in a recent work (Buisseret et al. 2022), in which we showed that an adiabatic invariant exists in the vertical motion of the COM. Here we go further in the analysis to assess whether or not the variability of the latter adiabatic invariant is modelled by Eq. (6.8).

Data processing

For a given participant, the position of the centre-of-mass is defined as the average position of the four markers: $\vec{x}_{COM} = \sum_a \vec{x}_a/4$. A focus in the study here is on the vertical component of the COM motion, $Q(t)$. To reduce measurement artefacts, $Q(t)$ was filtered with a fourth-order Butterworth low-pass filter, preserving 99.99% of the signal power. Cubic spline interpolation of the data was also performed, multiplying the frequency by 10 to 1200 Hz. The speed $\dot{Q}$ is computed from the time series Q by finite differentiation.

An identification $P = \dot{Q}$ is performed, i.e., we assume standard Hamiltonian dynamics and set the mass scale equal to 1 (this normalisation removes the variability induced by participants' masses). We then identify gait cycles by analysing the peaks in $Q(t)$: The duration of gait cycles i, $T_i = t_{i+2} - t_i$, were computed from the times t_i at which the peaks occur. The times t_i may be defined as the times at which a new step begin, a gait cycle consisting in two steps (left and right). Then the average kinetic energies, $\overline{E_{ci}}$, were computed as the mean values of $\dot{Q}^2/2$ on the successive cycles, and the adiabatic invariants

$$I_i = \frac{T_i \overline{E_{ci}}}{\pi} \tag{6.9}$$

were also computed.

The values collected in the sets $A_i = \{I_{j \leq i}\}$ are then binned according to Sturges rule (Sturges 1926), leading to n bins. The centres $I_a^{(i)}$ and frequencies $\varphi_a^{(i)}$, i.e. the number of items in bin$a$ divided by total number of items, are computed, with $a = 1, \ldots, n$. The experimentally computed distribution $\rho^{\text{exp}}(t_i, I)$ of the adiabatic invariant after a walking duration t_i is defined via $\rho^{\text{exp}}(t_i, I) = \left(I_a^{(i)}, \varphi_a^{(i)}\right)$.

A fit of the form (6.6) is then performed on the sets $\rho^{\text{exp}}(t_{i \geq 100}, I)$ using the least-squares method and the parameters I_{0i} and D_i are recorded. The latter parameters are the fitted values of I_0 and D at time t_i. No fit was made for the first 100 points. This threshold is arbitrary but avoids situations where the distribution has too little structure for the adjustment to be relevant. Finally, we compute the average values $I_0 = \boldsymbol{E}(I_{0i})$ and $D = \boldsymbol{E}(D_i)$, resulting in a distribution (6.6) called the model, $\rho^{\text{th}}(t, I)$.

The compatibility of the experimental distributions $\rho^{\text{exp}}(t_{i \geq 100}, I)$ and the model predictions $\rho^{\text{th}}(t_i, I)$ is assessed by a Kolmogorov-Smirnov test with a significance level 0.05. Let us note Π, the percentage of tests with $p > 0.05$, i.e., the percentage of cases in which the model is incompatible with the experimental data. One-sample t-tests were performed with null hypothesis of zero mean for I_0 and D.

All the above computations were performed using the free software R (R Core Team 2021, p. v. 4.1.0).

6.5 Results

The attractors of the centred vertical position and speed of the COM versus time are shown in Fig. 6.1 A and B, and a typical phase space trajectory is also shown in Fig. 6.1 C. The attractor is computed as follows. After each step cycle is identified, an average cycle is computed. For this purpose, each step was normalised to a duration of 1 time unit (0–100%). Then 1200 bins, one for each frame, were created and filled with the data of all steps of a given participant under a given condition. For each bin, the mean and standard deviation were computed. This yields the average cycle, which we refer to as the attractor, following works such as those of (Broscheid et al. 2018; Raffalt et al. 2020). The attractor may be interpreted as the basic motor pattern that a participant tries to achieve during each step cycle – without achieving

it exactly due to intrinsic physiological noise.

From the attractor, it is easy to see that the effective dynamics is not a pure harmonic oscillator, as it moves away from an elliptical shape in the first quadrant (indicated by a straight arrow in Fig. 6.1 C).[1] The deformation is systematic and present in all participants. Therefore, the model presented in section 6.3 may be applied since the diffusion coefficient can be nonzero. Here, each step cycle starts when the COM is at its higher position and its speed is null, i.e., when the subject is in midstance: one foot on the ground, the knee is extended and the other foot is in swing phase and crossing the stance leg. The direction of the trajectory of the COM in phase space is clockwise: from fourth to first quadrant. In the fourth and third quadrants, the COM position decreases (downward movement) and the speed is negative. The attractor shape is elliptical as in a spring-mass model of the stance leg (Whittington and Thelen 2008), inducing a harmonic motion. In the second and first quadrants, the COM position increases (upward movement) and its speed is now positive. In the fourth quadrant, the participant is in single leg stance (SS) on one foot and this phase continues during the first part of the third quadrant. In the second part of the third quadrant, the participant is in dual stance (DS), that begins when the COM speed is at its lowest value and ends when the COM postion is at its lowest value (Adamczyk and Kuo 2009). At the end of the second quadrant and the first one, the participant is in single leg stance on the other foot.

Table 6.2: Results of the fits of experimental distributions of the adiabatic invariants to model (6.6). Results are written under the form median [Q1−Q3]. The $p-$values of the one-sample t-tests are given in the last column.

D (10^{-9} m^2/s)	11.618 [6.024−37.712]	<0.001
π I_0 (J.s/kg)	0.0123 [0.0061−0.0178]	<0.001
Π (%)	100 [98.6-100]	

It appears that the fit is relevant since $\Pi > 97\%$ for 20 participants out of 25. Hence, the model (6.6) fairly well agrees with the time evolution of the distribution of the adiabatic invariant. Fitted parameters are summarized in Table 6.2. The mean value of I reads

$$\langle I \rangle = \int_0^{+\infty} \rho(I,t) dI = \frac{\Theta(t)}{\mathrm{erf}\left(\frac{I_0}{\sqrt{4Dt}}\right)} \, I_0 \, , \tag{6.10}$$

[1] We use the trigonometric convention in order to split the plane into four quadrants, with the angle going from 0 to $\pi/2$ in the first quadrant, from $\pi/2$ to π in the second quadrant, etc.

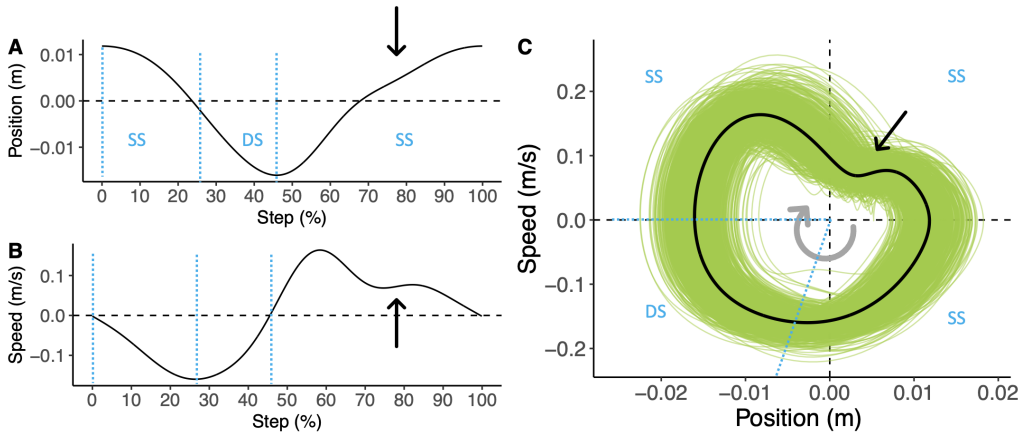

Figure 6.1: A: Attractor of the centred vertical position of the COM versus time, expressed in % of step time. B: Attractor of the vertical speed of the COM versus time, expressed in % of step time. C: Typical plot of COM vertical trajectory in phase space (solid green lines representing 508 gait cycles) during walking for a participant and of the corresponding attractor (solid black line). The straight arrows outline the deviation from genuine harmonic oscillator. The curved arrow is the arrow of time. Note that a closed loop corresponds to one step cycle, a complete gait cycle being composed of two step cycles. The blue dotted line separate the single stance (SS) and dual stance (DS) phases.

and its behaviour versus time is displayed in Fig. 6.2. The mean value stays of order I_0 during the protocol: Less than 10 % of variation is observed. The values obtained are comparable to the mean value found by an independent analysis in (Buisseret et al. 2022): $\pi\, I$ =0.0143±0.0058 J.s/kg.

The ability of the model to fit the data can be appraised in Fig. 6.3, where a typical plot of the fitted distributions versus experimental observations is displayed for one participant. All participants show the same qualitative agreement between the model and the data.

6.6 Discussion

By studying the vertical motion of the healthy participant during walking, we have shown that the phenomenon of phase space diffusion can be observed through the distribution of adiabatic invariant values over time. To our knowledge, this is the first time that such an observation is made in human motion.

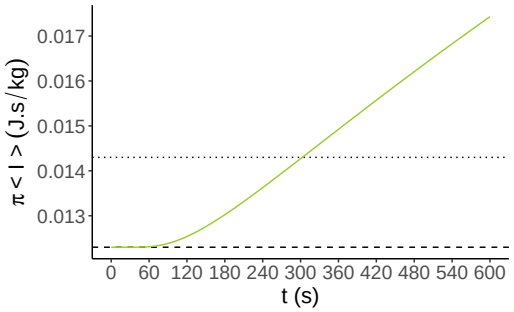

Figure 6.2: Plot of $\pi \langle I \rangle$ versus time (green line). The median value given in Table 6.2 is indicated (dashed line), as well as the average value found in (Buisseret et al. 2022) (dotted line).

The time evolution of the distribution of the adiabatic invariant over time is compatible with the Fokker-Planck equation with constant diffusion coefficient for healthy young adults walking at spontaneous speed of progression. Thus, up to our experimental precision, we observe no drift and no deformation of the constant-D distribution for high or low values of I. A change in the most likely value of I can presumably be associated with a change in energy expenditure during walking. As argued in (Buisseret et al. 2022), the value of the adiabatic invariant should be proportional to oxygen consumption during walking, and an increase in the former should be associated with an increase in the latter.

There are a number of immutable factors in the environment in which we live. One is gravity. The brain, instead of fighting against the effects caused by its presence (e.g. the emergence of a weight that counteracts movements) has developed strategies to make the most of it and optimize movements (White et al. 2020). In other words, humans move more optimally in the presence than in the absence of a gravitational field. One can make a parallel with the existence of noise in physiological systems. These emerge at every level of the decision-action chain, from perception to motoneurons. Authors have proposed in the optimal movement variability framework, that the central nervous system could actually exploit the presence of noise and hence, act more optimally in the presence of certain levels of uncertainties. Following (Emmerik et al. 2016; Goldberger et al. 2002; Stergiou et al. 2006) we interpret the variability measured by the distribution not as an "imperfection" but rather as an indication of the adaptability of the participants to the motor task. A given value of the adiabatic invariant corresponds to a given area in phase space for the step cycle under consideration. Thus, the changes in I indicate that the participants have access to a wide range of

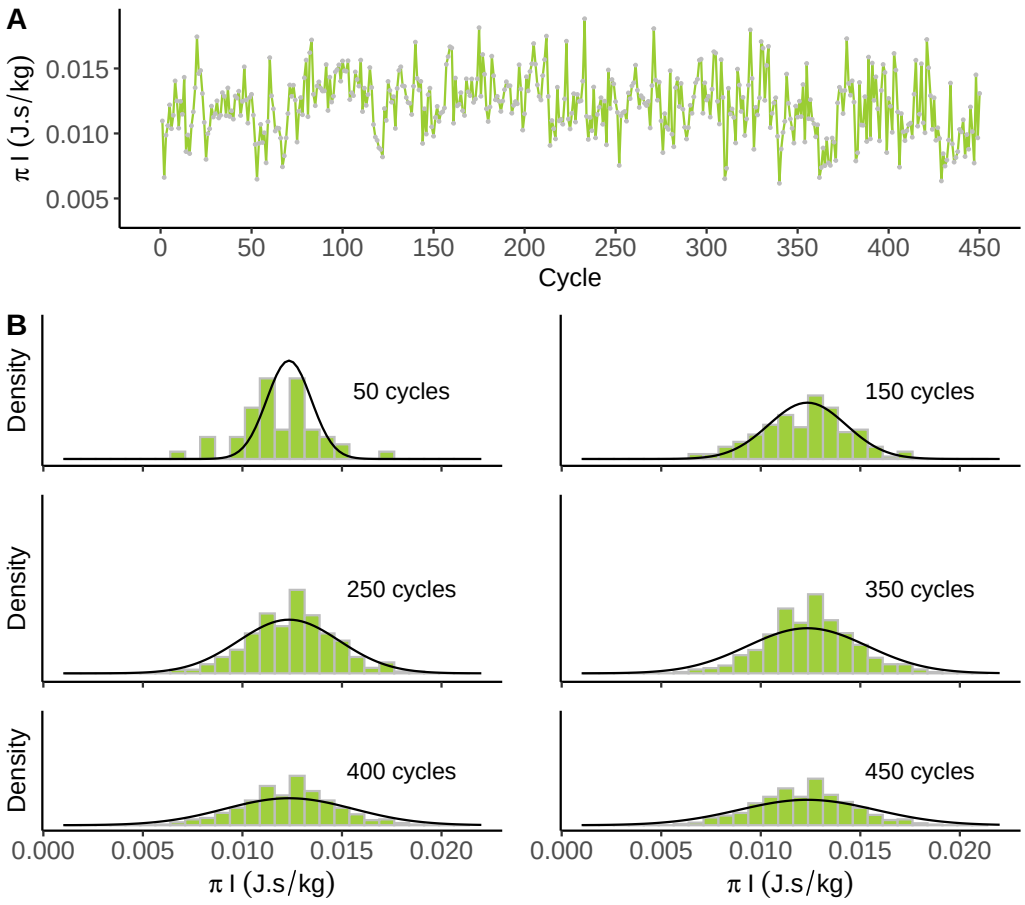

Figure 6.3: A: Adiabatic invariant versus time (gray points) for a given participant. Lines are added to guide the eyes, and time is expressed in cycle number. B: Typical plots showing the comparison between the theoretical distribution $\rho^{\text{th}}(t_i, I)$ (solid line) and the experimental one $\rho^{\text{exp}}(t_i, I)$ (histograms) after 50, 150, 250, 350, 400 and 450 cycles for the same participant as in A, with $\Pi = 99.4\%$. Fitted parameters are equal to $\pi\, I_0 = 0.0123$ J.s/kg and $D = 1.05\, 10^{-8}$ m^2/s.

motor strategies, visualised as closed step cycles in phase space. The distribution becomes wider and wider over time: more and more different motor patterns are "explored". In the approach given in this paper, there is no drift: the most likely value of I, i.e. the attractor defined as the ideal trajectory in phase space that the participant is aiming for, does not change with time.

We conjecture that the shape of the distribution $\rho(I, t)$ might be sensitive to the experimental condition and/or to each participant, as shown in Fig.

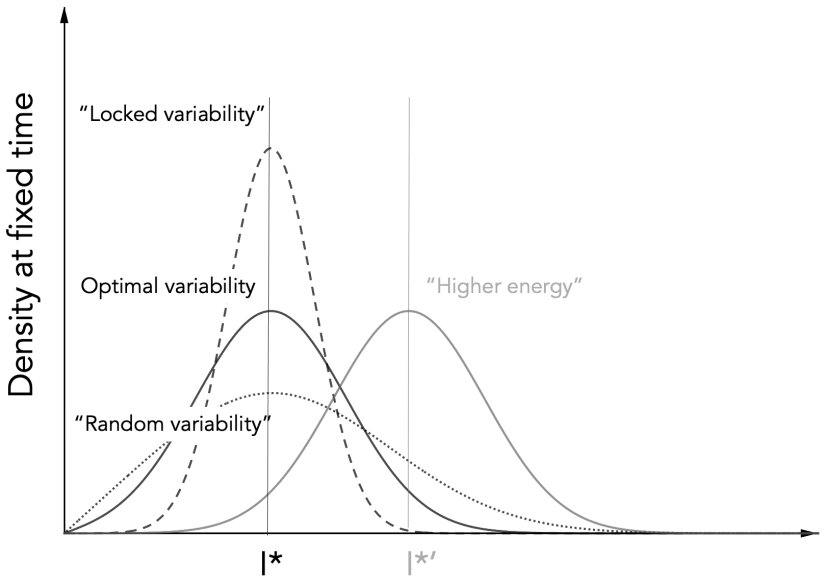

Figure 6.4: Schematic representation of several types of adiabatic invariant densities. Here is assumed that the black solid line is the density of a young, healthy, individual. The "locked" (dashed line) and "random" (dotted line) curves correspond to, respectively, smaller and higher diffusion coefficients than the optimal one. The "higher energy" curve (gray solid line) has an optimal diffusion coefficient but a higher maximally probable I^*, denoted $I^{*\prime}$ on the horizontal axis.

6.4. In particular, there should be an optimal value for the diffusion coefficient D and for I_0 for a young, healthy individual. Too large a value for D would reflect a lack of or altered motor control of the participant, leading to variability that tends to be random, as observed in stride interval variability of patients with neurodegenerative diseases (Moon et al. 2016) for example. Too small a value for D could be related to insufficient adaptability of the participant: the number of available patterns (i.e. different values of I) is not maximal. Such a case is observed, for example, in the electrocardiographic signal of patients with cardiovascular disease (Goldberger et al. 2002) or in healthy children, whose walking patterns are more stereotyped than in adults (Hausdorff et al. 1999). The diffusion coefficient then offers a novel way to quantify the general behaviour of internal models developed for a given task. Indeed, wide distribution (high D) are observed after time spent to experience or explore a task. On the other hand, narrow distributions (small D) may reflect a lack of generalisation of the motor strategies adopted. In motor control – and rehabilitation in particular – the concept of generalisa-

tion is tightly linked to the one of transfer (Criscimagna-Hemminger et al. 2003; Dizio and Lackner 1995; Sarwary et al. 2015). When working toward recovering lost or impaired motor functions, the challenge is to find the best possible movements that may be transferred to as many functional tasks as possible. These movements may be interpreted as fundamental bricks of the action repertoire. An interesting question is why would a participant opt for a narrow distribution? One possible explanation for this is related to the way motor learning works. There are different learning mechanisms, the most powerful being error-based learning. In this one, one plans the best possible action by minimising a cost function that includes target reaching in the general sense and effort. An error signal is observed in case of discrepancy between observation and what has been predicted by forward models (Shadmehr and Mussa-Ivaldi 1994; Thoroughman and Shadmehr 2000) which induces strategic changes, and encourage exploration. Another learning mechanisms, however, co-exists, with a slower dynamics: use-dependent-learning. When relying on this mechanism, one tends to repeat the same action if it led to success in the past, thereby discouraging exploration in task space. Adopting this strategy results from a compromise between cost and benefit: the target may be reached, but the control policy may be stuck in a local minima of the cost function.

We hope to apply the present formalism to participants with different ages or experimental conditions to investigate the effects of deviations from the optimal "healthy young adult state" on $\rho(I, t)$ in future work. More precisely, we hope to design appropriate experimental contexts that would manipulate I and D independently, then providing a better functional understanding of these indexes in motor control.

Acknowledgements The authors thank G. Henry and F. Piccinin for data acquisition.

Author contributions **Conceptualization**, N. Boulanger and F. Buisseret; **methodology**, F. Buisseret and V. Dehouck; **software**, V. Dehouck and F. Buisseret; **formal analysis**, N. Boulanger and F. Buisseret; **data curation**, V. Dehouck; **writing–original draft preparation**, N. Boulanger, F. Buisseret and V. Dehouck; **writing–review and editing**, N. Boulanger, F. Buisseret, F. Dierick, O. White and V. Dehouck. All authors have read and agreed to the published version of the manuscript. More information can be found about the authors in the published version: (Boulanger et al. 2023).

Chapter 7

Rhythmic arm motion in centrifuge

7.1 Summary

In this third experiment, we have investigated the true potential of adiabatic invariants, namely their capacity to describe changes in the system when its parameters vary slowly with time, which is a typical limitation of biomechanical models of motion. While there are many candidate parameters to fluctuate during motion, one of the most fundamental quantity for motion on Earth, gravity, appears as a natural candidate as it is routinely taken into account by the central nervous system to optimize motion. Nonetheless, very few people have experienced environments outside of 1 g for extended periods of time, and probing those environments might provide insights as to how the nervous system copes.

To achieve that goal, we have exposed six participants to two sessions of centrifugation, such that the acceleration along the body axis varied from one to three g. During those sessions participants performed voluntary rhythmic one-dimensional motion with their forearm at a free pace.

While participants have never experienced such gravitoinertial environments, we now observe a linear relationship between the adiabatic invariant and gravity, as expected from adiabatic theory. This further highlights the fact that adiabatic invariants seem to reveal generic hidden constraints of motion, naturally taken into account in time-varying environments.

The content of this chapter as been published as Boulanger N., Buisseret F., **Dehouck V.**, Dierick F., White O., (2020) **Adiabatic invariants drive rhythmic human motion in variable gravity**, *Physical Review E* DOI: 10.1103/PhysRevE.102.062403.

7.2 Introduction

All living organisms experience a constant terrestrial gravitational acceleration, denoted as $1g$ (9.81 m/s^2). Gravity, "the first thing which you don't think" (A. Einstein), is the most persistent sensory signal in the brain. However, the sensory experiences it generates lack the clear phenomenology of an identifiable stimulus event that characterises sound, sight and even taste. Critically, gravity influences human behaviour more pervasively than any other sensory signal. Exposure to Earth-discrepant gravity – as during spaceflight – leads to dramatic structural and functional changes in the human physiology, including alterations in the cardiovascular (Aubert et al. 2016), neural (White et al. 2016) and musculoskeletal systems (Lang et al. 2017). Nowadays the cerebellum appears to be a major structure in gravity perception (Angelaki et al. 2004; MacNeilage and Glasauer 2018). From experiments done on rhesus monkeys, the latter reference reports on results showing the relevance of the cerebellum in the detection of the gravitational field and inertial motions. This includes the neural network analyses sensed by the otolith organs in the inner ear, see (Angelaki et al. 2004) and refs. therein.

Recent neurocomputational approaches explain behaviour by a mixture of feedback and feedforward mechanisms, conceptualized by internal models (Kawato 1999): the brain plans an action using available sensory information and makes predictions about the consequences of that action in the environment. Any mismatch between this prediction and the information conveyed by feedback will yield a prediction error used to improve other actions. This mechanism drives motor adaptation. On Earth, gravity is immutable and plays a primary role in minimizing prediction errors by providing a strong prior reference.

What is the best way to fundamentally address the role of gravity in motor control? One approach consists in challenging the brain by changing a feature of the environment that is never supposed to change: gravity itself. Our original approach is to assess the impact of time-changing gravity on rhythmic biological motion from a purely mechanical vantage point, thereby providing further insights into the fundamental representation of gravity that shapes motor actions. In Mechanics, the more robust way to track the adaptation of a dynamical system to a slow change in the external conditions

is through the study of adiabatic invariants and their related action-angle variables describing the system, see *e.g.* (Landau and Lifchitz 1988) and Sec. 7.3.

Obviously, living organisms are extraordinarily more complex than a simple point-particle body. It is not at all clear a priori that the actions of a minded human being can be reduced to a standard, simple Lagrangian. Let us give an everyday example: Lifting a glass of water off a table requires estimating its weight to adjust the grasping force accordingly. Drinking half of its content with a straw while the glass rests on the table does not, however, allow the brain to program a smaller grasping force, more adapted to the lighter glass (Nowak and Hermsdörfer 2003). Explicit knowledge of the simplest change in object dynamics is not sufficient to update internal models, and one can hardly hope to model such behaviours by a standard Lagrangian or Hamiltonian. Nevertheless our working hypothesis is that some human actions, one of them being presented in Sec. 7.4, comply with the behaviour of a simple mechanical system, even if subject to a slowly changing environment, like a slowly varying gravitational field.

7.3 Adiabatic invariants and human motion

An adiabatic invariant determines a property of a system that stays approximately constant when external changes occur slowly. Despite their power in revealing constraints on complex dynamical systems, adiabatic invariants have been poorly investigated in biomechanics. For instance, in arm rhythmic motion, the changes in frequency (df) occurring during a one-dimensional periodic motion are correlated with changes in energy (dE) (Turvey et al. 1996) such that the action variable

$$I = \frac{1}{2\pi}\frac{dE}{df} \tag{7.1}$$

is constant. Action-angle coordinates are usually adopted when the Hamiltonian does not depend explicitly on time. The present work goes beyond previous approaches by immersing participants in a time-dependent gravitational environment where the action variables are not necessarily constant unless the changes in time are adiabatic.

The action-angle variables appeared in the context of classical mechanics in order to study the integrability of dynamical systems with finitely many degrees of freedom. Such systems are said to be *integrable* if the Hamilton-Jacobi equation describing them is completely separable. In the early sixties, the famous Kolmogorov-Arnold-Moser theorem — see (Dumas 2013) for a

very interesting book telling the history behind this theorem — brought back the action-angle variables on the scene of classical Mechanics in order to characterise chaotic Hamiltonian systems. Since then and with the seminal works of Nekhoroshev (Nekhoroshev 1972, 1977) their importance has never faded out. When a Hamiltonian $H(P_\alpha, Q^\alpha)$, $\alpha = 1, \ldots, n$, is integrable and leads to bounded trajectories in phase space, action variables may be defined as follows, in terms of a set of phase-space coordinates that separates the Hamiltonian:

$$I_\alpha = \frac{1}{2\pi} \oint_{\Gamma_\alpha} P_\alpha \, dQ^\alpha \ , \tag{7.2}$$

where Γ_α is the projection of the bounded trajectory in the plane (P_α, Q^α) for fixed α. Once the Hamilton-Jacobi equation is separated in the variables (Q^α, P_α), on the solution of Hamilton's canonical equations each momentum variable P_α will depend only on its canonically conjugate variable Q^α and on the initial conditions. The action variables give all the conserved quantities of the dynamical system under study, as certified by the Bour-Liouville theorem. They can be geometrically interpreted as the area enclosed by Γ_α.

If the Hamiltonian is time-dependent and slowly varying in comparison with the typical period of a cycle, then the action variables are slowly varying too. They are called adiabatic invariants (Henrard 1993; Jose and Saletan 1998; Landau and Lifchitz 1988) and may be used in a wide range of applications such as in electromagnetism (Tennyson et al. 1986), plasma physics (Notte et al. 1993) and cosmology (Cotsakis et al. 1998). Previous works in biomechanics showed the invariance of the action variable when experimental conditions are time-independent (Kadar et al. 1993; Kugler et al. 1990; Turvey et al. 1996). To the best of our knowledge, this concept has never been applied to human motion in time-varying environments. Our approach can reveal the important and otherwise hidden quantities on which the brain relies to plan actions. Advances in this field can potentially not be reached with other, more classical, methods that rest on energy conservation (Alexander 1997). We therefore designed an experimental set up in which external factors are time-dependent. It is described in the next section, together with its mechanical model.

7.4 The experiment

Setup

Six right-handed male participants (40.1 ± 7.2 years old) took part in two centrifugation sessions at QinetiQ's Flight Physiological Centre in Linköping, Sweden. The centrifuge was controlled to deliver specific $g(t)$-profiles. The real-time control of the orientation of the gondola ensured alignment of local gravity with the long body axis (Fig. 7.1 inset). One session of centrifugation consisted in a ramp up followed by a ramp down $g(t)$-profile for 180s. There were two equivalent sessions separated by a five-minute break bringing the centrifuge back to idle position. The initial $1g$ phases (idle) lasted for 27.4s. Then, the system generated $1.5g$, $2g$, $2.5g$, $3g$, $2.5g$, $2g$, $1.5g$ and $1g$. Each phase lasted 18.4s and transitions lasted 1.6s (average rate of $0.31g$/s), except for the first and last ones. We label a given transition by $T_n^{\pm}$ where it is meant that $g(t)$ goes from the value $(n+1)g/2$ to the value $(n+1+\eta)g/2$, with $\eta = \pm 1$. The increasing (decreasing) gravitational transitions correspond to $\eta = +1$ (-1). In both cases, $n \in \{1, 2, 3, 4\}$. The first decreasing-g series is T_4^- while the last one is T_1^- (Fig. 7.1). A medical flight doctor assessed the participant's health status before the experiment.The clinical examination consisted in the recording of an electrocardiogram and the measurement of arterial pressure in addition to a health questionnaire that aimed at estimating life style (smoker, sport activities etc). The protocol was reviewed and approved by the Facility Engineer from the Swedish Defence Material Administration (FMV) and an independent medical officer. The experiment was overseen by a qualified medical officer. The study was conducted in accordance with the Declaration of Helsinki (1964). All participants gave informed and written consent prior to the study. A similar protocol was used in a previous study where the human centrifuge is described in detail (White et al. 2018).

Participants were ask to perform upper arm rhythmic movements about the elbow at a free, comfortable pace and amplitude only during the transitions between gravitational environments, to limit fatigue. The elbow was first in contact with the support. When prompted by a GO signal, the participant started to perform the movement while holding a test object. This wireless test object (mass of 0.13 kg) embedded an accelerometer that measured combined gravitational and kinematic accelerations along the object's long axis (AIS326DQ, range 30m/s^2, accuracy $\pm$0.2m/s^2). The acceleration signal was sampled at a frequency of 120Hz. The upper arm produced movements of about 30^o with the horizontal. When the operator announced the STOP signal, the participant gently let the object touch the support again

while still securing it with his hand. A schematic representation of raw data (acceleration vs time) of one session for one subject is displayed in Fig. 7.1. We refer the interested reader to (White et al. 2018) for more detail and pictures about the experimental setup.

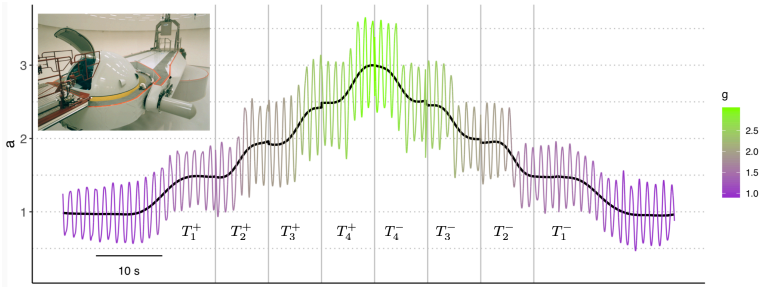

Figure 7.1: Typical plot of raw data recorded by the accelerometer (coloured line) during a single session of centrifugation (inset). The black line depicts local gravity. All measured accelerations are expressed in units of $g = 9.81$ m/s^2. The plateau phases are shown for the first and last transitions. For the other transitions, plateau phases and rest periods are not displayed for the sake of clarity but are replaced by vertical lines.

Harmonic oscillator and participant's motion

Accelerations $a(t)$ were numerically integrated and linearly detrended after subtraction of $g(t)$ to yield the object's speed and position $x(t)$. The link

$$a = -\omega^2 \, x \tag{7.3}$$

is observed for all participants within a given transition (96 time series): averaged Pearson's correlation coefficient between a and x is indeed equal to -0.82 ± 0.1. A typical plot is shown in Fig. 7.2; the behaviour observed for all the participants is similar. In average, $\omega = 6.3$ Hz leading to a typical period of T= 0.99 s. Hence, we are on safe grounds to assume that the effective dynamics of the test object along the body axis is compatible with that of a harmonic oscillator, *i.e.*, with a Hamiltonian of the form

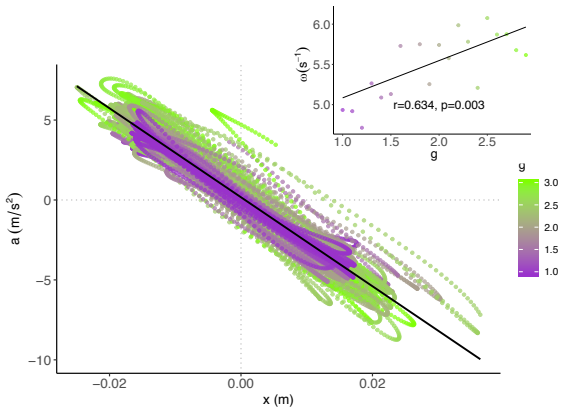

Figure 7.2: Typical plot of acceleration versus position for the test object during one centrifugation session, same participant as Fig. 7.1 (coloured points). A global linear regression is shown (solid line). The inset quantifies the significant linear relationship between ω and g. Dots result from a fit of the form (7.3) by bins of 0.1 g.

$$H = \frac{P^2}{2} + \frac{1}{2}\omega(t)^2 Q^2 \ , \quad \text{with} \quad P = \dot{Q} \quad \text{and } Q = x \ . \tag{7.4}$$

The parameter of model (7.4) is the function $\omega(t)$. Careful inspection of experimental data let us conclude that $\omega(t)$ versus $g(t)$ is compatible with a weakly increasing linear shape, see Fig. 7.2 inset. Hence we assume

$$\omega(t) = \varpi \left(1 + \frac{\epsilon}{g}\, g(t)\right) \tag{7.5}$$

and we will perform computations up to first order in ϵ through the rest of the paper. Equation (7.5) has the following physiological interpretation: muscle stiffness increases with gravitational acceleration to account for the larger motor commands required to perform the same movement. This leads to a modified frequency and to $\epsilon > 0$.

Figure 7.3 depicts a typical phase-space of a complete centrifugation session. Elliptic cycles are clearly visible and are the consequence of the harmonic-oscillator dynamics. The area of these ellipses is slowly changing with g as expected from adiabatic invariant's theory (Landau and Lifchitz 1988) that we now use to model the experiment described above.

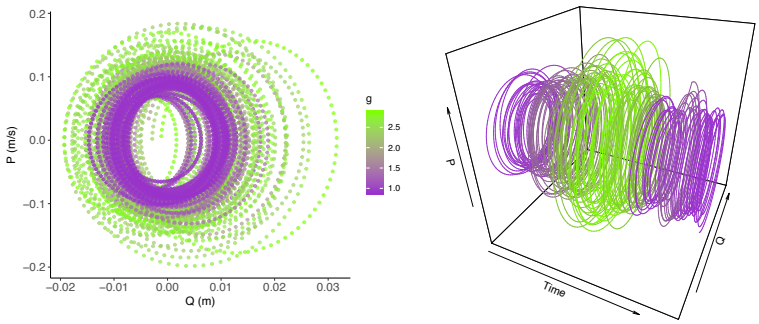

Figure 7.3: Left panel: Typical phase-space plot of the test object trajectory during one centrifugation session, same participant as Fig. 7.1. Right panel: Same data but the consecutive cycles are now unfolded along the time dimension.

The model

Let us now focus on a given transition $T_n^{\pm}$. Equation (7.5) can be adapted to the peculiar shape of $g(t)$ imposed during the centrifugation, compatible with

$$\begin{aligned} \omega_n(t) &= \varpi_n\,(1+\epsilon\,s(t))\ , \quad \varpi_n = \omega_0\Big(1+\frac{\epsilon}{2}\,(n-\tfrac{1}{2})\Big)\ , \\ s(t) &= \frac{\eta}{4}\,\sin(\Omega t)\ ,\ \eta=\pm 1\ , \quad \text{with } t\in\Big[-\frac{\pi}{2\Omega},\frac{\pi}{2\Omega}\Big]\ . \end{aligned} \tag{7.6}$$

Action-angle coordinates (I,ϕ) may be defined from (7.4) through the standard definition (Landau and Lifchitz 1988)

$$Q=\sqrt{\frac{2I}{\omega}}\sin\phi\ ,\ P=\sqrt{2I\omega}\cos\phi \tag{7.7}$$

and their equations of motion read

$$\dot I=-\frac{\dot\omega}{\omega}I\,\cos 2\phi\ ,\ \dot\phi=\omega+\frac{\dot\omega}{2\omega}\sin 2\phi\ . \tag{7.8}$$

We have shown in (Boulanger et al. 2019) that $I(t)$ and $\phi(t)$ can be analytically computed at order ϵ from Eq. (7.8) when $g(t)$ is of trigonometric form. This gives

$$I(t) = \bar{I}\left[1 - \epsilon\,\eta\,\frac{\Omega}{16}\left(\frac{1}{\omega^+}\sin[2(\omega^+ t + \alpha)] + (+ \leftrightarrow -)\right)\right] , \tag{7.9}$$

$$\phi(t) = \alpha + \varpi_n t - \epsilon\,\eta\,\frac{\omega_0}{4\Omega}\cos(\Omega t) - \epsilon\,\eta\,\frac{\Omega}{32}\left(\frac{1}{\omega^+}\cos[2(\omega^+ t + \alpha)] + (+ \leftrightarrow -)]\right) , \tag{7.10}$$

with $\omega^\pm = \omega_0 \pm \frac{\Omega}{2}$ and $\omega_0 > \Omega$.

The action variable takes a simpler form when $P = 0$, *i.e.* for t_k such that

$$\phi(t_k) \;=\; (2k+1)\pi/2 =: \phi_k , \quad k \in \mathbb{Z} , \tag{7.11}$$

see Eq. (7.7). The analytical shape of the times t_k such that $\phi(t_k) = \phi_k$ may be complicated but since our goal is the computation of $I(t_k)$, it is sufficient to work with the lowest order solution $t_k = \frac{\phi_k - \alpha}{\omega_0}$, leading to

$$I(t_k) = \bar{I}\left(1 - \epsilon\,\frac{\Omega^2}{4\omega_0^2 - \Omega^2}\,s(t_k)\right). \tag{7.12}$$

For a given transition $T_n^\pm$, $g(t)/g = \frac{n+6}{2} + s(t)$. Hence, $I(t_k) = A_{n,\eta} + B\,g(t_k)$, where $A_{n,\eta}$ and B are real constants, and where $B = dI/dg$ does not depend on n and η. It allows us to append the transitions and get an affine relation between $I(t_k)$ and $g(t_k)$ during the whole centrifugation session:

$$I(t_k) \;=:\; I_0 + I_1\,g(t_k) , \tag{7.13}$$

with $I_0 \in \mathbb{R}^+$ and $I_1 \in \mathbb{R}$. The shift in $I(t)$ predicted by Eqs. (7.9) and (7.13) extend previous results obtained in Ref. (Kulsrud 1957) where an analytical shape is obtained for $I(t)$ with arbitrary $\omega(t)$ provided that the latter is not C^∞. Equation (7.13) defines a model that can be compared to experimental data.

7.5 Results

We have computed phase-space trajectories of all participants in both centrifugation sessions. It is therefore possible to compute the action variable as a function of time. Indeed, Eq. (7.2) can be rewritten as $I(t) = \int_t^{t^*} \dot{Q}^2\,dt$

from (7.4), with t^* the end of the phase-space cycle starting at t. The instant $t^* > t$ is such that the distance between the points $(Q(t), P(t))$ and $(Q(t^*), P(t^*))$ in phase space is minimal and the difference $t^* - t$ is numerically as close as possible to T. Once the action variables $I(t)$ are known, the times t_k such that $P(t_k) = 0$ are computed as well as the action variables $I(t_k)$. Continuous values $I(t_k)$ of all participants and all trials are finally discretized into 0.1 g-bins ranging from 1 to 3 g. Each bin contains between 14 and 23 data points. Average values and standard deviations (SD) of I normalized to the $1g$ value (I_{norm}) are finally displayed in Fig. 7.4.

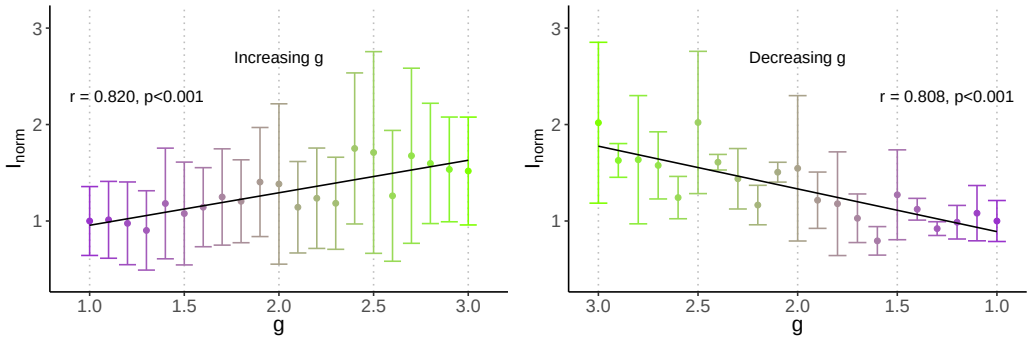

Figure 7.4: Mean values (and 1 SD error bars) of the adiabatic invariant I_{norm} per bin, normalized to the $1g$ value, versus $g(t)$. Significant linear regressions of the experimental data are depicted as a solid black line together with their Pearson's correlation coefficients and p-values. The left panel presents data in the ascending $g(t)$ phase and the right panel presents data in the descending $g(t)$ phase. Note that in the descending phase, the horizontal axis is decreasing in order to provide a continuous and chronological reading of the evolution of I_{norm}.

The adiabatic invariant exhibits a strong and significant positive ($I_1 > 0$) linear relationship with gravity both in the increasing and decreasing phases (Fig. 7.4). According to Eq. (7.1), it shows an expected higher energetic cost in high gravity for a given change in frequency, which is expected since raising the test object by a height Δh has a potential energetic cost of order $mg\Delta h$.

Despite this overall coherent dependence of I over g, we observed asymmetries in the slopes I_1 Eq. (7.13) between ascending and descending phases. To quantify this effect, we ran a 2-way repeated measures ANOVA with factors session (1 or 2) and phase (increasing or decreasing). This analysis shows that the slope I_1 is significantly larger in the increasing phase than in the decreasing phase ($I_1 = 0.296 \pm 0.306 > 0.523 \pm 0.219$, $p = 0.037$). This

asymmetry was not influenced by session ($p = 0.130$). Behavioral asymmetries with respect to gravity have already been reported in other tasks such as collisions between an object and a target (White et al. 2012) and in grip-load force modulation in rhythmic movements executed in ascending and descending hyper-gravity phases (White et al. 2018). The stronger reliance of the adiabatic invariant on g may reflect a more salient cognitive strategy in situations when mechanical constraints become more challenging due to the increase of gravity.

It may be conjectured that the adiabatic invariant is eventually modulated by vestibular and/or proprioceptive gains and re-adjustments of central pattern generators (CPGs) during that phase. At a spinal cord level indeed, rhythmic movements in mammals are organized by a network of interneurons and motor neurons called CPGs (Marder and Bucher 2001; Zehr et al. 2004). The observation of rapid adaptation of rhythmic forearm movements may suggest that vestibular and proprioceptive feedback are the major source of information used by CPGs to ensure adjustments to altered gravity, especially when it increases and becomes more demanding for the control of the task.

The variability of I_{norm} at a given g is globally lower in the decreasing than in the increasing-g phase as can be seen from the error bars in Fig. 7.4. It suggests habituation takes place because the decreasing-g phase always followed the increasing-g one. The higher variability during the increasing phase is consistent with the realization of a movement in a new situation. During the decreasing phase, motor learning achieved in the previous phase made it possible to induce a gradual reduction of variability in order to optimize the movement patterns that are compatible with a simple harmonic oscillator.

Of course, anharmonic corrections are expected at higher orders in ϵ. Still, it is remarkable that such a simple textbook model of harmonic oscillator with time-dependent frequency can capture the essential features of human motor control when facing variable gravity.

7.6 Conclusion

In summary, participants show a spontaneous adaptation of their motion that is compatible with the expectation of a simple harmonic oscillator with weakly gravity-dependent frequency. Previous analyses using the same centrifuge data did not involve the computation of the action variable and focused instead on other physical quantities, like the grip force (White et al. 2018). Here participant's adaptation is assessed by the computation of adi-

abatic invariants, whose experimental behaviour versus g complies with our model's prediction. Adiabatic invariants may thus be a relevant model of the choices made by spinal and supraspinal nervous structures among an infinite number of possible solutions to a given problem, *i.e.*, the motion of our test object in the present case. It is worth noting that, according to our model, $I \sim \mathrm{T}\,\bar{E}_c$, with T one cycle's period and $\bar{E}_c$ the average kinetic energy on this period. The behaviour of I versus g reveals a "hidden" constraint in participants movements: They may show variability in the cycle durations and speed profiles, still they will be such that the product $\mathrm{T}\,\bar{E}_c$ will be that imposed by adiabatic invariants theory. It is the first time, to our knowledge, that such a simple mechanical constraint is revealed behind the complexity of the human actions involved in the forearm motion.

Future works might go beyond the harmonic oscillator description of the effective dynamics but still in a phase-space based formalism. As shown in (Boulanger et al. 2019), adiabatic invariants can be computed in the case of higher-derivative Hamiltonians of Pais-Uhlenbeck type. Such Hamiltonians could describe rhythmic motions with several frequencies and discrete movements through, *e.g.*, minimal jerk models (Flash and Hogan 1985). We are currently investigating how our model can be generalized by analyzing complex trajectories performed during parabolic flight, therefore also including the very particular case of an absence of gravity (Boulanger et al. 2021; White et al. 2008).

Acknowledgements This research was supported by the European Space Agency (ESA) in the framework of the Delta-G Topical Team (e), the "Institut National de la Santé et de la Recherche Médicale" (INSERM) and the "Conseil Général de Bourgogne" (France) and by the "Centre National d'Etudes Spatiales" grant 4800000665 (CNES).

Author contributions **Conceptualization**, N. Boulanger, F. Buisseret and O. White; **methodology**, F. Buisseret and O. White; **formal analysis**, N. Boulanger and F. Buisseret; **data acquisition** O. White, J.-L. Thonnard and J. Hermsdörfer; **data curation**, V. Dehouck; **software**, V. Dehouck; **writing–draft preparation, review and editing**, N. Boulanger, F. Buisseret, V. Dehouck, F. Dierick and O. White. All authors have read and agreed to the published version of the manuscript. More information about the authors in the published version: (Boulanger et al. 2020).

Chapter 8

Parabolic flight and rhythmic arm motion

8.1 Summary

For this fourth study, we continued to study the adiabatic invariant model with the varying of fundamental parameters of the environment, namely gravity, and went a step further and tried to probe more complex motion and also the singular case $g = 0$. We also probed the adaptation of periodic human motion in a new environment when under constraint, again with a metronome keeping task.

For the purpose of this study, experiments were conducted in parabolic flights where airplanes perform a series of maneuvers to expose participants to 0, 1 and 1.8g. Eleven participants were recruited each performing lemniscate-shaped motion with their entire arm during six parabola. The participants were divided into two groups, a free pace and a metronome keeping one.

The linear link between gravity and the adiabatic invariant is once again observed for both constraints in the vertical direction of motion, and stays true even at the extreme $g = 0$ case, a common point of failure. As expected, the adiabatic invariant stays constant in the horizontal direction where gravity does not act. Differences between the free and metronome-driven conditions show that participants' adaptation to variable gravity is maximal without constraint. Our results show that adiabatic invariants are relevant quantities to show the changes in motor strategy in time-dependent environments. Interestingly, higher derivative dynamics are hinted at in the third direction, suggesting further directions of studies.

The content of this chapter as been published as Boulanger N., Buisseret F., **Dehouck V.**, Dierick F., White O., (2021) **Motor strategies and**

adiabatic invariants: The case of rhythmic motion in parabolic flights, *Physical Review E* DOI: 10.1103/PhysRevE.104.024403.

8.2 Introduction

Gravity obviously plays a role in human motor control, but it is not easy to isolate. On one hand, the perception and internal representation of gravity in the brain results from a widely distributed sensory process, including the vestibular system, vision, and somatosensory information (White et al. 2020). On the other hand, the constant immersive nature of the body in the Earth gravitational field calls for holistic experimental approaches in contrast to focused interventions on isolated body parts. In these settings, participants are exposed to variable gravito-inertial fields generated by human centrifuges or parabolic flights. The rationale behind these experimental approaches rest on Einstein's equivalence principle (see *e.g.* (Einstein 1916; Wald 1984)): Physics in an accelerated spacecraft (1g) is undistinguishable from physics on the ground. It does, however, not mean that the brain does not attempt to identify the possible different sources that give rise to the same consequences. Beyond the brain's role, it is well-known that variable gravity induces various changes in human physiology, typically at the cardiovascular (Aubert et al. 2016), neural (White et al. 2016) and musculoskeletal levels (Lang et al. 2017). In the present work, we do not focus on a particular physiological aspect but rather adopt a global (bio)mechanical point of view. Our main goal is to show that tools derived from mechanics may lead to conserved measurable parameters that the brain can exploit to plan and execute actions instead of relying on an estimate of gravity acquired through a noisy and distributed process.

Finding such conserved quantities demands to know the underlying dynamics, which is not an easy task in human motion where a same – even simple – action requires sometimes very different motor commands. For instance, consider reaching for a cup of coffee on the breakfast table or in an aircraft subject to turbulences, or drinking while seated or while walking. Planning efficient actions is challenging for the brain. It is therefore natural that the central nervous system relies on constants in this jungle of variability. Previous research demonstrated that some classes of actions result from an optimization process in which movements features are taken into account, such as minimizing jerk (Viviani and Flash 1995), metabolic cost (Alexander

1997; Berniker et al. 2013) or maintaining a nearly constant mechanical energy in level walking (Cavagna et al. 1976). Here we study rhythmic motion in time-changing gravity as a peculiar case of time-dependent dynamical system with bounded motion. The most powerful tools known so far to study such systems are adiabatic invariants (Henrard 1993; Jose and Saletan 1998; Landau and Lifchitz 1988). They have been applied in a wide range of applications such as plasma physics (Notte et al. 1993) and cosmology (Cotsakis et al. 1998). In biomechanics, several studies have shown the invariance of the action variable in time-independent conditions (Kadar et al. 1993; Kugler et al. 1990; Turvey et al. 1996). In a previous work, we went a step further and proposed to use adiabatic invariants to study the changes in the motion of upper arm rhythmic movements about the elbow at free pace and amplitude in a centrifuge where the perceived gravity's intensity changed stepwise from 1 to 3 g and from 3 back to 1 g (Boulanger et al. 2020). The direction of $\vec{g}$ was unchanged. It appeared that the behaviour of the adiabatic invariant $I = \frac{1}{2\pi} \oint_\Gamma P\, dQ$ computed from the latter one-degree-of-freedom motion was compatible with a theoretically predicted linear increase with g (Boulanger et al. 2019).

An obvious direction to generalize the framework of Ref. (Boulanger et al. 2020) is that of motions involving more than 1 degree of freedom. We first show in Sec. 8.3 that a linear link between the adiabatic invariant and g is expected for any potential energy, only assuming a separable dynamics. Our model is then applied to analyse the data of Ref. (White et al. 2008) in Sec. 8.4. In this last work, participants were asked to continually perform an $\infty-$shaped trajectory during a parabolic flight. The three-dimensional kinematics of the hand has been recorded and adiabatic invariants can be computed from it. Gravity during the parabolas varied between 0 and 1.8 g. We present our results in Sec. 8.5 and discuss them in Sec. 8.6.

8.3 The model

Adiabatic invariants in variable gravity

We assume that human voluntary rhythmic motion in variable gravity $g(t)$ may be seen as a dynamical system with bounded motion in phase space, described by a separable Hamiltonian $H(I_\alpha, \theta^\alpha, \lambda(t)) = \sum_{\alpha=1}^{D} H_j(I_\alpha, \theta^\alpha, \lambda(t))$. The Hamiltonian depends on action-angle variables I_α and θ^α respectively and on a time-dependent function $\lambda(t)$, accounting for the modifications induced by $g(t)$. The various ingredients underlying the latter assumption deserve further comments. First, Hamiltonian dynamics being the most power-

ful formulation of classical Mechanics, it is rather natural to adopt a Hamiltonian approach. This being said, not every dynamics is Hamiltonian: A sufficient criterion for a Hamiltonian to exist is that the total time-derivative applied to the Poisson bracket of two functions defined on phase-space obeys the Leibniz rule (Jose and Saletan 1998, Chapter 5). The latter criterion cannot a priori be checked from our experimental setup: We will a posteriori confirm that the observed phase-space trajectories are not incompatible with a Hamiltonian dynamics. Second, the dynamics has a priori no reason to be separable. The main interest we have in assuming the separability is that it allows a clear separation between vertical and horizontal directions (with respect to $\vec{g}$), the dynamics in the vertical direction being intuitively the most strongly impacted by the variations of g . Again, the separability hypothesis will only be checked a posteriori by observing the phase-space trajectories, see next Section.

It can then be shown that (Landau and Lifchitz 1988, Eqs (50, 10)-(50, 11))

$$\dot{I}_\alpha = -\frac{\partial H}{\partial \theta^\alpha} = -\left(\frac{\partial \Lambda}{\partial \theta^\alpha}\right)_{I_\alpha,\lambda} \dot{\lambda} \,, \tag{8.1a}$$

$$\dot{\theta}^\alpha = \frac{\partial H}{\partial I_\alpha} = \omega_\alpha + \left(\frac{\partial \Lambda}{\partial I_\alpha}\right)_{\theta^\alpha,\lambda} \dot{\lambda} \,, \tag{8.1b}$$

where the partial derivatives have to be computed while keeping constant the indexed variables and where ω_α are the motion's frequencies. The function Λ is the action of the system; it is sufficient for our purpose to state that it is a periodic function of the angle variables. Hence, according to (Landau and Lifchitz 1988), $\Lambda = \sum_{\ell_1=-\infty}^{+\infty} \cdots \sum_{\ell_D=-\infty}^{+\infty} \mathrm{e}^{i\vec{\ell}\cdot\vec{\theta}} \Lambda_{\vec{\ell}}$ with $\Lambda_{\vec{\ell}} \in \mathbb{C}$, $\vec{\ell} = (\ell_1, \ldots, \ell_D) \in \mathbb{Z}^D$ and

$$\frac{\partial \Lambda}{\partial \theta^\alpha} = \sum_{\ell_1=-\infty}^{+\infty} \cdots \sum_{\ell_D=-\infty}^{+\infty} i\ell_\alpha \mathrm{e}^{i\vec{\ell}\cdot\vec{\theta}} \Lambda_{\vec{\ell}} \,. \tag{8.2}$$

We moreover assume that $\lambda = \lambda_0 + \epsilon g(t)$ with $\epsilon g(t) \ll \lambda_0$, *i.e.* that the modifications induced by variable gravity may be computed at first-order in ϵ. Equation (8.1a) therefore leads to

$$\dot{I}_\alpha = -\epsilon\, \dot{g} \sum_{\ell_1=-\infty}^{+\infty} \cdots \sum_{\ell_D=-\infty}^{+\infty} i\ell_\alpha \mathrm{e}^{i\vec{\ell}\cdot\vec{\theta}} \Lambda_{\vec{\ell}} \,, \tag{8.3}$$

or

$$\frac{dI_\alpha}{dg} = -\epsilon \sum_{\ell_1=-\infty}^{+\infty} \cdots \sum_{\ell_D=-\infty}^{+\infty} i\ell_\alpha \mathrm{e}^{i\vec{\ell}.\vec{\theta}} \Lambda_{\vec{\ell}} \,. \tag{8.4}$$

Let us define the times t_n such that the values $\theta^\alpha(t_n)$ are all equal (modulo 2π). The existence of t_n is guaranteed for periodic dynamics such as the one that we consider here. Then it can be said that

$$\left.\frac{dI_\alpha}{dg}\right|_{t=t_n} = I_1 \Rightarrow I_\alpha(t_n) = I_{\alpha;0} + I_{\alpha;1}\, g(t_n), \tag{8.5}$$

with $I_{\alpha;0}$ and $I_{\alpha;1}$ two real numbers such that $|I_{\alpha;1}/I_{\alpha;0}| \ll 1$. Equation (8.5) defines our model: The adiabatic invariant is expected to behave linearly in g when computed at a given position in the consecutive cycles performed.

Definition of I_α

The action variables are defined from positions (Q^α) and momenta (P_α) degrees of freedom as follows:

$$I_\alpha = \frac{1}{2\pi} \oint_{\Gamma_\alpha} P_\alpha \, dQ^\alpha \ , \tag{8.6}$$

where Γ_α is the projection of the bounded trajectory in the plane (Q^α, P_α) for fixed α. Note that, with a kinetic energy of the standard form $E_c \sim \sum_{\alpha=1}^{D} \dot{Q}^{\alpha\,2}$, one is led to a form for the adiabatic invariant which is straightforward to compute:

$$I_\alpha(t) \sim \int_t^{t+T} \dot{Q}^{\alpha\,2}(u)\, du \,, \tag{8.7}$$

with T the period of the phase-space cycle Γ_α starting at t.

This last equation provides a way to compute the adiabatic invariant from experimental data provided $Q^\alpha(t)$ is known, which is not so obvious since a mathematical description of voluntary human motion may involve higher derivative dynamics, see *e.g.* (Hagler 2015; Hogan 1984; Nelson 1983). Two cases should therefore be considered. First, the motion's dynamics does not involve higher derivative terms. In this case Q^α may directly be identified to, say, one anatomical landmark's trajectory $x^\alpha(t)$, and $P_\alpha \sim \dot{x}^\alpha$. Second, the motion's dynamics is a higher-derivative one. Then Q^α and P_α can, in principle, be computed from $x^\alpha(t)$ but their definition is more involved. We refer the interested reader to the case of Pais-Uhlenbeck oscillator (Pais and

Uhlenbeck 1950), that is a higher-derivative generalization of standard harmonic oscillator for which adiabatic invariants can be analytically computed (Boulanger et al. 2019).

8.4 The experiment

Parabolic flights

During parabolic flights, participants were asked to continually perform an ∞-shaped trajectory oriented crosswise to the body around two virtual obstacles situated 3 m in front of them. An optoelectronic device (OptoTrak 3020 system, Northern Digital, Waterloo, Ontario, Canada) recorded the position of three infrared LEDs placed on the object with a resolution of 0.1 mm. A three-dimensional accelerometer fixed on the floor of the aircraft recorded its acceleration. The two synchronized acquisition systems recorded parameters at a sampling rate of 200 Hz. During a parabola, the aircraft performs a series of manoeuvres to allow for changes of effective gravity. This allows one to run experiments at 0 (microgravity), 1 and approximately 1.8 g (hypergravity), albeit for a short time. The micro and hyper gravity phases last around 20 s with transition periods shorter than 5 s. Typical plots of the motion performed and of the $g(t)$-profile are shown in Fig. 8.1. The cartesian frame we use is also displayed.

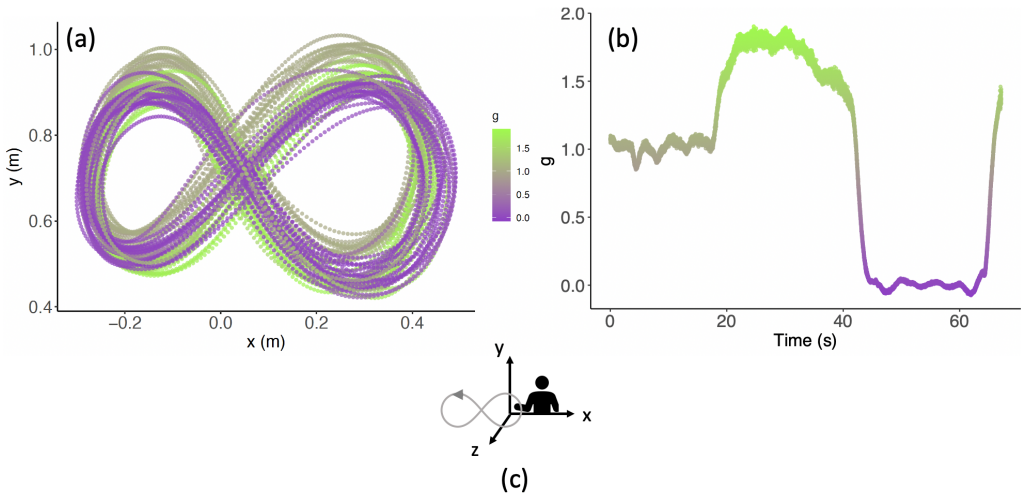

Figure 8.1: (a) Typical plot of the $\infty-$shaped motion in frontal plane (x, y) during one parabola. A participant in FREE condition has been chosen. (b) $g(t)$ profile during the same parabola. (c) The Cartesian frame is displayed.

Participants executed $\infty-$shaped movements in two conditions. In the free condition (FREE), the motion was self-paced. Four participants, totalling 24 parabolas, performed the motion in FREE condition. In the metronome condition (METRO), participants had to adopt 1.5-second constant pace prompted by a metronome. Seven participants, totalling 42 parabolas, performed the motion in METRO condition. Before starting the parabolic flights, participant's health was assessed by their individual National Centres for Aerospace Medicine as meeting the requirement "Jar Class II" for parabolic flight. No participant reported sensory or motor deficits and they all had normal or corrected-to-normal vision. All participants gave their informed consent to participate in this study and the procedures were approved by the European Space Agency (ESA) Safety Committee and by the local ethics committee. Their motion was recorded during 6 consecutive parabolas. We refer the reader to Ref. (White et al. 2008) for a more detailed presentation of the experiment.

Phase-space trajectories and action variables

The speeds $v_\alpha = \dot{x}^\alpha$ are first computed from the positions x^α recorded by the optoelectronic device through a finite differentiation. Typical speed-position plots are shown in Fig. 8.2.

The x and y directions show (quasi)-periodic trajectories of elliptic type, compatible with a standard Hamiltonian dynamics. Hence we proceed as follows to compute the action variables. First, we identify Q^α to x^α and P_α to $\dot{Q}^\alpha$ – up to an arbitrary mass scale that is set equal to 1 kg. Second, the beginning and end of each cycle Γ_α in phase-space plane (Q^α, P_α) are computed. The end of the cycle starting at t is chosen as the time $t^\star$ which is the smallest time after t at which the euclidean distance between $(Q^\alpha(t^\star), P_\alpha(t^\star))$ and $(Q^\alpha(t), P_\alpha(t))$ is minimal. Once $t^\star$ is identified, the adiabatic invariant is computed by quadrature from Eq. (8.4): $I_\alpha(t) = \int_t^{t+t^\star} \dot{Q}^{\alpha\,2}(u)\,du$. Then, to apply our model, only adiabatic invariants corresponding to a given value of the angle variable have to be collected. We only consider the instants at which $P_\alpha = 0$ and Q^α was maximal since they are easily identified.

As can be seen in Fig. 8.2, the trajectory in (z, v_z) plane intersects itself during one cycle. The underlying dynamic is therefore called *non-autonomous*, in the theory of dynamical systems. Participant's motion in the $z-$direction actually contains two distinct frequencies. One is the whole ∞-shaped movement's pulsation, say ω, and the other is a forward-backward oscillation at 2ω. A trajectory of the form

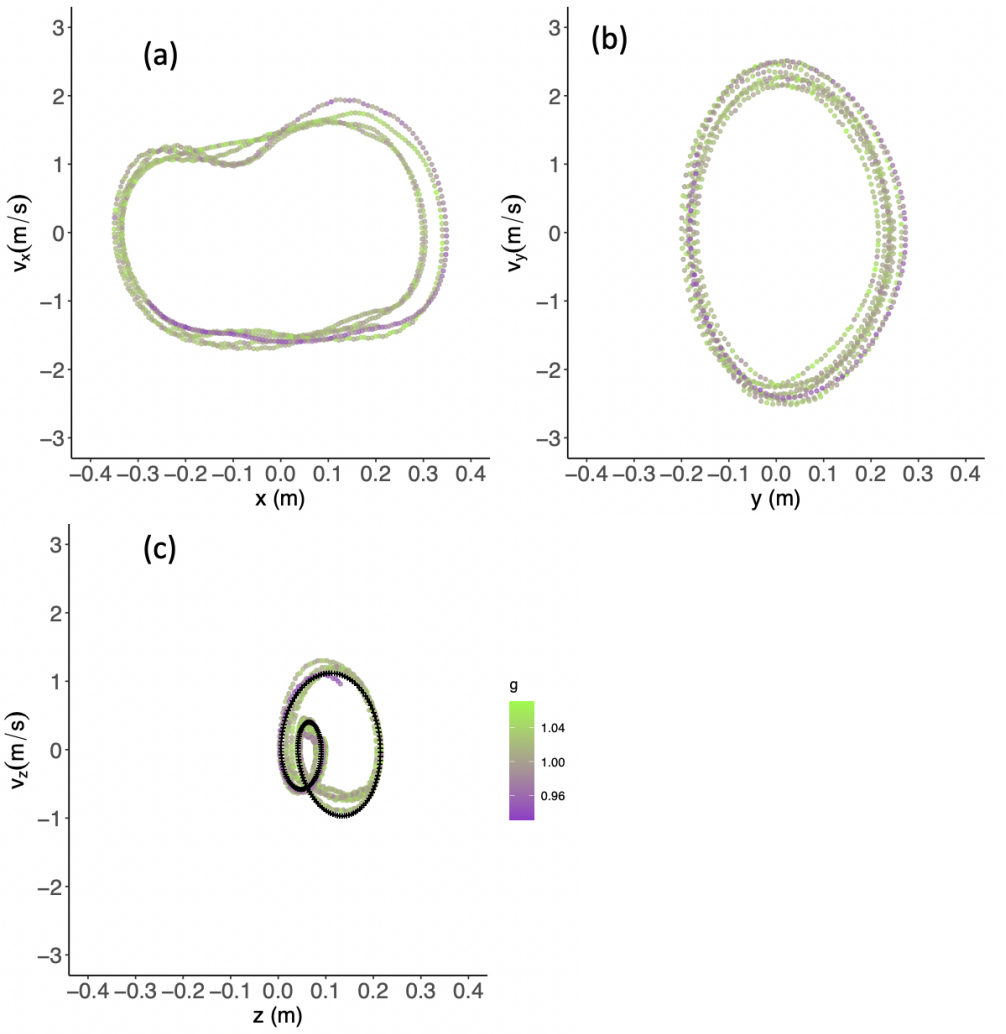

Figure 8.2: (a) Typical speed-position plot of the motion in (x, v_x) plane during several cycles, same participant as Fig. 8.1. (b) and (c) Same data in the (y, v_y) and (z, v_z) planes respectively. The crosses show the trajectory obtained from Eq. (8.8) with $A_0 = 0.092$ m, $A_1 = 0.065$ m, $A_2 = 0.060$ m, $\omega = 2\pi$ rad/s, $\phi_1 = 0$ rad and $\phi_2 = -1$ rad.

$$z(t) = A_0 + \sum_{j=1,2} A_j \sin(j\omega t + \phi_j) \tag{8.8}$$

has the qualitative features of what is observed in the (z, v_z) plane for appropriate values of the real constants ω, A_i and ϕ_i.

Several effective models may produce trajectories such as (8.8). (1) An os-

cillator with pulsation ω plus an external, time-dependent, periodic force with pulsation 2ω. A textbook example is the Duffing oscillator. The complete set of solutions of a forced, non-harmonic oscillator is unknown a priori but some special solutions are known that perfectly match the observed motion. (2) A system of coupled harmonic oscillators oscillating near its equilibrium position provided that the frequencies of some normal modes are equal to ω and 2ω. The dynamics of the various joints of the arm may be approximated by such a system. (3) A second-order Pais-Uhlenbeck harmonic oscillator. As shown in Appendix B, an autonomous higher-derivative oscillator may actually mimic the dynamics of one peculiar degree of freedom in a system of coupled oscillators. An obvious advantage in resorting to Pais-Uhlenbeck harmonic oscillators is that the effective dynamics in the $z-$direction would be autonomous and that adiabatic invariants are well-defined once phase-space is properly built from the position degree of freedom and its time derivatives (Boulanger et al. 2019). Hence, our model can in principle be adapted to the $z-$direction. However, such higher-derivative adiabatic invariants involve not only $\dot{z}$ but at least $\ddot{z}$ and $\dddot{z}$ (Boulanger et al. 2019). The experimental precision reached in the measurement of z does not allow for a reliable computation of those higher derivatives from our experimental data and we chose not to make further computations as far as the (z, v_z) plane is concerned.

8.5 Action variables in terms of gravity: The results

We have linearly fitted I_α versus g for each available parabola in order to check whether Model (8.5) is observed at an individual level or not. The variable g refers to the average value of $g(t)$ within the considered cycle Γ_α. The parameters of the fit are $I_{1;\alpha}$ (slope), r_α (Pearson's correlation coefficient) and $I_{0;\alpha}$ (intercept). A two-way ANOVA may be performed on the parameters of the fit with factors condition (FREE or METRO) and parabola number (1 to 6). The latter factor is introduced to check whether a learning effect is present or not during the consecutive parabolas a given participant has experienced. The ANOVA was performed using SigmaPlot software (v.11.0, Systat Software, San Jose, CA, United States of America), with significance level 0.05. It appears that no significant effect of the parabola number can be found in the fit parameters which means that the model parameters are stable over time, with values set from the outset. Interactions between condition and parabola number are not significant either. However, the condition

has a significant impact on $I_{0;\alpha}$, $I_{1;y}$ and r_y, as shown in Table 8.1.

From Table 8.1, the following global features of participant's motion can be deduced. (a) The action variable I_x does not show a well-defined linear behaviour versus g: both the slopes and the Pearson's correlation coefficients are comparable with 0. The action variable I_x can be considered as constant with g, although it is significantly lower in METRO condition than in the FREE condition. Let us note that the $x-$direction is orthogonal to gravity while the $y-$direction is aligned with gravity (see frame in Fig. 1). This observation may intuitively explain why there is no trend versus g for the $x-$dynamics. (b) However, the trend of I_y vs g is compatible with model (8.5) for positive $I_{1;y}$ well smaller than the intercept $I_{0;y}$. It is coherent with our initial assumption to work at first-order in g. Furthermore, the slope and the intercept are significantly lower in METRO condition than in the FREE one. (c) The clearest linear trend is observed for the action variable I_y in the FREE condition. An example of linear fit is displayed in Fig. 8.3.

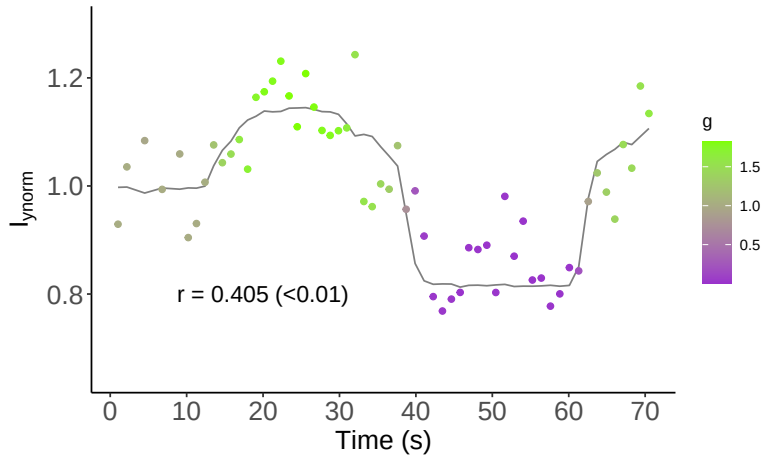

Figure 8.3: Adiabatic invariant I_y versus g computed from experimental data in the FREE condition for the same participant as in Fig. 8.1 (points), compared to the best linear fit of the form (8.5). Pearson's correlation coefficients is also indicated. I_y has been normalized so that its average value is 1 at $1g$.

The global trend of I_y vs g can be observed by averaging I_y over participants by condition (FREE and METRO) and by gravity condition, *i.e.* by gathering computed adiabatic invariants into bins of 0.1 g, ranging from 0 to 1.8 g. Only the bins containing more than 10 points were finally kept. This threshold is arbitrary but avoids almost empty bins in the fast transition regions between 0 and 1 g and between 1 and 1.6 g. The results of this analysis are displayed in Fig. 8.4. The observed trends are com-

Direction	Condition	$I_{1;\alpha}$ (kg.m)	r_α	$I_{0;\alpha}$ (J.s)
x	FREE	$[-0.014, 0.005]$	$[-0.150, 0.082]$	$[0.327, 0.371]$
	METRO	$[-0.010, 0.004]$	$[-0.182, 0.109]$	$[0.177, 0.205]$
	p	0.884	0.969	< 0.001
y	FREE	$[0.017, 0.033]$	$[0.291, 0.518]$	$[0.187, 0.296]$
	METRO	$[0.005, 0.14]$	$[0.117, 0.332]$	$[0.106, 0.120]$
	p	< 0.001	0.014	< 0.001

Table 8.1: 95 % confidence intervals for the slopes $I_{1;\alpha}$, Person's correlation coefficients r_α and intercepts $I_{0;\alpha}$ obtained through the fit (8.5) of the computed I_α vs g in each parabola for all conditions. The $p-$ values of the ANOVA for the effect of condition are also given.

patible with $I_y^{FREE} = 0.210 + 0.015\,g$ and $I_y^{METRO} = 0.106 + 0.015\,g$; an ANCOVA further shows that the slopes are not significantly different with condition ($p = 0.994$), while the intercepts significantly depend on condition ($p < 0.001$). Finally, it is also worth highlighting the fact that some bins (e.g. $[1.3; 1.4[$) capture values of gravity in the ascending but also descending parts of the parabolic profile.

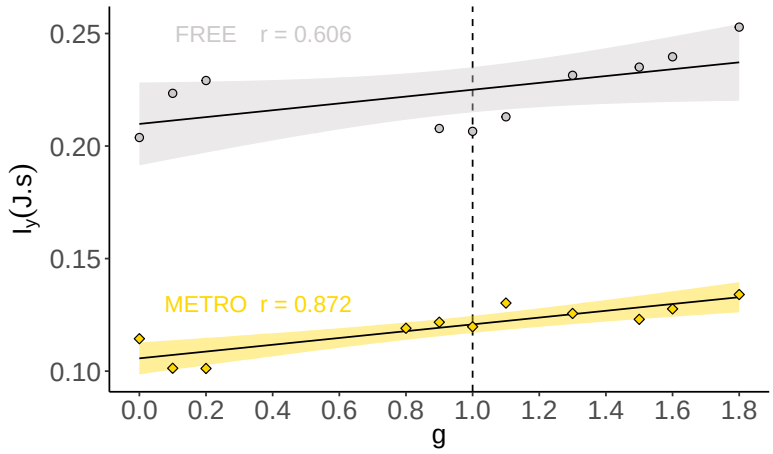

Figure 8.4: Adiabatic invariant I_y versus g computed from experimental data in the FREE (grey points) and METRO (yellow points) conditions. A linear fit is given (solid lines) with its 95% confidence interval (colored bands) in each condition. Pearson's correlation coefficients are also indicated. The 1-g bin is marked with a vertical dashed line.

8.6 Discussion of the results

The trajectory in the $z-$direction contains two distinct frequencies leading to intersecting trajectories in the (z, v_z) plane, see Fig. 8.2. Effective dynamics in this plane therefore cannot be described by a time-independent standard dynamics: Either higher-derivatives or time-dependent forces have to be included. We believe that the appearance of such features could be explained by shoulder biomechanical constraints. The main shoulder movements required to execute the $\infty-$shaped movement are abduction and adduction. During shoulder abduction-adduction movements, rotations are usually observed (Assi et al. 2016). It is well known that external rotation of the shoulder is adopted during abduction to clear the major tubercule of humerus from beneath acromion for preventing impingement (Hurov 1986; Peat 1986). The movement strategy spontaneously chosen by participants is therefore not located on a single plane with constant z, leading to the observed nontrivial pattern. As previously said, the current experimental accuracy along the $z-$axis does not allow for a more detailed study of a potential higher-derivative effective dynamics. Note that it has already been successfully conjectured that a higher-derivative action principle such as $S = \int \dddot{x}^2\, dt$ – a jerk-based cost function – may constrain non-rhythmic voluntary human motion (Hogan 1984). However, such an action principle does not lead to periodic solutions, that is why a Pais-Uhlenbeck oscillator seems more relevant to us. In the motion we observe, the two frequencies have an integer ratio, therefore stability of the motion is not guaranteed in such a resonant case (Boulanger et al. 2019). It has recently been understood that extra interaction terms may stabilize periodic solutions of resonant higher-derivative oscillators (Kaparulin et al. 2020): We hope to investigate the applicability of such models to human rhythmic motion in future works.

By definition, the adiabatic invariant in x and $y-$directions is proportional to

$$I_\alpha \sim T \left\langle E_{c,\alpha} \right\rangle , \tag{8.9}$$

where T is a given cycle duration in the vertical direction – the duration of the cycle starting at the same time is twice that value in the $x-$direction –, and where $\langle E_{c,\alpha} \rangle$ is the averaged kinetic energy on the considered cycle. The protocol of White et al. 2008 is such that $T^{FREE} < T^{METRO}$: The pace imposed by the metronome was chosen to be slower than participants' spontaneously chosen paces. Since, at given g, the adiabatic invariant in FREE condition is always larger than in METRO condition, it can be concluded that $\left\langle E_{c,\alpha}^{FREE} \right\rangle > \left\langle E_{c,\alpha}^{METRO} \right\rangle$. The smaller kinetic energy in METRO condition thus follows from the fact that participants have to move slower

than in FREE condition in order to follow metronome's pace. Note that $I_{1;y}^{METRO} < I_{1;y}^{FREE}$: The extra constraint imposed by the metronome actually prevents the participant from optimally adapting his/her motion when g is changing, assuming that the optimal motor strategy is reached in FREE condition. It is also known that T is a decreasing function of g in either METRO or FREE conditions (White et al. 2008). Since $I_{1;y} > 0$, $\langle E_{c,y} \rangle$ has to be an increasing function of g: The participant's arm moves with higher typical vertical speed at higher values of g.

Definition (8.9) explicitly makes appear the links between adiabatic invariant and kinetic energy. Another interpretation of the adiabatic invariant, focusing on external forces, is relevant to clarify the influence of gravity on it. To this aim, the virial theorem may be used to state that

$$I_\alpha \sim T \left\langle F_\alpha x^\alpha \right\rangle , \tag{8.10}$$

where F_α is an external force acting on the point-like object whose trajectory is x^α. The latter force should involve muscular forces as well as gravity. One can reasonably assume that $F_\alpha = F_{0\alpha} + F_{1\alpha} g$, in coherence with the previously found linear trend of I_α vs g. A priori, $F_{1y} \gg F_{1x}$ since gravity's influence should mostly concern the vertical direction. Changes induced by F_{1x} are probably unnoticeable up to our current experimental precision.

Around $1g$, I_y is lower than expected from the 95% confidence interval of the linear fit. In that familiar environment, participants "know" the most economic strategy when they are allowed to move freely in Earth's gravity. In METRO condition, that drop in I_y is not observable: The extra constraint imposed by the metronome does not allow participants to follow that optimal strategy. Furthermore, our results also reveal that microgravity is a special case. While the linear fit holds true for the whole explored gravitational values ($[0g; 1.8g]$), there is a significant gap between 0.3 g and 0.7 g in our data. Hypogravity values are not explored. Our study again reveals that 0 g acts as a singular value for the brain (White et al. 2008). Finally, adiabatic invariants do not behave like parameters measured in most motor control investigations. Indeed, while errors in reaching movements perturbed by force fields require tens of trials to vanish (Shadmehr and Mussa-Ivaldi 1994), safety margins in object manipulation in altered gravity need an exposure to 6 parabolas to decrease to normal values (Augurelle et al. 2003) and some behaviours in conflicting force-fields or visuomotor rotations do not even adapt at all (Cothros et al. 2008), adiabatic invariants seem to be set to their nominal values from the outset.

8.7 Concluding comments

To conclude this work, it is worth linking them to well-known frameworks in motor control.

Participants have many more kinematic degrees of freedom than necessary to fulfill the demanded task, *i.e.* the $\infty-$shaped movement. The coordination of kinematically redundant systems was formulated by Bernstein as the degrees of freedom problem (Bernstein 1967). The main difficulty of Bernstein's problem is that the nervous system must conciliate two apparently conflicting abilities: (1) the realization of a movement from the choice of one among an infinite number of motor patterns; (2) the absence of univocal relationship between the movement realized and motor patterns used, known as motor equivalence. Although it remains unclear as to whether and how the brain can estimate adiabatic invariants, such quantities puts constraints on the allowed strategies, *i.e.* strategies keeping I_α invariant at constant g. In this picture, an increase (decrease) in $I_\alpha(g)$ may be related to an increase (decrease) of the allowed motor patterns.

When subjects are free to point to a target, they automatically scale movement duration with movement amplitude and choose a trade off between movement speed and accuracy to touch the target. It is known as Fitts's law (Fitts 1954). The adiabatic invariant is the area of a closed trajectory in phase space: $I_\alpha \sim A_\alpha\, v_\alpha^{\max}$, with A_α and $v_\alpha^{\max}$ the amplitude and maximal speed of the movement in the direction α respectively. Its invariance at given g implies that, if maximal speed increases (decreases), amplitude decreases (increases). In our experiment, the maximal speed is an obvious measure of movement's speed, and the amplitude can be seen as an index of precision. Indeed,the instruction given to the participant is to avoid 2 targets by turning around. Thus, if amplitude decreases (increases), the participant increases (decreases) the chances of hitting the target, and he/she is less (more) precise. The adiabatic invariant can then be seen as an explicit realization of the speed-accuracy-trade off scenario. The modification of its value with g actually changes the acceptable values of maximal speed and amplitude involved in this trade off.

In summary, our results indicate that adiabatic invariants deserve a particular attention in biomechanical approaches of human motion. They are indeed able to capture one individual's reaction to time-dependent external conditions, even in extreme cases such as variable gravity. Adiabatic invariants seem very robust in this context. Further studies are now needed to clarify the links between adiabatic invariant theory and celebrated motor control paradigms such as speed-accuracy-trade off.

Acknowledgements This research was supported by grants from Prodex

and IAP; Belgian Federal Office for Scientific, Technical, and Cultural Affairs; Fonds Spécial de Recherche; and Canadian Space Agency Contract 9F007-033026.

Author contributions **Conceptualization**, N. Boulanger, F. Buisseret and O. White; **methodology**, F. Buisseret and O. White; **formal analysis**, N. Boulanger and F. Buisseret; **data acquisition** O. White, N. Dowling, R.M. Bracewell and J. Diedrichsen; **data curation**, V. Dehouck; **software**, V. Dehouck; **writing–draft preparation, review and editing**, N. Boulanger, F. Buisseret, V. Dehouck, F. Dierick and O. White. All authors have read and agreed to the published version of the manuscript. More information about the authors in the published version: (Boulanger et al. 2021).

Chapter 9

Conclusion

Our agility within our movements is, among other things, what makes us (healthy) human beings. Bipedal locomotion allowed us to distinguish ourselves from our evolutionary ancestors and develop our brain, to become the dominant species on the planet. This mobility is both so fundamental and complex that some neuroscientists argue that it is the reason why evolution has "given" us a brain in the first place.

Although mobility is not exclusive to the animal kingdom, its study for beings equipped with a nervous system is its own field of study: motor control. This field spans many disciplines as it is interested in the integration of sensory information, the neural structures and the nature of the signals involved, the biomechanics of the system under investigation, the differences between reflexes and voluntary motion, etc. Motor control has evolved a lot since its inception, and is now very different from the first essays on the subject written by Aristotle. Nevertheless, one of the central questions in the coordination of motion, namely Bernstein's degrees of freedom problem is still without a definitive answer decades after its formulation.

Many approaches have been explored. One of the most common among them appears within the framework of optimal control theory and is based on the minimization of a cost function, such as jerk. This approaches are well-suited to describe reaching motion, but are not adapted to periodic problems, which are the subject of this work.

To derive general principles *a priori*, we based our approach in the world of physics. Between the three main formulations of mechanics –Newtonian, Lagrangian and Hamiltonian– we selected the latter for its interesting properties for the study of (quasi-)periodic motion, such as adiabatic invariance.

We explored this property in the context of voluntary human motion over the course of several experiments.

In a first experiment (chapter 5), we probed the use of adiabatic invari-

ants to characterize gait. In that context, they act as a global constraint on motion as they link different variables together thereby reducing the degrees of freedom in motor coordination. This was indeed observed in a very simple whole-body center-of-mass model, highlighting the ease of use of our approach. Furthermore, this stayed true regardless of the experimental condition: free-pace or metronome, even though they exhibit wildly different local variability. This confirms the adiabatic invariant to be a dynamical constraint on variability to preserve the global stability of gait, as speed and frequency do not evolve arbitrarily but such that their ratio stays constant.

In a second experiment (chapter 6), we reused the experimental data of the first study. This was done specifically to explore the variability inherent in human motion which is now a staple of motor control. In fact, gait is at best merely quasi-periodic and there are variations from one step to the next due to the presence of physiological noise. Adiabatic invariants, which have been used for the study of chaotic systems, are still relevant in this context. Indeed, by simply adding a small perturbation term to the system the Fokker-Planck equation now dictates the distribution of values that adiabatic invariants can take. This was observed experimentally and we extracted the shape of those distributions. Furthermore, noise does not detail imperfection in motion, but rather is an indication of our adaptability. Therefore, we interpret the distribution of the adiabatic invariant to be a way to assess this adaptability.

In a third experiment (chapter 7), we explored using adiabatic invariants to characterize motion in gravity-varying environments. Indeed, gravity appears as the most pervasive signal dictating motion, and is readily taken into account by the central nervous system. Therefore, it is not clear how motion is planned by the brain when gravity changes. In this context, adiabatic invariants are once again relevant quantities as they can easily be computed even when changes in parameters occur during motion. Experimentally, we observed rhythmic arm motion during centrifugation and saw agreement with our mechanistic approach, revealing spontaneous adaptation of movements to a new environment. This points towards adiabatic invariants being constraints that the central nervous system relies on.

In a fourth experiment (chapter 8), ostensibly a continuation of the third experiment this time in parabolic flights, we also explored hypogravity regimes and more complex motion with different experimental conditions. Again, we observe experimentally what is expected from adiabatic theory. A salient result of this experiment is the absence of effect of the parabola number on the value of the adiabatic invariants while adaptation to a new environment usually requires plenty of trials. This reinforces the hypothesis that adiabatic invariance is a global constraint on motion.

It is important to note that adiabatic invariance constitutes a physi-

cal property of periodic motion that is applicable in human motion as we have shown in this work and not something that the central nervous system achieves through motor planning. Indeed, the central nervous system is bound by the laws of physics. However, this does not mean that motor strategies cannot be molded by this property, just like they are by fundamental parameters such as gravity. This is of course speculative as it is unclear how the central nervous system would incorporate such a property. It might rule out "unphysical" trajectories that result in arbitrary kinetic energy and frequency of motion, but probing such behavior would surely involve novel and exotic experimental designs that go beyond the scope of this thesis.

All in all, this thesis has revealed the formulation of motor control problems within the framework of Hamiltonian mechanics to be valuable in a novel way, as it has shown how the laws of physics necessarily constrain and guide motion; particularly for periodic motion with time-dependent perturbations.

Perspectives

This thesis being in nature exploratory is open-ended and allows for many new directions of study, in this section we outline a few of these directions and also ways to make this first fray into Hamiltonian mechanics richer.

Firstly, we have so far only been interested in point-like kinematic data of the parts of the body under investigation, mainly because this is the type of data that we have been able to gather during our experiments. While this already reveals rich possibilities for human motion study, it could be further enriched by the use of other types of data. For example, electromyography can be used to probe the tension in a muscle which can be likened to the stiffness of a spring. In our gravity-changing experiments, where the motions performed are harmonic, this could be used to model the change of muscle activity as a result of stress or poor internal model planning due to the novelty of the environment.

As we have just pointed out, our models are based on harmonic motion. While this is a natural candidate for rhythmic motion, real world motion rarely is, but rather necessitates small corrections, indeed harmonic oscillators are already a small-angle approximation of planar pendulums. This is particularly apparent when we look at the center-of-mass motion in our gait experiment (figure 9.1) or at the motion performed during parabolic flights. This departure from harmonicity might be modeled by adding anharmonic terms to the Hamiltonian of the system, or by using different types of oscillators. Fortunately, the identification of the oscillator describing the motion of the system can be readily made by looking at the curves it produces in phase

space, as can be seen in figure 8.2 where we see the similarities between the horizontal motion and a Duffing oscillator, interestingly known to produce chaotic regimes.

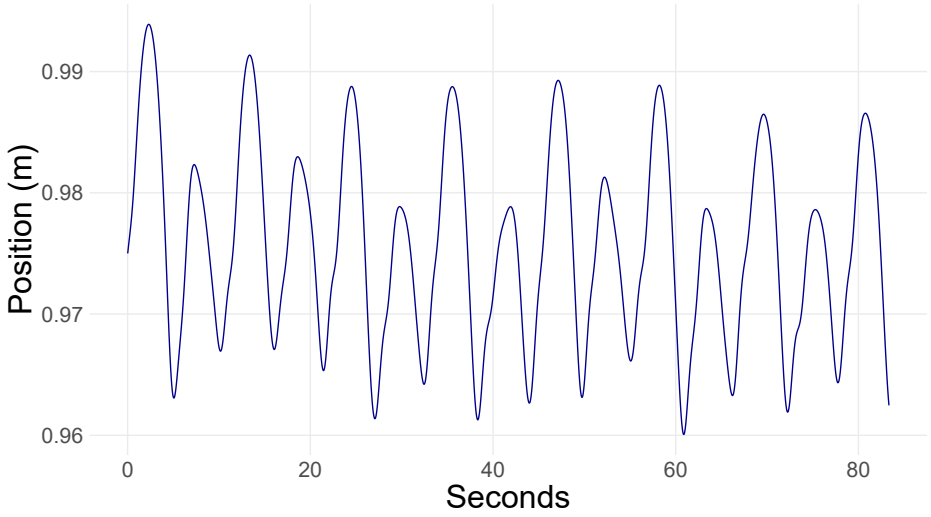

Figure 9.1: Typical COM profile for the gait of a participant during experiment 5.

As discussed with our parabolic flight experiment, sometimes higher derivatives are needed to accurately describe and model motion. Unfortunately, we could not explore this idea due to poor experimental precision. Access to this type of data could help reveal new insights, and draw parallel to other paradigms using higher derivatives, like minimum-jerk models.

Another common issue with this type of experiment is the averaging over all participants in order to obtain robust statistics, glossing over individual differences. It could be beneficial to perform longer experiments on a single participant, or repeat the experiment over long periods of time (e.g. days, weeks, etc.) to be able to follow the evolution of an individual and meaningfully study their specificities.

Furthermore, what we have studied here constitutes different types of perturbations to a system; sometimes controlled, deterministic i.e. changes in gravity or following a regular metronome, and sometimes stochastic i.e. the distribution of the adiabatic invariant as it diffuses in phase space. But, as we discussed in our first gait experiment (chapter 5), the nature of physiological signals lies between those two regimes, in an auto-correlated state. During this thesis we have tried to probe this regime in the framework of optimal variability and Hamiltonian mechanics, unfortunately without being able to finalize the analysis, this is discussed in appendix C.

Moreover, the variations of the scaling of I with g around the mean, as seen in figure (8.3), present a limit of the current analysis. Indeed, we make several assumptions with regards to motion and its perturbation in order to observe adiabatic invariance. As previously stated, the motion performed here is not strictly harmonic and corrections should be added for a better fit. The other two assumptions are that the perturbation is small compared to the main Hamiltonian term, both in its value and its timescale. Unfortunately, there is no agreed-upon threshold as to what constitutes a change "small enough", and we might be at the limit of application. For example, the transition from one effective gravity to the next is of the order of $2 - 3s$, while the motion has a cycle period of $1.5s$. This might not be "slow enough" for adiabatic theory to be applied without further corrections.

More so, the variations around the mean may reflect modulation of motion induced by neural control going further than a passive mechanical approach. The interplay between the physical nature of the body and its ability to change strategies to account for changes in the environment could be explored by tightening the experimental protocols closer to the assumptions of adiabatic invariance, i.e., slower and smaller transitions. This would also alleviate the amount of stress that participants experience in already quite exotic experimental environments.

As said at the beginning of this section, this only covers a small set of possible directions that the use of Hamiltonian mechanics brings to the table. We hope to be able to engage in further research brought by ideas this thesis sparked, and we urge the motor control community to use the tools laid out here to further understand human motion.

Bibliography

Abram, Sabrina J., Jessica C. Selinger, and J. Maxwell Donelan (June 2019). "Energy optimization is a major objective in the real-time control of step width in human walking". *Journal of Biomechanics* 91, pp. 85–91. DOI: 10.1016/j.jbiomech.2019.05.010.

Acharya, U. Rajendra et al. (2015). "A Novel Depression Diagnosis Index Using Nonlinear Features in EEG Signals". *European Neurology* 74.1-2, pp. 79–83. DOI: 10.1159/000438457.

Adamczyk, Peter G. and Arthur D. Kuo (Aug. 2009). "Redirection of center-of-mass velocity during the step-to-step transition of human walking". *Journal of Experimental Biology* 212.16, pp. 2668–2678. DOI: 10.1242/jeb.027581.

Ahn, Jooeun and Neville Hogan (Sept. 2013). "Long-Range Correlations in Stride Intervals May Emerge from Non-Chaotic Walking Dynamics". *PLOS ONE* 8.9, pp. 1–10. DOI: 10.1371/journal.pone.0073239.

Alexander, R. McN. (Feb. 1997). "A minimum energy cost hypothesis for human arm trajectories". *Biological Cybernetics* 76.2, pp. 97–105. DOI: 10.1007/s004220050324.

Angelaki, Dora E. and Kathleen E. Cullen (July 2008). "Vestibular System: The Many Facets of a Multimodal Sense". *Annual Review of Neuroscience* 31.1, pp. 125–150. DOI: 10.1146/annurev.neuro.31.060407.125555.

Angelaki, Dora E. et al. (2004). "Neurons compute internal models of the physical laws of motion". *Nature* 430.6999, pp. 560–564. DOI: 10.1038/nature02754.

Ariani, Giacomo, Young Han Kwon, and Jörn Diedrichsen (May 2020). "Repetition facilitates online planning of sequential movements". *Journal of Neurophysiology* 123.5, pp. 1727–1738. DOI: 10.1152/jn.00054.2020.

Arnold, V. I. (1989). *Mathematical methods of classical mechanics*. Second edition. Graduate Text in Mathematics. Springer-Verlag.

Arnold, Vladimir I (Oct. 1963). "Proof of a theorem of A.N. Kolmogorov on the invariance of quadi-periodic motions under small perturbations of the hamiltonian". *Russian Mathematical Surveys* 18.5, pp. 9–36. DOI: 10.1070/rm1963v018n05abeh004130.

Assi, A. et al. (2016). "Three-dimensional kinematics of upper limb anatomical movements in asymptomatic adults: Dominant vs. non-dominant". *Human movement science* 50, pp. 10–18. DOI: 10.1016/j.humov.2016.09.002.

Aubert, André E et al. (Dec. 2016). "Towards human exploration of space: the THESEUS review series on cardiovascular, respiratory, and renal research priorities". *npj Microgravity* 2.1, p. 16031. DOI: 10.1038/npjmgrav.2016.31.

Augurelle, Anne-Sophie et al. (Feb. 2003). "The effects of a change in gravity on the dynamics of prehension". *Experimental Brain Research* 148.4, pp. 533–540. DOI: 10.1007/s00221-002-1322-3.

Bazzani, A., S. Siboni, and G. Turchetti (1994a). "Diffusion in Hamiltonian systems with a small stochastic perturbation". *Physica D: Nonlinear Phenomena* 76.1, pp. 8–21. DOI: https://doi.org/10.1016/0167-2789(94)90246-1.

— (1995). "Diffusion in stochastically and periodically modulated Hamiltonian systems". *AIP Conference Proceedings* 344.1, pp. 68–77. DOI: 10.1063/1.48970.

Bazzani, A. et al. (1994b). "A model of modulated diffusion. I. Analytical results". *Journal of Statistical Physics* 76.3, pp. 929–967. DOI: 10.1007/BF02188693.

Bazzani, Armando and Luca Beccaceci (1998). "Diffusion in Hamiltonian systems driven by harmonic noise". *Journal of Physics A: Mathematical and General* 31.28, pp. 5843–5854. DOI: 10.1088/0305-4470/31/28/004.

Berniker, Max et al. (Jan. 2013). "An Examination of the Generalizability of Motor Costs". *PLOS ONE* 8.1, pp. 1–11. DOI: 10.1371/journal.pone.0053759.

Bernstein, N.A. (1967). *The Co-Ordination and Regulation of Movements*. Pergamon Press.

Boulanger, N. et al. (2019). "Higher-derivative harmonic oscillators: stability of classical dynamics and adiabatic invariants". *Eur. Phys. J.* C79.1, p. 60. DOI: 10.1140/epjc/s10052-019-6569-y.

Boulanger, N. et al. (2020). "Adiabatic invariants drive rhythmic human motion in variable gravity". *Phys. Rev. E* 102 (6), p. 062403. DOI: 10.1103/PhysRevE.102.062403.

— (2021). "Motor strategies and adiabatic invariants: The case of rhythmic motion in parabolic flights". *Phys. Rev. E* 104 (2), p. 024403. DOI: 10.1103/PhysRevE.104.024403.

Boulanger, Nicolas et al. (Feb. 2023). "Diffusion in Phase Space as a Tool to Assess Variability of Vertical Centre-of-Mass Motion during Long-Range Walking". *Physics* 5.1, pp. 168–178. DOI: 10.3390/physics5010013.

Brizard, Alain J. (2013). "Jacobi zeta function and action-angle coordinates for the pendulum". *Communications in Nonlinear Science and Numerical Simulation* 18.3, pp. 511–518. DOI: 10.1016/j.cnsns.2012.08.023.

Broscheid, Kim-Charline, Christian Dettmers, and Manfred Vieten (2018). "Is the Limit-Cycle-Attractor an (almost) invariable characteristic in human walking?" *Gait and Posture* 63, pp. 242–247. DOI: 10.1016/j.gaitpost.2018.05.015.

Buisseret, Fabien et al. (2022). "Adiabatic Invariant of Center-of-Mass Motion during Walking as a Dynamical Stability Constraint on Stride Interval Variability and Predictability". *Biology* 11.9. DOI: 10.3390/biology11091334.

Cavagna, GA., H. Thys, and A. Zamboni (1976). "The sources of external work in level walking and running". *J Physiol.* 262, pp. 639–657. DOI: 10.1113/jphysiol.1976.sp011613.

Cavagna, Giovanni A. and Mario A. Legramandi (Nov. 2020). "The phase shift between potential and kinetic energy in human walking". *Journal of Experimental Biology* 223.21. jeb232645. DOI: 10.1242/jeb.232645.

Cogburn, R. and J. A. Ellison (1992). "A stochastic theory of adiabatic invariance". *Communications in Mathematical Physics* 149.1, pp. 97–126. DOI: 10.1007/BF02096625.

Cothros, Nicholas, Jeremy Wong, and Paul L. Gribble (Apr. 2008). "Distinct Haptic Cues Do Not Reduce Interference when Learning to Reach in Multiple Force Fields". *PLOS ONE* 3.4, pp. 1–10. DOI: 10.1371/journal.pone.0001990.

Cotsakis, S., R. L. Lemmer, and P. G. L. Leach (1998). "Adiabatic invariants and mixmaster catastrophes". *Phys. Rev. D* 57 (8), pp. 4691–4698. DOI: 10.1103/PhysRevD.57.4691.

Crevecoeur, F. et al. (2010). "Towards a "gold-standard" approach to address the presence of long-range auto-correlation in physiological time series". *Journal of Neuroscience Methods* 192.1, pp. 163–172. DOI: 10.1016/j.jneumeth.2010.07.017.

Criscimagna-Hemminger, Sarah E. et al. (2003). "Learned Dynamics of Reaching Movements Generalize From Dominant to Nondominant Arm". *Journal of Neurophysiology* 89.1. PMID: 12522169, pp. 168–176. DOI: 10.1152/jn.00622.2002.

Degond, Pierre, Maxime Herda, and Sepideh Mirrahimi (2020). "A Fokker-Planck approach to the study of robustness in gene expression". *Mathematical Biosciences and Engineering* 17.6, pp. 6459–6486. DOI: 10.3934/mbe.2020338.

Dierick, Frédéric et al. (Nov. 2017). "Fractal analyses reveal independent complexity and predictability of gait". *PLOS ONE* 12.11. Ed. by Steven Allen Gard, e0188711. DOI: 10.1371/journal.pone.0188711.

Dierick, Frédéric et al. (May 2020). "Digital natives and dual task: Handling it but not immune against cognitive-locomotor interferences". *PLOS ONE* 15.5, pp. 1–13. DOI: 10.1371/journal.pone.0232328.

Dierick, Frédéric et al. (2021). "Benefits of nonlinear analysis indices of walking stride interval in the evaluation of neurodegenerative diseases". *Human Movement Science* 75, p. 102741. DOI: 10.1016/j.humov.2020.102741.

Dizio, P. and J. R. Lackner (1995). "Motor adaptation to Coriolis force perturbations of reaching movements: endpoint but not trajectory adaptation transfers to the nonexposed arm". *Journal of Neurophysiology* 74.4. PMID: 8989414, pp. 1787–1792. DOI: 10.1152/jn.1995.74.4.1787.

Dumas, H Scott (Sept. 2013). *The KAM Story*. Hackensack, NJ: WORLD SCIENTIFIC. DOI: 10.1142/8955.

Einstein, Albert (1916). "The Foundation of the General Theory of Relativity". *Annalen Phys.* 49.7. Ed. by Jong-Ping Hsu and D. Fine, pp. 769–822. DOI: 10.1002/andp.200590044.

Emmerik, Richard E.A. van et al. (Mar. 2016). "Comparing dynamical systems concepts and techniques for biomechanical analysis". *Journal of*

Sport and Health Science 5.1, pp. 3–13. DOI: 10.1016/j.jshs.2016.01.013.

Fa, Kwok Sau (2005). "Exact solution of the Fokker-Planck equation for a broad class of diffusion coefficients". *Phys. Rev. E* 72 (2), p. 020101. DOI: 10.1103/PhysRevE.72.020101.

Fisk, Arthur D. and Walter Schneider (1984). "Memory as a function of attention, level of processing, and automatization." *Journal of Experimental Psychology: Learning, Memory, and Cognition* 10.2, pp. 181–197. DOI: 10.1037/0278-7393.10.2.181.

Fitts, Paul M. (1954). "The information capacity of the human motor system in controlling the amplitude of movement." *Journal of Experimental Psychology* 47.6, pp. 381–391. DOI: 10.1037/h0055392.

Flash, T and N Hogan (1985). "The coordination of arm movements: an experimentally confirmed mathematical model". *The Journal of Neuroscience* 5.7, pp. 1688–1703. DOI: 10.1523/jneurosci.05-07-01688.1985.

Gates, DH, JL Su, and JB Dingwell (2007). "Possible biomechanical origins of the long-range correlations in stride intervals of walking". *Physica A: Statistical Mechanics and its Applications* 380, pp. 259–270. DOI: 10.1016/j.physa.2007.02.061.

Gaveau, Jérémie et al. (Jan. 2014). "Energy-related optimal control accounts for gravitational load: comparing shoulder, elbow, and wrist rotations". *Journal of Neurophysiology* 111.1, pp. 4–16. DOI: 10.1152/jn.01029.2012.

Gentili, R., C. Papaxanthis, and T. Pozzo (Jan. 2006). "Improvement and generalization of arm motor performance through motor imagery practice". *Neuroscience* 137.3, pp. 761–772. DOI: 10.1016/j.neuroscience.2005.10.013.

Goldberger, Ary L. et al. (2002). "Fractal dynamics in physiology: Alterations with disease and aging". *Proceedings of the National Academy of Sciences* 99.suppl_1, pp. 2466–2472. DOI: 10.1073/pnas.012579499.

Goldstein, Herbert, Charles P. Poole, and John L. Safko (2002). *Classical Mechanics (3rd Edition)*. Addison Wesley, p. 680.

Hagler, Stuart (2015). "On the principled description of human movements". en. DOI: 10.13140/RG.2.2.13192.62723.

Hairer, Ernst, Gerhard Wanner, and Syvert P. Norsett (1993). *Solving Ordinary Differential Equations I*. Springer Berlin Heidelberg. DOI: 10.1007/978-3-540-78862-1.

Hausdorff, J. M. et al. (1995). "Is walking a random walk? Evidence for long-range correlations in stride interval of human gait". *Journal of Applied Physiology* 78.1. PMID: 7713836, pp. 349–358. DOI: 10.1152/jappl.1995.78.1.349.

Hausdorff, J. M. et al. (Mar. 1999). "Maturation of gait dynamics: stride-to-stride variability and its temporal organization in children". *Journal of Applied Physiology* 86.3, pp. 1040–1047. DOI: 10.1152/jappl.1999.86.3.1040.

Hausdorff, Jeffrey M. et al. (Jan. 1997). "Altered fractal dynamics of gait: reduced stride-interval correlations with aging and Huntington's disease". *Journal of Applied Physiology* 82.1, pp. 262–269. DOI: 10.1152/jappl.1997.82.1.262.

Hedenström, Anders et al. (Nov. 2016). "Annual 10-Month Aerial Life Phase in the Common Swift Apus apus". *Current Biology* 26.22, pp. 3066–3070. DOI: 10.1016/j.cub.2016.09.014.

Henrard, J. (1993). "The Adiabatic Invariant in Classical Mechanics". *Dynamics Reported*. Springer Berlin Heidelberg, pp. 117–235. DOI: 10.1007/978-3-642-61232-9_4.

Hoffman, Errol R. (Apr. 1991). "A comparison of hand and foot movement times". *Ergonomics* 34.4, pp. 397–406. DOI: 10.1080/00140139108967324.

Hogan, N (Nov. 1984). "An organizing principle for a class of voluntary movements". *The Journal of Neuroscience* 4.11, pp. 2745–2754. DOI: 10.1523/jneurosci.04-11-02745.1984.

Hogan, Neville (June 1982). "Control and Coordination of Voluntary Arm Movements". *1982 American Control Conference*. IEEE. DOI: 10.23919/acc.1982.4787906.

Hooren, Bas Van et al. (Dec. 2019). "Is Motorized Treadmill Running Biomechanically Comparable to Overground Running? A Systematic Review and Meta-Analysis of Cross-Over Studies". *Sports Medicine* 50.4, pp. 785–813. DOI: 10.1007/s40279-019-01237-z.

Hurov, J. (1986). "Anatomy and mechanics of the shoulder: review of current concepts." *Journal of hand therapy* 22, pp. 328–343. DOI: 10.1016/j.jht.2009.05.002.

Hurst, H. E. (Jan. 1951). "Long-Term Storage Capacity of Reservoirs". *Transactions of the American Society of Civil Engineers* 116.1, pp. 770–799. DOI: 10.1061/taceat.0006518.

Hutchinson, B. (Nov. 1823). "Observations on the Tread-Mill." *The London medical and physical journal* 50 (297), pp. 372–381. ppublish.

Jose, J.V. and E.J Saletan (1998). *Classical dynamics: a contemporary approach*. Cambridge: Cambridge Univ. Press.

Kadar, E.E., R.C. Schmidt, and M.T. Turvey (1993). "Constants underlying frequency changes in biological rhythmic movements". *Biol. Cybern.* 68, pp. 421–430. DOI: doi.org/10.1007/BF00198774.

Kantz, Holger and Thomas Schreiber (Nov. 2003). *Nonlinear Time Series Analysis*. Vol. 7. Cambridge: Cambridge University Press. DOI: 10.1017/cbo9780511755798.

Kaparulin, Dmitry S., Simon L. Lyakhovich, and Oleg D. Nosyrev (2020). "Resonance and stability of higher derivative theories of a derived type". *Phys. Rev. D* 101.12, p. 125004. DOI: 10.1103/PhysRevD.101.125004.

Kawato, Mitsuo (1999). "Internal models for motor control and trajectory planning". *Current Opinion in Neurobiology* 9.6, pp. 718–727. DOI: 10.1016/s0959-4388(99)00028-8.

Kerr, Robert (Sept. 1973). "Movement Time in an Underwater Environment". *Journal of Motor Behavior* 5.3, pp. 175–178. DOI: 10.1080/00222895.1973.10734962.

Khasminski, R. Z. (Jan. 1966). "On Stochastic Processes Defined by Differential Equations with a Small Parameter". *Theory of Probability & Its Applications* 11.2, pp. 211–228. DOI: 10.1137/1111018.

Kolmogorov, A N (1954). "On conservation of conditionally periodic motions for a small change in Hamilton's function". *Dokl. Akad. Nauk SSSR* 98, pp. 527–530.

Kominis, Y., A. K. Ram, and K. Hizanidis (2010). "Kinetic Theory for Distribution Functions of Wave-Particle Interactions in Plasmas". *Phys. Rev. Lett.* 104 (23), p. 235001. DOI: 10.1103/PhysRevLett.104.235001.

Kritzinger, Duane (2016). *Aircraft System Safety Assessments for Initial Airworthiness Certification. Assessments for Initial Airworthiness Certification*. Elsevier, p. 422.

Kugler, P.N. et al. (1990). "Investigating a Nonconservative Invariant of Motion in Coordinated Rhythmic Movements". *Ecological Psychology* 2.2, pp. 151–189. DOI: 10.1207/s15326969eco0202_4.

Kulsrud, R.M. (1957). "Adiabatic Invariant of the Harmonic Oscillator". *Phys. Rev.* 106, pp. 205–207. DOI: 10.1103/PhysRev.106.205.

Landau, L. and E. Lifchitz (1988). *Physique théorique Tome 1 : Mécanique*. Moscow: E. MIR.

Lang, Thomas et al. (Feb. 2017). "Towards human exploration of space: the THESEUS review series on muscle and bone research priorities". *npj Microgravity* 3.1, p. 8. DOI: 10.1038/s41526-017-0013-0.

Lawson, B. and B. Riecke (Sept. 2014). "Vision and Virtual Environments". *Handbook of Virtual Environments*. CRC Press. DOI: 10.1201/b17360-10.

Lima, F. M. S. and P. Arun (Oct. 2006). "An accurate formula for the period of a simple pendulum oscillating beyond the small angle regime". *American Journal of Physics* 74.10, pp. 892–895. DOI: 10.1119/1.2215616.

Lin, W.-T. and C.-L. Ho (Feb. 2012). "Similarity solutions of the Fokker–Planck equation with time-dependent coefficients". *Annals of Physics* 327.2, pp. 386–397. DOI: 10.1016/j.aop.2011.11.004.

Lozier, Daniel W., Ronald F. Boisvert, and Charles W. Clark (2010). *NIST Handbook of Mathematical Functions Hardback and CD-ROM*. Cambridge University Press, p. 968.

MacNeilage, Paul R. and Stefan Glasauer (Nov. 2018). "Gravity Perception: The Role of the Cerebellum". *Current Biology* 28.22, R1296–R1298. DOI: 10.1016/j.cub.2018.09.053.

Marder, Eve and Dirk Bucher (Nov. 2001). "Central pattern generators and the control of rhythmic movements". *Current Biology* 11.23, R986–R996. DOI: 10.1016/s0960-9822(01)00581-4.

Marmelat, Vivien et al. (2014). "Persistent Fluctuations in Stride Intervals under Fractal Auditory Stimulation". *PLoS ONE* 9.3. Ed. by Alfonso Fasano, e91949. DOI: 10.1371/journal.pone.0091949.

Minassian, Karen et al. (2017). "The Human Central Pattern Generator for Locomotion: Does It Exist and Contribute to Walking?" *The Neuroscientist* 23.6. PMID: 28351197, pp. 649–663. DOI: 10.1177/1073858417699790.

Moon, Yaejin et al. (June 2016). "Gait variability in people with neurological disorders: A systematic review and meta-analysis". *Human Movement Science* 47, pp. 197–208. DOI: 10.1016/j.humov.2016.03.010.

Möser, J (1962). "On invariant curves of area-preserving mappings of an annulus". *Nachr. Akad. Wiss. Göttingen, II*, pp. 1–20.

Nekhoroshev, Nikolaï (1972). "Behavior of Hamiltonian systems close to integrable". *Functional Analysis and Its Applications* 5.4, pp. 338–339. DOI: 10.1007/bf01086753.

— (Dec. 1977). "An exponential estimate of the time of stability of nearly-integrable Hamiltonian systems". *Russian Mathematical Surveys* 32.6, pp. 1–65. DOI: 10.1070/rm1977v032n06abeh003859.

Nelson, W. L. (Feb. 1983). "Physical principles for economies of skilled movements". *Biological Cybernetics* 46.2, pp. 135–147. DOI: 10.1007/bf00339982.

Notte, J. et al. (1993). "Experimental breaking of an adiabatic invariant". *Phys. Rev. Lett.* 70 (25), pp. 3900–3903. DOI: 10.1103/PhysRevLett.70.3900.

Nowak, D.A. and J. Hermsdörfer (2003). "Sensorimotor memory and grip force control: does grip force anticipate a self-produced weight change when drinking with a straw from a cup?" *Eur. J. Neurosci* 18, pp. 2883–92. DOI: doi.org/10.1111/j.1460-9568.2003.03011.x.

Ortega, Justus D. and Claire T. Farley (2005). "Minimizing center of mass vertical movement increases metabolic cost in walking". *Journal of Applied Physiology* 99.6, pp. 2099–2107. DOI: 10.1152/japplphysiol.00103.2005.

Pais, A. and G. E. Uhlenbeck (1950). "On Field theories with nonlocalized action". *Phys. Rev.* 79, pp. 145–165. DOI: 10.1103/PhysRev.79.145.

Peat, M. (1986). "Functional anatomy of the shoulder complex". *Physical therapy* 66, pp. 1855–1865. DOI: 10.1093/ptj/66.12.1855.

Peng, C.-K. et al. (Feb. 1994). "Mosaic organization of DNA nucleotides". *Physical Review E* 49.2, pp. 1685–1689. DOI: 10.1103/physreve.49.1685.

Peng, C.-K. et al. (Mar. 1995). "Quantification of scaling exponents and crossover phenomena in nonstationary heartbeat time series". *Chaos: An*

Interdisciplinary Journal of Nonlinear Science 5.1, pp. 82–87. DOI: 10.1063/1.166141.

Penzel, T. et al. (Oct. 2003). "Comparison of detrended fluctuation analysis and spectral analysis for heart rate variability in sleep and sleep apnea". *IEEE Transactions on Biomedical Engineering* 50.10, pp. 1143–1151. DOI: 10.1109/tbme.2003.817636.

Pérez, Enric (Sept. 2008). "Ehrenfest's adiabatic theory and the old quantum theory, 1916–1918". *Archive for History of Exact Sciences* 63.1, pp. 81–125. DOI: 10.1007/s00407-008-0030-1.

Phinyomark, Angkoon, Robyn Larracy, and Erik Scheme (2020). "Fractal Analysis of Human Gait Variability via Stride Interval Time Series". *Frontiers in Physiology* 11, p. 333. DOI: 10.3389/fphys.2020.00333.

Pozzo, Thierry et al. (Nov. 1998). "The sensorimotor and cognitive integration of gravity". *Brain Research Reviews* 28.1-2, pp. 92–101. DOI: 10.1016/s0165-0173(98)00030-7.

R Core Team (2021). *R: A Language and Environment for Statistical Computing*. R Foundation for Statistical Computing. Vienna, Austria.

Raffalt, PC. et al. (2020). "To walk or to run - a question of movement attractor stability". *J Exp Biol.* 223.13, p. 1. DOI: 10.1242/jeb.224113.

Rahmani, Bahareh et al. (July 2018). "Dynamical Hurst analysis identifies EEG channel differences between PTSD and healthy controls". *PLOS ONE* 13.7. Ed. by Lutz Jäncke, e0199144. DOI: 10.1371/journal.pone.0199144.

Ravi, Deepak K. et al. (2020). "Assessing the Temporal Organization of Walking Variability: A Systematic Review and Consensus Guidelines on Detrended Fluctuation Analysis". *Frontiers in Physiology* 11. DOI: 10.3389/fphys.2020.00562.

Risken, H. and T. K. Caugheyz (Sept. 1991). *The Fokker-Planck Equation: Methods of Solution and Application, 2nd ed.* Vol. 58. 3. ASME International, pp. 860–860. DOI: 10.1115/1.2897281.

Rock, Chase G. et al. (Nov. 2018). "Interaction between step-to-step variability and metabolic cost of transport during human walking". *Journal of Experimental Biology* 221.22. jeb181834. DOI: 10.1242/jeb.181834.

Rose, Jessica and James Gibson Gamble (2006). *Human walking*. Third edition. Lippincott Williams and Wilkins.

Rosenbaum, David A. (2009). *Human motor control*. Academic Press, p. 528.

Saini, M. et al. (1998). "The Vertical Displacement of the Center of Mass During Walking: A Comparison of Four Measurement Methods". *Journal of Biomechanical Engineering* 120.1, pp. 133–139. DOI: 10.1115/1.2834293.

Sarvestan, Javad et al. (Apr. 2022). "The effects of mobile phone use on motor variability patterns during gait". *PLOS ONE* 17.4. Ed. by Yih-Kuen Jan, e0267476. DOI: 10.1371/journal.pone.0267476.

Sarwary, A. M. E. et al. (2015). "Generalization and transfer of contextual cues in motor learning". *Journal of Neurophysiology* 114.3. PMID: 26156381, pp. 1565–1576. DOI: 10.1152/jn.00217.2015.

Selinger, Jessica C. et al. (Oct. 2019). "How humans initiate energy optimization and converge on their optimal gaits". *Journal of Experimental Biology* 222.19. jeb198234. DOI: 10.1242/jeb.198234.

Shadmehr, R and FA Mussa-Ivaldi (May 1994). "Adaptive representation of dynamics during learning of a motor task". *The Journal of Neuroscience* 14.5, pp. 3208–3224. DOI: 10.1523/jneurosci.14-05-03208.1994.

Stergiou, Nicholas (Sept. 2018). *Nonlinear Analysis for Human Movement Variability*. Ed. by Nicholas Stergiou. CRC Press. DOI: 10.1201/9781315370651.

Stergiou, Nicholas and Leslie M. Decker (Oct. 2011). "Human movement variability, nonlinear dynamics, and pathology: Is there a connection?" *Human Movement Science* 30.5, pp. 869–888. DOI: 10.1016/j.humov.2011.06.002.

Stergiou, Nicholas, Regina T. Harbourne, and James T. Cavanaugh (Sept. 2006). "Optimal Movement Variability". *Journal of Neurologic Physical Therapy* 30.3, pp. 120–129. DOI: 10.1097/01.npt.0000281949.48193.d9.

Steuer, Inge and Pierre A. Guertin (Jan. 2019). "Central pattern generators in the brainstem and spinal cord: an overview of basic principles, similarities and differences". *Reviews in the Neurosciences* 30.2, pp. 107–164. DOI: 10.1515/revneuro-2017-0102.

Sturges, Herbert A. (1926). "The Choice of a Class Interval". *Journal of the American Statistical Association* 21.153, pp. 65–66. DOI: 10.1080/01621459.1926.10502161.

Tai-jun, Chen et al. (Feb. 2013). "Higher derivative theories with constraints: exorcising Ostrogradski's ghost". *Journal of Cosmology and Astroparticle Physics* 2013.02, pp. 042–042. DOI: 10.1088/1475-7516/2013/02/042.

Takaishi, T., Y. Yasuda, and T. Moritani (1994). "Neuromuscular fatigue during prolonged pedalling exercise at different pedalling rates". *Eur J Appl Physiol Occup Physiol.* 69, pp. 154–158. DOI: 10.1007/BF00609408.

Tennyson, J. L., John R. Cary, and D. F. Escande (1986). "Change of the Adiabatic Invariant due to Separatrix Crossing". *Phys. Rev. Lett.* 56 (20), pp. 2117–2120. DOI: 10.1103/PhysRevLett.56.2117.

Terrier, Philippe and Olivier Dériaz (Feb. 2011). "Kinematic variability, fractal dynamics and local dynamic stability of treadmill walking". *Journal of NeuroEngineering and Rehabilitation* 8.1. DOI: 10.1186/1743-0003-8-12.

Terrier, Philippe and Olivier Dériaz (2012). "Persistent and anti-persistent pattern in stride-to-stride variability of treadmill walking: Influence of rhythmic auditory cueing". *Human Movement Science* 31.6, pp. 1585–1597. DOI: 10.1016/j.humov.2012.05.004.

Tesio, Luigi and Viviana Rota (2019). "The Motion of Body Center of Mass During Walking: A Review Oriented to Clinical Applications". *Frontiers in Neurology* 10. DOI: 10.3389/fneur.2019.00999.

Thoroughman, Kurt A. and Reza Shadmehr (2000). "Learning of action through adaptive combination of motor primitives". *Nature* 407.6805, pp. 742–747. DOI: 10.1038/35037588.

Turvey, M.T., K.G. Holt, J. Obusek, et al. (1996). "Adiabatic transformability hypothesis of human locomotion". *Biol. Cybern.* 74.107, pp. 107–115. DOI: 10.1007/BF00204199.

Viviani, Paolo and Tamar Flash (1995). "Minimum-jerk, two-thirds power law, and isochrony: converging approaches to movement planning." *Journal of Experimental Psychology: Human Perception and Performance* 21.1, pp. 32–53. DOI: 10.1037/0096-1523.21.1.32.

Wald, Robert M (1984). *General relativity.* Chicago, IL: Chicago Univ. Press.

Wang, Yang and Manoj Srinivasan (2014). "Stepping in the direction of the fall: the next foot placement can be predicted from current upper body state in steady-state walking". *Biology Letters* 10.9, p. 20140405. DOI: 10.1098/rsbl.2014.0405.

Whinnery, Typ and Estrella M Forster (June 2013). "The Gz-induced loss of consciousness curve". *Extreme Physiology & Medicine* 2.1. DOI: 10.1186/2046-7648-2-19.

White, Olivier et al. (Nov. 2008). "Altered Gravity Highlights Central Pattern Generator Mechanisms". *Journal of Neurophysiology* 100.5, pp. 2819–2824. DOI: 10.1152/jn.90436.2008.

White, Olivier et al. (Sept. 2012). "Active Collisions in Altered Gravity Reveal Eye-Hand Coordination Strategies". *PLoS ONE* 7.9. Ed. by Nicole Wenderoth, e44291. DOI: 10.1371/journal.pone.0044291.

White, Olivier et al. (Aug. 2016). "Towards human exploration of space: the THESEUS review series on neurophysiology research priorities". *npj Microgravity* 2.1, p. 16023. DOI: 10.1038/npjmgrav.2016.23.

White, Olivier et al. (Feb. 2018). "Grip Force Adjustments Reflect Prediction of Dynamic Consequences in Varying Gravitoinertial Fields". *Frontiers in Physiology* 9, p. 131. DOI: 10.3389/fphys.2018.00131.

White, Olivier et al. (July 2020). "The gravitational imprint on sensorimotor planning and control". *Journal of Neurophysiology* 124.1, pp. 4–19. DOI: 10.1152/jn.00381.2019.

Whittington, Ben R. and Darryl G. Thelen (Nov. 2008). "A Simple Mass-Spring Model With Roller Feet Can Induce the Ground Reactions Observed in Human Walking". *Journal of Biomechanical Engineering* 131.1. 011013. DOI: 10.1115/1.3005147.

Wolpert, Daniel (2011). *The real reason for brains*. Ed. by TED.

Yentes, J.M. et al. (2013). "The Appropriate Use of Approximate Entropy and Sample Entropy with Short Data Sets". *Ann Biomed Eng* 41.1, pp. 349–365. DOI: 10.1007/s10439-012-0668-3.

Zbären, Gabrielle Aude et al. (May 2023). "Physical inference of falling objects involves simulation of occluded trajectories in early visual areas". *Human Brain Mapping* 44.10, pp. 4183–4196. DOI: 10.1002/hbm.26338.

Zehr, E Paul et al. (July 2004). "Possible contributions of CPG activity to the control of rhythmic human arm movement". *Canadian Journal of Physiology and Pharmacology* 82.8-9, pp. 556–568. DOI: 10.1139/y04-056.

Appendix A

Adiabatic invariants and random noise

The dynamical state of a system coordinatized by configuration space variables Q^α, $\alpha = 1, \ldots, n$ can be summarized by its trajectory in $2n-$dimensional phase-space (Q^α, P_α), where P_α are the momentum degrees of freedom. In standard dynamics, $P_\alpha = m\,\dot{Q}^\alpha$ with m a mass scale, although Hamiltonian dynamics can be formulated for more general systems. The trajectory is generated by a set of initial conditions $(Q_0^\alpha, P_{0\alpha})$ and an evolution operator called a Hamiltonian, $H(Q^\alpha, P_\alpha)$, which leads to the equations of motion (Landau and Lifchitz 1988, Ch. 45)

$$\dot{Q}^\alpha = \frac{\partial H}{\partial P_\alpha}, \quad \dot{P}_\alpha = -\frac{\partial H}{\partial Q_\alpha}. \tag{A.1}$$

If the Hamiltonian has a standard, separable, time independent form, $H = \sum_{\beta=1}^{n} \left[\frac{1}{2}P_\beta^2 + V_\beta(Q^\beta)\right]$, then $\dot{Q}^\alpha = P_\alpha$ and the momentum can be interpreted as the body velocity. Separability allows to focus on a Hamiltonian system with $n = 1$, knowing that the results can be straightforwardly extended. Let us consider the Hamiltonian $H = \frac{P^2}{2} + V(Q)$. If the potential V allows for bounded trajectories in phase-space, the action variable can be defined as

$$I = \frac{1}{2\pi} \oint_\Gamma P\, dQ\ , \tag{A.2}$$

where Γ is the bounded trajectory in the plane (Q, P). The relation (Eq. 5.1) is equivalent to (Eq. A.2) in our case. Then, the Hamiltonian can be reformulated as a function of only the action variables: $H = H_0(I)$ which is always true for an integrable system. The equations of motion for the integrable system now reads (Landau and Lifchitz 1988, Ch. 45)

$$\dot{I} = -\frac{\partial H_0}{\partial \theta} = 0, \quad \dot{\theta} = \frac{\partial H_0}{\partial I} = \omega(I), \tag{A.3}$$

where θ is the angle variable. The action variables are therefore invariant and $\theta = \omega(I)\, t + \theta_0$.

In attempting to model the quasiperiodic nature of human motion, it is of interest to assume that

$$H = H_0(I) + \epsilon\ \xi(t)\ \mathcal{V}(I, \theta), \tag{A.4}$$

where $0 < \epsilon \ll 1$, and where $\xi(t)$ is a stochastic noise with vanishing mean value. It is also assumed that $H_0(I)$ must satisfy the assumptions underlying the Nekhoroshev theorem (Nekhoroshev 1972, 1977). According to (Khasminski 1966, theorems 1.1 and 3.1), the action variable becomes time-dependent because of the random noise (I becomes $I_\epsilon(t)$), but the deviation from the value I (which can be taken as the initial value) remains small, of order $\sqrt{\epsilon}$, up to a time of order $1/\epsilon$ or even better (Cogburn and Ellison 1992), up to time of order $1/\epsilon^2$. More precisely, $|I_\epsilon(t) - I| = \sqrt{\epsilon}\ Y(t)$ with $Y(t)$ a Gaussian Markov process.

Assuming that deviations from the time-independent dynamics are of order ϵ, a given observable Λ should behave approximately as $\Lambda(t) = \Lambda(1 + \epsilon\, f(t))$. Hence, the coefficient of variation of Λ, CV_Λ, defined as the ratio between its standard deviation and its mean value Λ, is of order ϵ: $CV_\Lambda \sim \epsilon$.

Appendix B

Higher derivative dynamics and rhythmic motion

Let us consider a system with N degrees of freedom x^α described by the Lagrangian

$$L = \frac{1}{2} g_{\alpha\beta}(x) \dot{x}^\alpha \dot{x}^\beta - U(x^\gamma) \tag{B.1}$$

with $g_{\alpha\beta}$ the components of a real, symmetric and positive-definite matrix G that we call the kinetic matrix. Note that it is not necessarily constant and may depend on the dynamical variables. If necessary after a translation of the origin of the coordinates, we may assume that $x^\alpha = 0$ $(\forall\, \alpha)$ is an equilibrium position: $\frac{\partial U}{\partial x^\alpha}\big|_{x^\gamma=0} = 0$. Such a Lagrangian may model the motion of several joints, the potential energy U being an a priori complicated function of the degrees of freedom. If only small oscillations around equilibrium position are considered, the equations of motion read $\ddot{x}^\alpha + \gamma^{\alpha\delta} U_{\delta\beta} x^\beta = 0$, with $\gamma^{\alpha\beta}$ the components of the inverse of the matrix G_0 of components $\gamma_{\alpha\beta} := g_{\alpha\beta}(0)$. In other words, one has $\gamma^{\alpha\delta}\gamma_{\delta\beta} = \delta^\alpha_\beta$. One defines the potential matrix U with components

$$U_{\alpha\beta} = \left.\frac{\partial^2 U}{\partial x^\alpha \partial x^\beta}\right|_{x^\delta=0}. \tag{B.2}$$

Solving the eigenequation $V^\alpha{}_\beta\, \xi^\beta_a = \lambda_a\, \xi^\alpha_a$ for the matrix $V = G_0^{-1} U$ with components $V^\alpha{}_\beta = \gamma^{\alpha\delta}\, U_{\delta\beta}$, with $a = 1, \ldots, N$, allows to solve the equations of motion in terms of the normal coordinates $Q^a(t)$:

$$x^\alpha = \xi^\alpha_a\, Q^a(t) \qquad \text{with} \qquad \ddot{Q}^a = -\lambda_a\, Q^a \tag{B.3}$$

and without any summation over the index a. Therefore, for the given dynamical system described by the variables x^α, any small oscillatory motion about the minimum of the potential in configuration space can therefore be decomposed as a linear combination of elementary oscillations along the normal modes, each one at the frequency $\nu_a = \omega_a/2\pi$, where $\lambda_a = \omega_a^2$. In particular, for appropriate initial conditions it is possible to only excite the normal mode $Q^a(t)$ for a given value of the index a. The dynamical system as a whole will then oscillate at the single frequency ν_a, without exciting the modes $Q^b(t)$ with $b \neq a$. The interested reader may find a detailed discussion about small oscillations around an equilibrium position in (Landau and Lifchitz 1988, Chapter 5), or in (Arnold 1989, Part 2, Chapter 5) for a more precise mathematical formulation.

Note that, from the datum of the normal modes Q's with their frequencies ν's, one can go back and access the information contained in the kinetic and potential matrices G and U. This is because the normal modes are orthogonal with respect to the metric G, and using the latter metric together with the eigenvalues of $V := G^{-1}U$ gives U up to a reordering of the dynamical variables x^α.

In a human rhythmic motion, if the participant is asked to perform a periodic motion, say with the forearm, one observes that the projection of the motion of the hand along the three spatial directions gives rise to a very small set of frequencies that are all integer multiples of a fundamental one. In this description, we neglect the quasi-periodic motion of the forearm due to physiological noise. Of course, the forearm is a very complicated system with dozens of components linked in a complicated fashion, giving rise to a configuration space $\mathbb{Q}$ of very large dimension N. In principle (but not in practice), it is possible to describe it by a Lagrangian of the form (B.1) and there will N normal modes Q^a's with possible degeneracies in the frequencies. The observed motion of the forearm of the participants is, instead, very simple and degenerate.

Instead of trying to find the realistic Lagrangian description (B.1) of the forearm, from the sole observation of a very limited set of forced periodic motions with distinct frequencies ω_a's, motions that we view as analogous to the distinct normal modes of a dynamical system, we propose an effective model whose purpose it to reproduce those "normal modes" without any diagonalisation of any potential matrix V. The operator

$$F = \Pi_{a=1}^{n} \left(1 + \frac{1}{\omega_a^2} \frac{d^2}{dt^2} \right) \tag{B.4}$$

is such that $Fx^\alpha = 0$ *for all* α because $FQ^a = 0$ for all a, by construction. Here, by an abuse of notation we have denoted by $Q^a(t)$ the $n \ll N$

simple and pure harmonic modes observed in the participant's motion. The latter describes the motion in a configuration space of very large dimension N whereas we effectively reduce the dynamics to a configuration space of dimension n way smaller than N. Therefore, in our effective description of the motion based on a specific set of harmonic oscillations observed in the forearm's motion, every single dynamical variable x^α for α fixed obeys the equation of motion of a Pais-Uhlenbeck oscillator whose Lagrangian reads $L_{P-U} = -\frac{1}{2}\, x^\alpha\, F\, x^\alpha$ (Pais and Uhlenbeck 1950). If at least two frequencies ω_a are different, the effective dynamics of a given degree of freedom can be mimicked by a particular solution of the equations of motion of a higher-derivative harmonic oscillator.

Appendix C

Experiment on pointing task with fractal stimulus

Introduction

For a long time, noise has been considered detrimental to experimental studies and seen as something to minimize, correct or outright remove to obtain robust results. Recently though, after observing variability in numerous signals (for example in humans: electroencephalograms (Acharya et al. 2015; Rahmani et al. 2018), heart beat and heart beat variability (Peng et al. 1995; Penzel et al. 2003), gait (Dierick et al. 2017; Hausdorff et al. 1995), etc.) it has been hypothesized that variability is actually an important feature of a healthy system (Stergiou and Decker 2011). Indeed, in these situations, healthy, optimal or energy-minimizing systems have a variability that lies in an auto-correlated regime i.e. neither completely random nor strictly deterministic. This can be affected by health condition, or external stimuli such as cognitive load like metronome keeping (Marmelat et al. 2014).

Variability is a nebulous term used in many contexts. In this appendix we use the term variability to refer to the Hurst exponent, i.e. the measure of the long-term memory of a signal. It has been measured here by using Detrended Fluctuation Analysis (DFA) a technique developed in (Peng et al. 1994) and Rescaled range methods first proposed in (Hurst 1951). A Hurst exponent H of 0 refers to a perfectly anti-correlated time series i.e. a time series where adjacent values switch between highs and lows, $H = 0.5$ corresponds to a random time series and $H = 1$ to a completely auto-correlated one. Healthy systems being somewhat auto-correlated usually lie in the $0.5 < H < 1$ regime, that is to say that high values tend to be followed by high values, and similarly for low values of the time series.

In this experiment, instead of measuring the variability inherent in human motion, we tried to synthetically force the participant into a certain variability to probe its effect on performance. To do so we devised a tracing task during which participants followed targets appearing with a timing following a certain variability and we computed its effect on various indices. We hypothesize that motion is most efficient and therefore optimal from a performance point of view for Hurst exponents lying in a somewhat auto-correlated regime, i.e., far from $H = 1$ or $H = 0.5$, but rather around intermediate values $H \sim 0.7$.

Protocol

The protocol was validated by a local ethics committee and was performed over a period of 90 minutes. Thirteen participants were selected, they were healthy students from the University of Burgundy (Dijon, France). The participants gave their informed consent after being briefed about the study. The same experimenter (V. Dehouck) was responsible for all measurements.

Participants' hand motion was recorded using a drawing tablet (Wacom DTH-3220, Wacom; Kazo, Saitama, Japan) and its stylus. Participants were sat comfortably in front of the tablet and were allowed to manipulate and trace on the tablet to familiarize themselves with the device. The stylus position was sampled at a frequency of 100Hz.

Participants took part in 18 (3x6 conditions) blocks composed of 10 trials each. The order of the blocks was randomized for each participant. At the start of each block a ready check was performed by the participant themselves. Participants were then instructed to follow the appearance of green dots on the screen with the stylus. The timing of appearance followed not an isochronous metronome but a fractal one, identified by its Hurst exponent (H = 0.5, 0.6, 0.7, 0.8, 0.9, 1; a condition) generated via a Gaussian noise generator and controlled using Detrended Fluctuation Analysis and Rescaled Range techniques. Each of the timing series was 256-point long. After a period during which the participant was asked to follow the metronome, a red dot was randomly flashed on the screen (a trial). The participant was instructed to connect with the dot as quickly as possible.

The green dots were placed on the vertices of a square of side 14.5 cm centered in the middle of the screen. The red target was flashed randomly on the screen within a square of side 21.8 cm.

Limits

This experiment had to overcome several hurdles. First of all, this experiment was originally designed for a Phantom system (Phantom Premium, 3Dsystems; Rock Hill, USA) allowing for motion in three directions. Unfortunately, after a few participants took part in the experiment, the machine was broken heavily delaying us. After being assured that the machine could not be fixed, the experiment had to be quickly ported to a new system with its own limitations, the drawing tablet. Most obviously, the motion performed on the tablet is akin to writing on a table, already strongly changing the nature of the expected motion from a whole-arm 3D motion, to a 2D movement mostly with the forearm; therefore severely reducing the number of degrees of freedom available.

Secondly, the targets, with which the performance indices were computed, were randomly flashed on the screen, both in time and position. This resulted in enormous error bars with regards to the time it took for participants to reach the target but also the speed at which they did, and therefore negatively impacted the analysis.

Furthermore, the protocol was hard to follow. Indeed, the time series dictating the isochronous metronome pace had a very large coefficient of variation, of the order of 25%. This further worsened the problem discussed above, but also made the interval of time between two ticks of the metronome vary between $0.4s$ and $1.2s$, putting participants between a continuous and a discrete motion regime.

Finally, this experiment was heavily delayed because of the COVID-19 pandemic, and with the time constraints that came with porting the experiment to another system, we were unable to rework and fine tune the experiment. We hope to be able to revise the protocol and revisit our hypothesis in the future with the experience gained with this exploration.